JPTM

Journal of Pathology and Translational Medicine

July 2020
Vol. 54 / No.4
jpatholtm.org
pISSN: 2383-7837
eISSN: 2383-7845

Evolving Concepts of Serrated Colorectal Lesions

Journal of Pathology and Translational Medicine

Volume 54 • Number 4 • July 2020 (bimonthly)
Published since 1967
Printed on 11 July 2020 Published on 15 July 2020

J Pathol Transl Med
pISSN: 2383-7837
eISSN: 2383-7845

Aims & Scope

The Journal of Pathology and Translational Medicine is an open venue for the rapid publication of major achievements in various fields of pathology, cytopathology, and biomedical and translational research. The Journal aims to share new insights into the molecular and cellular mechanisms of human diseases and to report major advances in both experimental and clinical medicine, with a particular emphasis on translational research. The investigations of human cells and tissues using high-dimensional biology techniques such as genomics and proteomics will be given a high priority. Articles on stem cell biology are also welcome. The categories of manuscript include original articles, review and perspective articles, case studies, brief case reports, and letters to the editor.

Subscription Information

To subscribe to this journal, please contact the Korean Society of Pathologists/the Korean Society for Cytopathology. Full text PDF files are also available at the official website (http://jpatholtm.org). *Journal of Pathology and Translational Medicine* is indexed by Emerging Sources Citation Index (ESCI), PubMed, PubMed Central, Scopus, KoreaMed, KoMCI, WPRIM, Directory of Open Access Journals (DOAJ), and CrossRef. Circulation number per issue is 50.

Contact the Korean Society of Pathologists/the Korean Society for Cytopathology

Publishers: Choi, Chan, MD, Hong, Soon Won, MD
Editors-in-Chief: Jung, Chan Kwon, MD, Park, So Yeon, MD
Published by the Korean Society of Pathologists/the Korean Society for Cytopathology

Editorial Office
Room 1209 Gwanghwamun Officia, 92 Saemunan-ro, Jongno-gu, Seoul 03186, Korea
Tel: +82-2-795-3094 Fax: +82-2-790-6635 E-mail: office@jpatholtm.org

#1508 Renaissancetower, 14 Mallijae-ro, Mapo-gu, Seoul 04195, Korea
Tel: +82-2-593-6943 Fax: +82-2-593-6944 E-mail: office@jpatholtm.org

Printed by iMiS Company Co., Ltd. (JMC)
Jungang Bldg. 18-8 Wonhyo-ro 89-gil, Yongsan-gu, Seoul 04314, Korea
Tel: +82-2-717-5511 Fax: +82-2-717-5515 E-mail: ml@smileml.com

Manuscript Editing by InfoLumi Co.
210-202, 421 Pangyo-ro, Bundang-gu, Seongnam 13522, Korea
Tel: +82-70-8839-8800 E-mail: infolumi.chang@gmail.com

Front cover image: Histologic features of traditional serrated adenomas (Fig. 3). p279.

Journal of Pathology and Translational Medicine

J Pathol Transl Med
pISSN: 2383-7837
eISSN: 2383-7845

Volume 54, Number 4, July 2020

CONTENTS

REVIEWS

ORIGINAL ARTICLES

CASE REPORTS

CONTENTS CONTINUED

Instructions for Authors for *Journal of Pathology and Translational Medicine* are available at http://jpatholtm.org/authors/authors.php

JPTM
Journal of Pathology and Translational Medicine 2020; 54: 265-275
https://doi.org/10.4132/jptm.2020.04.07

REVIEW

Clinicopathological characteristics of *BRCA*-associated breast cancer in Asian patients

Eun-Kyu Kim[1], So Yeon Park[2], Sung-Won Kim[3]

Departments of [1]Surgery and [2]Pathology, Seoul National University Bundang Hospital, Seoul National University College of Medicine, Seongnam; [3]Department of Surgery, Daerim St. Mary's Hospital, Seoul, Korea

BRCA1/2 germline mutations account for the majority of hereditary breast cancers. Since the identification of the *BRCA* genes, several attempts have been made to define the clinicopathological characteristics of *BRCA*-associated breast cancer in comparison with sporadic breast cancer. Asians constitute 60% of the world population, and although the incidence of breast cancer in Asia remains low compared to the West, breast cancer is the most prevalent female cancer in the region. The epidemiological aspects of breast cancer are different between Asians and Caucasians. Asian patients present with breast cancer at a younger age than Western patients. The contributions of *BRCA1/2* mutations to breast cancer incidence are expected to differ between Asians and Caucasians, and the different genetic backgrounds among races are likely to influence the breast cancer phenotypes. However, most large-scale studies on the clinicopathological characteristics of *BRCA*-associated breast cancer have been on Western patients, while studies on Asian populations were small and sporadic. In this review, we provide an overview of the clinical and pathological characteristics of *BRCA*-associated breast cancer, incorporating findings on Asian patients.

Key Words: Breast neoplasms; Genes, BRCA1; Genes, BRCA2; Asian Continental Ancestry Group

Received: March 23, 2020 **Accepted:** April 7, 2020
Corresponding Author: Sung-Won Kim, MD, PhD, Department of Surgery, Daerim St. Mary's Hospital, 657 Siheung-daero, Yeongdeungpo-gu, Seoul 07442, Korea
Tel: +82-2-829-9515, Fax: +82-2-833-6224, E-mail: brcakorea@gmail.com

Breast cancer is the most frequent female cancer that remains the leading cause of cancer death in women globally, which amounted to 25% (1.7 million) of all new cancers and 15% (521,900) of all cancer deaths in year 2012 [1]. Genetic predisposition is one of the major risk factors in breast cancer which constitutes 5%–10% of all breast cancers [2]. About 20%–40% of inherited breast cancers are attributed to deleterious mutations in the breast cancer-associated genes *BRCA1* and *BRCA2* [3]. Women who have *BRCA* germline mutations are at an increased risk of developing breast and ovarian cancers [4]. Meta-analyses indicate that *BRCA1* and *BRCA2* carriers have a 57%–65% and 45%–49% probability of developing breast cancer over lifetime, respectively [5,6]. *BRCA1/2* germline mutations are more common in patients with a family history of breast or ovarian cancer, personal history of breast cancer at young age, or triple-negative phenotype (for *BRCA1* only) [7-9]. The prevalence of these genetic mutations varies among ethnic groups and countries. However, most studies of hereditary breast cancer have been on Caucasians in Europe and North America.

Asians make up 60% of the world population. Although the incidence is low compared with Western countries [10], breast cancer is the most prevalent female cancer in Asia, and its incidence is continuously increasing [11-14]. Asian patients develop breast cancer at younger age than their Caucasian counterparts [13,15]. Thus, the contributions of *BRCA1/2* germline mutations to breast cancer incidence are expected to differ between Asians and Caucasians. In addition to the age of onset, epidemiological aspects of breast cancer are quite different between patients in Asia and those in the West. The different racial background leads to different genetic backgrounds, which in turn, may result in different breast cancer phenotypes.

The reported prevalence of *BRCA1/2* germline mutations in Asian patients with familial breast cancer ranges from 8.0% to 31.8% and in those with early-onset breast cancers from 2.8% to 21.4% [13]. The prevalence of *BRCA1/2* mutations in familial breast cancer in Asians is similar to that of African and His-

pISSN 2383-7837
eISSN 2383-7845

panic Americans but lower than Ashkenazi-Jews and North Americans of Caucasian descent. The prevalence of *BRCA1/2* mutations in early-onset breast cancer in Asians is similar to that of Caucasians and African Americans. It has been reported that *BRCA2* mutations have a higher incidence in Asians with the exception of Indians and Pakistanis, whereas *BRCA1* mutations are more prominent in other ethnicities [13,16]. In a recent study from a Chinese cohort, *BRCA* mutations were identified in 9.1% of cases with at least one risk factor for hereditary breast cancer, 3.5% of sporadic patients, and 0.38% of healthy controls [17]. In Western countries, the estimated cumulative risk of breast cancer to the age of 70 years in *BRCA1* and *BRCA2* mutation carriers ranges from 72%–87% and 71%–84%, respectively [4,18-20]. The estimated cumulative risk of breast cancer to the age of 70 years is 72.1%–66.3% and 78%–80% for *BRCA1* and *BRCA2* mutation carriers in Korea and Japan, respectively [21,22].

Current treatment recommendations for *BRCA*-associated breast cancer are similar to sporadic breast cancers, which mainly include surgery, radiotherapy, and chemotherapy. However, as chemotherapeutic regimens are becoming increasingly tumor-specific, it is possible that patients with *BRCA* mutations will be treated differently in the future. Recently, for example, various clinical trials have investigated polyadenosine diphosphate-ribose polymerase (PARP) inhibitor treatment for advanced breast cancer patients with germline *BRCA1/2* mutation. Among the various PARP inhibitors, olaparib and talazoparib, which reached phase III clinical trials, showed a significant benefit over standard chemotherapy with respect to progression-free survival [23,24]. Thus, it is important to determine the clinical characteristics and tumor pathological features of *BRCA*-associated cancers that may affect treatment recommendations.

Most studies on Asian patients have focused on the incidence and prevalence of *BRCA* mutation in high-risk women and their families [13,25-28], and few studies have investigated the clinicopathological features of *BRCA*-associated breast cancer [17,26,29,30]. In this review article, we review the literature, including Asian studies, on clinical and pathological characteristics of BRCA-associated breast cancers.

CLINICAL CHARACTERISTICS OF *BRCA1/2*-ASSOCIATED BREAST CANCER

As opposed to sporadic breast cancers, breast cancers with mutations in high-penetrance susceptibility genes display distinctive clinical features: younger age at diagnosis, higher incidence of bilateral breast cancer, and association with other cancers including ovarian, colon, prostate, pancreatic, endometrial, and male breast cancers and sarcomas [31-33].

A patient's chance of having a *BRCA1* or *BRCA2* germline mutation is highly dependent on the age and family history of breast and ovarian cancers [20,34-38]. *BRCA1* mutations are observed in 6% to 16% of breast cancers diagnosed before the age of 36 years [34,36,38-40], while *BRCA2* mutations account for a similar to the smaller or similar percentage in such young patients [40-42]. These genes may have greater contributions in early-onset breast cancer in defined populations with founder mutations. A multicenter study of 457 Ashkenazi-Jewish women with breast cancer reported that three founder mutations in *BRCA1* and *BRCA2* were found in over 40% of breast cancers diagnosed before age 40 [38]. On the other hand, patients diagnosed at the age of 60 or older had mutation rates similar to that from population studies. A family history of ovarian or breast cancer, especially the number of first-degree relatives with breast cancer diagnosed before age 50, was an important predictor of *BRCA1* and *BRCA2* germline mutations in both affected and unaffected Ashkenazi-Jewish individuals [43-45].

In Asian patients, *BRCA*-associated breast cancers tend to develop at a younger age compared to sporadic breast cancers. It has been reported that in Korea, approximately 50% of breast cancer patients with *BRCA1/2* mutations were younger than 40 years of age [25]. In a Chinese cohort, the mean age at breast cancer diagnosis in *BRCA1/2* mutation carriers was 39–45 years [29,46,47], and 56.2% of *BRCA1* mutation carriers and 33.3% of *BRCA2* mutation carriers were diagnosed with breast cancer before the age of 40 years compared with only 16.4% of non-carriers [47]. In a Japanese cohort, *BRCA1/2* mutation carriers were significantly younger at the time of diagnosis compared with non-carriers [26]. A study from the Philippines reported that two-thirds of the Philippino breast cancer patients with *BRCA1/2* mutations were under 45 years of age [48].

Patients with *BRCA1/2* mutations have higher incidences of contralateral and second ipsilateral primary breast cancers [18,49-52]. *BRCA1/2* mutation carriers diagnosed with breast cancer have a long-term risk of developing a contralateral tumor as high as 60% to 70% [19,50,51]. However, considering such clinical feature as an independent predictor of *BRCA1/2* germline mutation remains controversial [35,41,53]. *BRCA1/2* mutations were found in 22.1% (15/68) of bilateral breast cancer patients in Korea [25].

Most studies, including those in Asian patients, have reported that there is no significant difference in tumor size between

 https://doi.org/10.4132/jptm.2020.04.07

BRCA1/2-associated and sporadic breast cancers [17,26,47,52,54-58]. Nonetheless, a few studies have reported a larger tumor size at presentation in *BRCA1/2*-associated breast cancers [51,59,60], whereas others have reported the association of smaller tumor size and BRCA-associated tumors [29,61]. An earlier Chinese study reported that tumor size was significantly smaller in *BRCA* carriers than in non-carriers [29]. However, in a recent large study on Chinese population, there was no difference in tumor size among *BRCA1* carriers, *BRCA2* carriers, and non-carriers [17].

Regarding lymph node status, several studies have shown that there was a tendency for *BRCA1* mutation carriers to have a higher percentage of lymph node-negative tumors compared with controls [35,49,51,55,61,62]. Earlier Chinese and Japanese cohort studies reported no differences in nodal status between *BRCA1/2* mutation carriers and non-carriers [26,29,47]. However, a recent Chinese study reported a significantly higher rate of lymph node metastasis in *BRCA2* mutation carriers compared with *BRCA1* carriers and non-carriers [17].

The reported clinical outcomes of *BRCA1/2* mutation carriers and non-carriers with breast cancer have been inconsistent. Some studies observed significantly worse survival in *BRCA* mutation carriers compared with sporadic breast cancer patients [63-68], whereas other studies have reported similar outcomes between *BRCA* mutation carriers and non-carriers [60,69,70]. Some earlier reports even suggested a superior outcome in hereditary breast cancer [71,72]. A large population-based study reported that 10-year survival rates were similar between *BRCA* mutation carriers and non-carriers [73]. Bordeleau et al. [74] also reported that prognosis of *BRCA1/2*-associated and sporadic breast cancers appeared to be similar based on their review of the literature. However, a meta-analysis assessing the effect of *BRCA1/2* mutations on survival by Lee et al. [75] concluded that *BRCA1*, but not *BRCA2*, mutation decreases short-term and long-term overall survivals and short-term progression-free survival. The majority of these results were from Western studies, and there have been few reports comparing the clinical outcomes of *BRCA* mutation carriers and non-carriers in Asian patients. In a Chinese cohort, *BRCA1/2* mutation was not associated with breast cancer-specific survival, and *BRCA1* mutation was not proven as an independent prognostic factor [76]. Another large Chinese cohort study reported no difference in disease-free survival among *BRCA1* carriers, *BRCA2* carriers, and non-carriers [17]. General opinion seems to be that *BRCA1/2* mutation carriers and non-carriers have a similar prognosis.

It remains inconclusive whether *BRCA* mutation carriers are more likely to develop local recurrence than non-carriers. Some studies have reported similar rates of local recurrence between *BRCA* mutation carriers and non-carriers [54,64,77,78] while others have observed more frequent ipsilateral breast cancer recurrence among *BRCA* mutation carriers [29,66,79,80].

PATHOLOGICAL CHARACTERISTICS OF *BRCA*-ASSOCIATED BREAST CANCER

Histological features

The most common histological subtype in hereditary breast cancers is invasive ductal carcinoma-not otherwise specified, and this type of breast cancer seems to be more frequent in *BRCA1/2* mutation carriers than in non-carriers [78]. However, *BRCA1*-associated breast cancers have consistently been shown to have a higher frequency of medullary and atypical medullary carcinomas than *BRCA2*-associated and sporadic breast cancers. In a report by the Breast Cancer Linkage Consortium (BCLC), which is the most extensive series on the histological features of *BRCA*-associated breast cancer, *BRCA1* mutation carriers were found to have a higher incidence of medullary or atypical medullary carcinomas (13%) than *BRCA2* carriers (3%) and non-carriers (2%) [81]. In a report by Eisinger et al. [82], 19% of *BRCA1*-associated cases were typical medullary type. Invasive lobular carcinoma seems to be more frequent in *BRCA2*-associated breast cancers [78]. Although the BCLC did not report a higher frequency of lobular cancers in *BRCA2*-associated breast cancers [81], Armes et al. [56] found that pleomorphic lobular carcinomas and extensive intraductal carcinomas were more frequent in *BRCA2* mutation carriers. Marcus et al. [49] reported a higher incidence of the 'tubular lobular group' in *BRCA2*-associated tumors, which includes invasive lobular, tubular, and cribriform carcinomas. A lobular phenotype is rarely found in *BRCA1*-associated breast cancers.

A more detailed examination of the cytological and architectural features of *BRCA*-associated tumors has been reported in a complementary collaborative study by the BCLC [83]. *BRCA1*-associated breast cancers were associated with pushing margins, marked nuclear atypia, high mitotic frequency, necrotic foci, and prominent lymphocytic infiltration, some of which features define medullary carcinoma (Fig. 1). On the contrary, *BRCA2*-associated cancers had less tubular differentiation, some tendency for pushing margins, and less mitotic activity compared with sporadic breast cancers. A multivariate analysis comparing *BRCA1*- and *BRCA2*-associated breast cancers revealed that higher mitotic count ($p < .001$) and lymphocytic infiltration ($p = .001$) in *BRCA1*-associated cancers and defective tubule formation

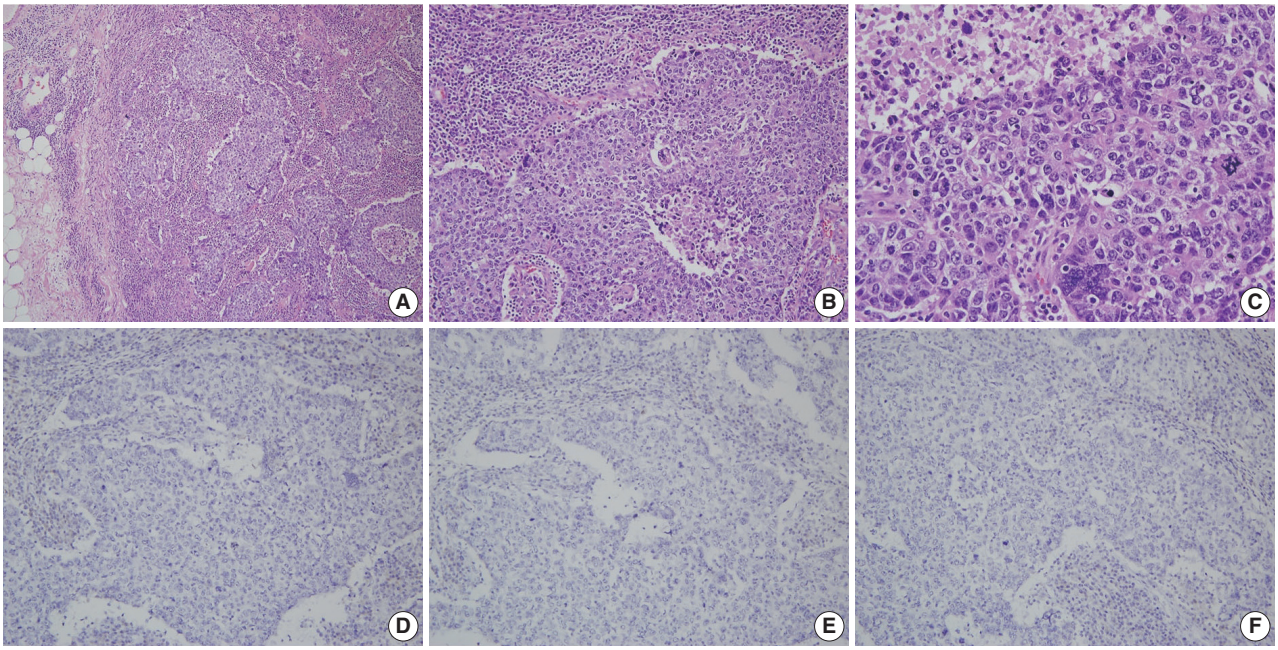

Fig. 1. A representative example of *BRCA1*-associated breast cancer diagnosed with invasive carcinoma with medullary features. (A) Low power view reveals a well-circumscribed tumor with a pushing margin and heavy lymphocytic infiltration. There are no desmoplastic stroma and no carcinoma in situ component. (B) The tumor shows a syncytial growth pattern with central necrosis. (C) Tumor cells show marked nuclear pleomorphism and frequent mitoses. Estrogen receptor (D), progesterone receptor (E), and human epidermal growth factor receptor-2 (F) are all negative on immunohistochemistry.

($p < .001$) in *BRCA2*-associated cancers were the only statistically significant features.

A consistent feature of *BRCA1*-associated tumors is high histologic grade. The incidence of grade III tumors has been reported to range from 66% to 84% in *BRCA1* mutation carriers and 30% to 40% in sporadic controls [81,84-86]. A detailed analysis of the BCLC report showed tumor specimens from *BRCA1*-associated breast cancer patients had less tubule formation, higher nuclear pleomorphism and higher mitotic activity compared with tumor specimens from age-matched sporadic controls [81]. *BRCA2*-associated tumors also tend to be of higher grade compared with sporadic tumors; however, this association is weaker than that for *BRCA1*-associated tumors. In the BCLC report, 66% of *BRCA1* tumors, 41% of *BRCA2* tumors, and 36% of sporadic tumors were grade III [81]. Most *BRCA2* tumors are grade II or III, and in comparison with sporadic tumors, show less tubule formation but similar cellular pleomorphism and mitotic counts (Fig. 2) [81]. However, in some series, nuclear pleomorphism and mitotic rates have been reported to be higher in *BRCA2* tumors than in sporadic tumors [87].

Hormonal receptors and human epidermal growth factor receptor-2 status

Expression status of estrogen receptor (ER), progesterone receptor (PR), and human epidermal growth factor receptor-2 (HER2) have critical clinical implications for breast cancer treatment and prognosis. *BRCA1*-associated breast cancers have strong associations with ER and PR expression [17,56,64,85,86,88-91]. The ER status has been reported to be negative in 71% to 90% of *BRCA1*-associated breast cancers in different series [17,56,85,88,89]. Lakhani et al. [88] reported that 90% of *BRCA1*-associated breast cancers showed negative ER expression compared with 35% of controls. Lang et al. [17] reported that the rate of ER negativity in tumors of *BRCA1* carriers, *BRCA2* carriers, and non-carriers among Chinese patients was 71.2%, 27.1%, and 42.8%, respectively. Younger age and higher tumor grade have been suggested to contribute to the lower rate of ER expression in *BRCA1*-associated breast cancers. However, even taking into account the earlier age of onset of *BRCA1*-associated breast cancers, ER-positive breast cancers are clearly underrepresented in this group. The likelihood of ER negativity was reported to be 4.8 times higher in high-grade *BRCA1*-associated tumors than in high-grade sporadic tumors [90]. PR expression has also been reported to be lower in *BRCA1*-associated tumors than sporadic tumors [17,56,85,88,89]. Lang et al. [17] reported the rate of PR negativity in tumors of *BRCA1* carriers, *BRCA2* carriers, and non-carriers as 71.2%, 31.8%, and 47.7%, respectively. In contrast to *BRCA1*-associated tumors, ER and

https://doi.org/10.4132/jptm.2020.04.07

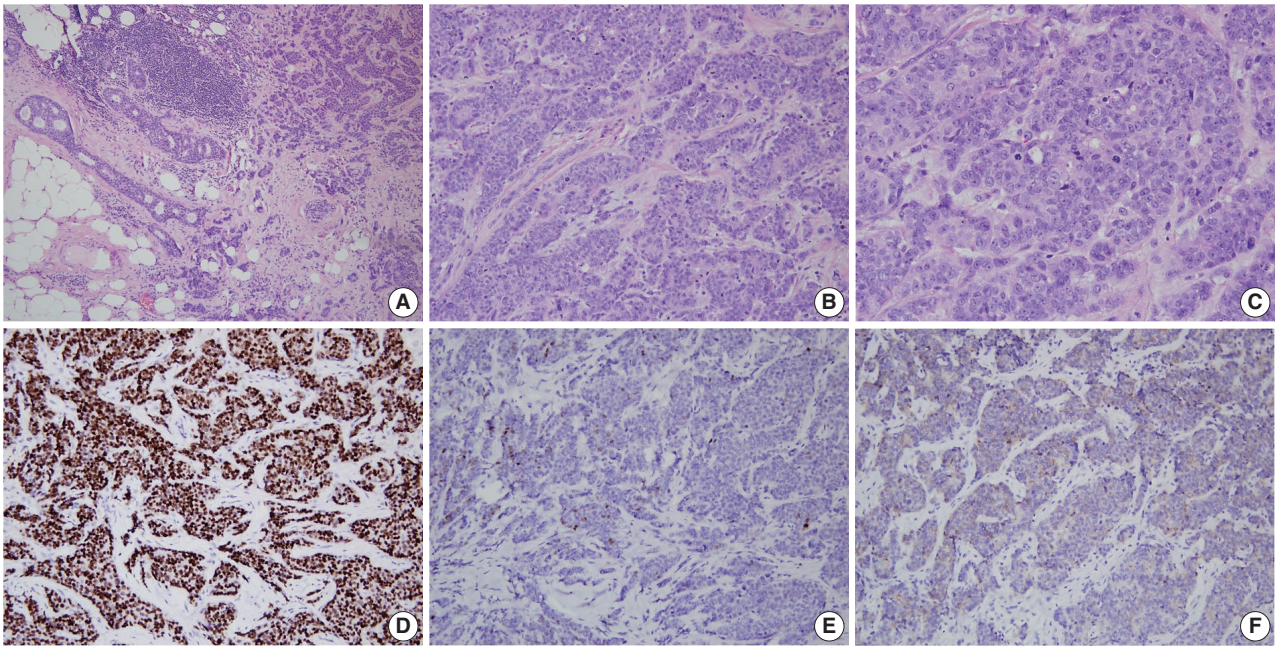

Fig. 2. A representative example of *BRCA2*-associated breast cancer diagnosed as high grade invasive ductal carcinoma (invasive carcinoma of no special type). (A) Low power view reveals an ill-defined tumor with an infiltrative margin. The tumor reveals desmoplastic stroma and ductal carcinoma in situ component on the left. (B, C) The tumor shows less tubule formation, moderate nuclear pleomorphism, and frequent mitoses. Estrogen receptor (D) is diffuse positive, progesterone receptor (E) is focal positive, and human epidermal growth factor receptor-2 (F) is 1+/3 on immunohistochemistry.

PR expression is similar between *BRCA2*-associated and sporadic breast cancers; the reported ER and PR expression levels in *BRCA2*-associated breast cancers are approximately 65%–72% and 40%–68%, respectively (Fig. 2) [17,56,64,88].

Data on HER2 expression in *BRCA*-associated tumors vary among series and is probably due to technical differences. However, most studies have reported that the frequency of HER2 overexpression in both *BRCA1*- and *BRCA2*-associated tumors ranges from 0% to 8% [17,55,88,89]. HER2 overexpression is classically associated with aneuploidy and high grade, which are two features encountered more frequently in *BRCA1*-associated tumors. Despite this association, a significantly lower incidence of HER2 overexpression has been observed among *BRCA1*-associated breast cancers [17,55,85,88,89,92-94]. The low incidence of *HER2/neu* amplification in *BRCA1*-associated carcinomas may be due to physical codeletion of one *HER2/neu* allele and nearby sequences during the loss of heterozygosity at the *BRCA1* locus as suggested in one study [94]. The reason behind the low incidence of *HER2/neu* amplification in *BRCA2*-associated tumors remains yet to be elucidated.

Triple-negative breast cancers (TNBCs), which lack expression of ER, PR, and HER2, comprise 15% to 20% of all sporadic breast cancers [9,95]. Most studies have shown a significantly higher frequency (57% to 75%) of the triple-negative phenotype among *BRCA1* mutation carriers (Fig. 1) [9,95-97]. The incidence of *BRCA1* mutations in TNBC patients has been reported to be 7.5% to 15.6% [9,97,98]. Sharma et al. [98] evaluated the prevalence of *BRCA1/2* mutations in 207 TNBC patients and reported that deleterious *BRCA1/2* mutations were present in 15.4% of patients with *BRCA1* in 11.1% and *BRCA2* in 4.3% of patients. However, the mutation prevalence differed according to patient age: it was 27.6%, 11.4%, and 4.9% in patients aged ≤50 years, 51–60 years, and ≥61 years, respectively [98]. A higher incidence of the triple-negative phenotype (50% to 100%) among Asian patients with *BRCA1* mutations has also been reported [17,29,30,46,47,58,76,99]. The reported incidence of *BRCA1* mutation among Asian patients with TNBC is 9.4% to 36.8% [29,47,76,99]. A recent Chinese cohort study reported the rate of triple-negative phenotype in *BRCA1* carriers, *BRCA2* carriers, and non-carriers was 61.6%, 23.9%, and 33.1%, respectively [17]. The rate of *BRCA1* mutation among patients with TNBC was 11.1% [17].

Key pathological characteristics of *BRCA1*- and *BRCA2*-associated breast cancers are summarized in Table 1.

Carcinoma in situ

The natural history of hereditary breast cancers from morphologically normal epithelium to invasive cancer is not well known.

Table 1. Key pathological characteristics of *BRCA1*- and *BRCA2*-associated breast cancers [9,55,63,80,82,84,87,88,94-96,103]

	BRCA1	*BRCA2*
Histology	Ductal, no special type (75%); medullary or atypical medullary (10%–20%); rare lobular	Ductal, no special type (75%); medullary or atypical medullary (<5%); lobular or ductal with lobular features more common than in BRCA1 (~10%)
Mitosis	High	Low
Prominent lymphocytic infiltration	Often	Rare
Histologic grade	High (grade III, 71%–75%)	Intermediate to high (grade II, 43%–45%; grade III, 45%–50%)
ER	Negative (73%–90%)	Positive (65%–77%)
PR	Negative (79%–81%)	Positive (40%–64%)
HER2	Negative (86%–95%)	Negative (72%–95%)
Triple-negative phenotype	Common (57%–75%)	Rare
Associated in situ carcinoma	Rare	Common
Others	p53 positive (50%–53%); CK5 positive (50%); bcl-2, low; CDKN2A, low; cyclin D1 negative (90%)	p53 positive (40%–52%); CK5 negative (90%); bcl-2, high; CDKN2A, high; cyclin D1 positive (60%)

ER, estrogen receptor; PR, progesterone receptor; HER2, human epidermal growth factor receptor-2; CK, cytokeratin; bcl-2, B-cell leukemia/lymphoma-2; CDKN2A, Cyclin dependent kinase inhibitor 2A.

It is difficult to assess and compare the incidence of in situ carcinoma between studies, and the incidence of in situ lesions in the absence of a concomitant invasive component has not been established in familial breast cancers.

Ductal carcinoma in situ (DCIS) around the invasive lesion is reported to be less common in *BRCA1* mutation carriers than in controls [78,81,84]. However, the results for lobular carcinoma in situ (LCIS) are uncertain [78]. In the BCLC study, *BRCA1* mutation carriers showed less DCIS around the invasive cancer compared to controls (41% vs. 56%, p = .001) [81]. LCIS was less common in familial cancers (p = .013) with no significant difference between *BRCA1* and *BRCA2* mutation carriers [81]. *BRCA1* and *BRCA2* mutations were found in three (0.8%) and nine (2.4%) of 369 DCIS cases, respectively [100].

Prophylactic mastectomy specimens have been used to investigate the different stages of breast cancer development in *BRCA1/2* mutation carriers [84]. Hoogerbrugge et al. [101] assessed prophylactic mastectomy specimens of 67 women who had an extremely high genetic risk of breast cancer (66% of patients were *BRCA1* or *BRCA2* mutation carriers) and reported that one or more types of high-risk histopathological lesions, such as DCIS, LCIS, atypical ductal hyperplasia (ADH), and atypical lobular hyperplasia (ALH), were present in 57% of the women [101]. Kauff et al. [102] also reported that lesions with risks of developing subsequent malignancy (DCIS, LCIS, ADH, and ALH) are more common in prophylactic mastectomy specimens from women with *BRCA* mutations than in autopsy specimens from unaffected women of unknown genetic predisposition.

Adem et al. [103] evaluated therapeutic mastectomy and prophylactic mastectomy specimens from high-risk women with or without *BRCA1/2* mutations. They observed that proliferative fibrocystic changes were less prevalent in *BRCA1/2* mutation carriers (7%) than controls (25%) and non-carriers with a family history of breast cancer (22%–33%). However, the prevalence of DCIS was not different among the groups (50%–60%), and invasive carcinomas were of higher grade in the *BRCA1/2* mutation carriers compared with controls and non-carriers. Based on these findings, they suggested that breast cancer progression is accelerated in *BRCA1/2*-mutation carriers.

Pathologic data from the Consortium of Investigators of Modifiers of *BRCA1/2*

The comprehensive pathology data of 4,325 *BRCA1* and 2,568 *BRCA2* mutation carriers were reported in 2012 from the Consortium of Investigators of Modifiers of *BRCA1/2* (CIMBA), the most extensive collaborative study of *BRCA1* and *BRCA2* mutation carriers [96]. In both *BRCA1* and *BRCA2* carriers diagnosed with breast cancer, invasive ductal carcinoma of no special type was the predominant histologic subtype. Medullary and atypical medullary carcinomas were more likely to be *BRCA1*-related ($p = 2.3 \times 10^{-15}$), while lobular carcinomas were *BRCA2*-related ($p = 4.4 \times 10^{-14}$). As for receptor status, 78%, 79%, 90%, and 69% of tumors diagnosed in *BRCA1* carriers were ER-negative, PR-negative, HER2-negative, and triple-negative, respectively, whereas 23%, 36%, 87%, and 16% of tumors from *BRCA2* carriers were ER-negative, PR-negative, HER2-negative, and triple-negative. The proportion of ER-negative breast cancers decreased with age among *BRCA1* carriers ($p = 1.2 \times 10^{-5}$) but increased with age among *BRCA2* carriers ($p = 6.8 \times 10^{-6}$). As for the proportion of TNBCs, it decreased with age in *BRCA1* carriers but increased with age in *BRCA2* carriers. In *BRCA1* and *BRCA2* carriers alike, ER-negative tu-

 https://doi.org/10.4132/jptm.2020.04.07

mors had higher histologic grade than ER-positive tumors.

REPORTS ASSESSING THE CHARACTERISTICS OF *BRCA*-ASSOCIATED BREAST CANCER IN ASIAN PATIENTS

To date, few studies have assessed characteristics of *BRCA1/2*-associated breast cancer in Asian patients. In 2009, Kwong et al. [29] reported the clinicopathological characteristics of Chinese patients with *BRCA*-associated breast cancer. Among 226 high-risk Hong Kong Chinese women, 28 women (12.4%) carried *BRCA* mutations (*BRCA1* mutation, 11 patients; *BRCA2* mutations, 17 patients), and 55.6% of these carriers were diagnosed with breast cancer before age 40 compared with 36.0% of non-carriers (p = .05). *BRCA* mutation carriers were more likely to have a family history of breast and ovarian cancers, high-grade cancers, and TNBCs. The prevalence of TNBC was significantly higher in *BRCA1* carriers (67.7%) than in *BRCA2* carriers (35.3%) and non-carriers (25.6%). ER-negative cancer was significantly associated with *BRCA1* mutations, especially in patients under 40 years of age.

In 2014, Yu et al. [58] compared the characteristics of breast cancers from 181 *BRCA1/2* mutation carriers cases (80 patients with *BRCA1* mutation and 101 patients with *BRCA2* mutation) and 55,387 sporadic breast cancers from the Korean Breast Cancer Registry. In this report, median patient age was significantly lower in the *BRCA1* and *BRCA2* mutation groups than in the registry group (37 years and 41 years vs. 48 years; p < .001 for both). Tumor size was not different between the *BRCA1* and *BRCA2* groups and the registry group. The proportion of patients with axillary node metastasis was not significantly different between the *BRCA1* and registry groups; however, axillary nodal involvement was present more often in the *BRCA2* group than in the registry group (45.5% vs. 33.5%, p = .002). Tumor size and axillary nodal involvement did not have significant correlations in the *BRCA1* and *BRCA2* groups. Tumors of the *BRCA1* group were of higher grade compared with those of the registry group (64.3% vs. 27.5%, p < .001). The *BRCA1* group had a higher proportion of hormone receptor-negative tumors and lower proportion of HER2-overexpressing tumors compared to the registry group. TNBCs were more prevalent in the *BRCA1* group than in the registry group (61.3% vs. 12.4%, p < .001). In contrast, hormone receptor expression was not significantly different between the *BRCA2* group and registry group. The frequency of DCIS was lower in the *BRCA1* (3.7%) and *BRCA2* (5%) groups than in the registry group (10.3%).

Recently, Lang et al. [17] reported the prevalence of *BRCA* mutation and features of *BRCA*-associated breast cancer in Chinese patients by using next-generation sequencing on 2,991 breast cancer patients and 1,043 healthy individuals as controls. *BRCA* mutations were present in 9.1% (232/2,560) of patients with at least one risk factor for hereditary breast cancer compared to 3.5% (15/431) in sporadic patients and 0.38% (4/1,043) in healthy controls. Family history of breast/ovarian cancer, young age, negative HER2, high Ki-67 index, and high tumor grade were associated with *BRCA* mutations. *BRCA1* carriers were more likely to be ER- or PR-negative than *BRCA1* non-carriers, whereas *BRCA2*-mutated breast cancers were more likely to be ER- or PR-positive. *BRCA1*-mutated patients also presented a higher stage at the time of diagnosis, and *BRCA2* mutation carriers showed more positive lymph nodes. There were no differences in disease-free survival among *BRCA1* carriers, *BRCA2* carriers, and non-carriers. However, among the non-TNBC patients, *BRCA2* mutation carriers showed decreased disease-free survival compared to *BRCA2* mutation non-carriers (hazard ratio, 1.892; 95% confidence interval, 1.132 to 3.161; p = .013).

In 2011, the Asian *BRCA* (ABRCA) Consortium was established to share knowledge and conduct collaborative researches on hereditary breast and ovarian cancer (HBOC) in Asia. To date, the ABRCA Consortium has members from 14 Asian countries (Korea, Japan, Malaysia, Singapore, Hong Kong, China, Indonesia, Thailand, the Philippines, India, Bangladesh, Pakistan, Taiwan, and Vietnam). The ABRCA Consortium has held regular meetings annually since 2011 and is open to new members who wish to participate in collaborative researches in Asia. The ABRCA working groups are conducting studies to assess the *BRCA* mutation spectrum and founder mutations in Asia as well as the status of genetic counseling and genetic testing for HBOC in Asian countries. Lifestyle modifiers of breast cancer and estimated penetrance of *BRCA* mutations in Asians may become clearer with the groups' efforts. A more comprehensive understanding of the clinicopathological characteristics of *BRCA1/2*-associated breast cancer in Asian populations is expected through this international collaboration.

CONCLUSION

BRCA1/2 germline mutations account for the majority of HBOCs. Ever since the *BRCA* genes were recognized, many have attempted to define the clinicopathological characteristics of *BRCA*-associated breast cancer in relation to sporadic breast cancer. *BRCA1/2*-associated breast cancers have certain distinc-

tive clinical features such as younger age at onset, higher prevalence of bilateral breast cancer, male family members with breast cancer, and association with other cancers in the ovary, colon, prostate, pancreas, and endometrium. *BRCA1/2*-associated breast cancers seem to have a similar prognosis as sporadic breast cancers. *BRCA1*-associated cancers have characteristic histopathologic features compared with sporadic cases: they are usually high grade, poorly differentiated, and infiltrating ductal carcinomas with a triple-negative phenotype. Medullary carcinomas are also more frequent in *BRCA1* mutation carriers. *BRCA2*-associated breast cancers seem to share similar pathologic characteristics with non-carriers with the exception of an increased frequency of high-grade tumors. Evidence to date suggests that the clinicopathological characteristics of BRCA-associated breast cancer are not different between Asian and Caucasian patients.

Ethics Statement

Not applicable.

ORCID

Eun-Kyu Kim https://orcid.org/0000-0003-1318-0939
So Yeon Park https://orcid.org/0000-0002-0299-7268
Sung-Won Kim https://orcid.org/0000-0001-5687-1380

Author Contributions

Project administration: SWK. Supervision: SWK. Writing—original draft: EKK. Writing—review & editing: SWK, SYP.

Conflicts of Interest

S.Y.P. is the Editor-in-Chief of the *Journal of Pathology and Translational Medicine* and was not involved in the editorial evaluation or decision to publish this article. All remaining authors declare that they have no potential conflicts of interest.

Funding Statement

The present research has been supported by Korea Breast Cancer Foundation (KBCF-2017R008).

References

1. Torre LA, Bray F, Siegel RL, Ferlay J, Lortet-Tieulent J, Jemal A. Global cancer statistics, 2012. CA Cancer J Clin 2015; 65: 87-108.
2. Ripperger T, Gadzicki D, Meindl A, Schlegelberger B. Breast cancer susceptibility: current knowledge and implications for genetic counselling. Eur J Hum Genet 2009; 17: 722-31.
3. Fackenthal JD, Olopade OI. Breast cancer risk associated with *BRCA1* and *BRCA2* in diverse populations. Nat Rev Cancer 2007; 7: 937-48.
4. Ford D, Easton DF, Stratton M, et al. Genetic heterogeneity and penetrance analysis of the *BRCA1* and *BRCA2* genes in breast cancer families. The Breast Cancer Linkage Consortium. Am J Hum Genet 1998; 62: 676-89.
5. Antoniou A, Pharoah PD, Narod S, et al. Average risks of breast and ovarian cancer associated with *BRCA1* or *BRCA2* mutations detected in case Series unselected for family history: a combined analysis of 22 studies. Am J Hum Genet 2003; 72: 1117-30.
6. Chen S, Parmigiani G. Meta-analysis of *BRCA1* and *BRCA2* penetrance. J Clin Oncol 2007; 25: 1329-33.
7. Ferla R, Calo V, Cascio S, et al. Founder mutations in *BRCA1* and *BRCA2* genes. Ann Oncol 2007; 18 Suppl 6: vi93-8.
8. Daly MB, Axilbund JE, Buys S, et al. Genetic/familial high-risk assessment: breast and ovarian. J Natl Compr Canc Netw 2010; 8: 562-94.
9. Gonzalez-Angulo AM, Timms KM, Liu S, et al. Incidence and outcome of *BRCA* mutations in unselected patients with triple receptor-negative breast cancer. Clin Cancer Res 2011; 17: 1082-9.
10. Jemal A, Bray F, Center MM, Ferlay J, Ward E, Forman D. Global cancer statistics. CA Cancer J Clin 2011; 61: 69-90.
11. Shin HR, Carlos MC, Varghese C. Cancer control in the Asia Pacific region: current status and concerns. Jpn J Clin Oncol 2012; 42: 867-81.
12. Ko BS, Noh WC, Kang SS, et al. Changing patterns in the clinical characteristics of Korean breast cancer from 1996-2010 using an online nationwide breast cancer database. J Breast Cancer 2012; 15: 393-400.
13. Kim H, Choi DH. Distribution of *BRCA1* and *BRCA2* mutations in Asian patients with breast cancer. J Breast Cancer 2013; 16: 357-65.
14. Yang L, Parkin DM, Ferlay J, Li L, Chen Y. Estimates of cancer incidence in China for 2000 and projections for 2005. Cancer Epidemiol Biomarkers Prev 2005; 14: 243-50.
15. Kurian AW, Fish K, Shema SJ, Clarke CA. Lifetime risks of specific breast cancer subtypes among women in four racial/ethnic groups. Breast Cancer Res 2010; 12: R99.
16. Anglian Breast Cancer Study Group. Prevalence and penetrance of *BRCA1* and *BRCA2* mutations in a population-based series of breast cancer cases. Anglian Breast Cancer Study Group. Br J Cancer 2000; 83: 1301-8.
17. Lang GT, Shi JX, Hu X, et al. The spectrum of *BRCA* mutations and characteristics of *BRCA*-associated breast cancers in China: screening of 2,991 patients and 1,043 controls by next-generation sequencing. Int J Cancer 2017; 141: 129-42.
18. Ford D, Easton DF, Bishop DT, Narod SA, Goldgar DE. Risks of cancer in *BRCA1*-mutation carriers. Breast Cancer Linkage Consortium. Lancet 1994; 343: 692-5.
19. Easton DF, Ford D, Bishop DT. Breast and ovarian cancer incidence in *BRCA1*-mutation carriers. Breast Cancer Linkage Consortium. Am J Hum Genet 1995; 56: 265-71.
20. Struewing JP, Hartge P, Wacholder S, et al. The risk of cancer associated with specific mutations of *BRCA1* and *BRCA2* among Ashkenazi Jews. N Engl J Med 1997; 336: 1401-8.
21. Han SA, Park SK, Ahn SH, et al. The breast and ovarian cancer risks in Korea due to inherited mutations in *BRCA1* and *BRCA2*: a preliminary report. J Breast Cancer 2009; 12: 92-9.
22. Ikeda N, Miyoshi Y, Ikeda N, Yoneda K, Kinoshita M, Noguchi S. Frequency of *BRCA1* and *BRCA2* germline mutations detected by protein truncation test and cumulative risks of breast and ovarian cancer among mutation carriers in Japanese breast cancer families. J Korean Breast Cancer Soc 2002; 5: 194-201.
23. Robson M, Im SA, Senkus E, et al. Olaparib for metastatic breast cancer in patients with a germline *BRCA* mutation. N Engl J Med 2017; 377: 523-33.

24. Litton JK, Rugo HS, Ettl J, et al. Talazoparib in patients with advanced breast cancer and a germline *BRCA* mutation. N Engl J Med 2018; 379: 753-63.
25. Han SA, Kim SW, Kang E, et al. The prevalence of *BRCA* mutations among familial breast cancer patients in Korea: results of the Korean Hereditary Breast Cancer study. Fam Cancer 2013; 12: 75-81.
26. Sugano K, Nakamura S, Ando J, et al. Cross-sectional analysis of germline *BRCA1* and *BRCA2* mutations in Japanese patients suspected to have hereditary breast/ovarian cancer. Cancer Sci 2008; 99: 1967-76.
27. Kwong A, Ng EK, Wong CL, et al. Identification of *BRCA1/2* founder mutations in Southern Chinese breast cancer patients using gene sequencing and high resolution DNA melting analysis. PLoS One 2012; 7: e43994.
28. Valarmathi MT, Sawhney M, Deo SS, Shukla NK, Das SN. Novel germline mutations in the *BRCA1* and *BRCA2* genes in Indian breast and breast-ovarian cancer families. Hum Mutat 2004; 23: 205.
29. Kwong A, Wong LP, Wong HN, et al. Clinical and pathological characteristics of Chinese patients with *BRCA* related breast cancer. Hugo J 2009; 3: 63-76.
30. Yip CH, Taib NA, Choo WY, Rampal S, Thong MK, Teo SH. Clinical and pathologic differences between *BRCA1*-, *BRCA2*-, and non-*BRCA*-associated breast cancers in a multiracial developing country. World J Surg 2009; 33: 2077-81.
31. Wooster R, Neuhausen SL, Mangion J, et al. Localization of a breast cancer susceptibility gene, *BRCA2*, to chromosome 13q12-13. Science 1994; 265: 2088-90.
32. Breast Cancer Linkage Consortium. Cancer risks in *BRCA2* mutation carriers. J Natl Cancer Inst 1999; 91: 1310-6.
33. Thompson D, Easton DF; Breast Cancer Linkage Consortium. Cancer incidence in *BRCA1* mutation carriers. J Natl Cancer Inst 2002; 94: 1358-65.
34. FitzGerald MG, MacDonald DJ, Krainer M, et al. Germ-line *BRCA1* mutations in Jewish and non-Jewish women with early-onset breast cancer. N Engl J Med 1996; 334: 143-9.
35. Shattuck-Eidens D, Oliphant A, McClure M, et al. *BRCA1* sequence analysis in women at high risk for susceptibility mutations: risk factor analysis and implications for genetic testing. JAMA 1997; 278: 1242-50.
36. Malone KE, Daling JR, Thompson JD, O'Brien CA, Francisco LV, Ostrander EA. *BRCA1* mutations and breast cancer in the general population: analyses in women before age 35 years and in women before age 45 years with first-degree family history. JAMA 1998; 279: 922-9.
37. Hodgson SV, Heap E, Cameron J, et al. Risk factors for detecting germline *BRCA1* and *BRCA2* founder mutations in Ashkenazi Jewish women with breast or ovarian cancer. J Med Genet 1999; 36: 369-73.
38. Warner E, Foulkes W, Goodwin P, et al. Prevalence and penetrance of *BRCA1* and *BRCA2* gene mutations in unselected Ashkenazi Jewish women with breast cancer. J Natl Cancer Inst 1999; 91: 1241-7.
39. Langston AA, Malone KE, Thompson JD, Daling JR, Ostrander EA. *BRCA1* mutations in a population-based sample of young women with breast cancer. N Engl J Med 1996; 334: 137-42.
40. Peto J, Collins N, Barfoot R, et al. Prevalence of *BRCA1* and *BRCA2* gene mutations in patients with early-onset breast cancer. J Natl Cancer Inst 1999; 91: 943-9.
41. Ligtenberg MJ, Hogervorst FB, Willems HW, et al. Characteristics of small breast and/or ovarian cancer families with germline mutations in *BRCA1* and *BRCA2*. Br J Cancer 1999; 79: 1475-8.
42. Krainer M, Silva-Arrieta S, FitzGerald MG, et al. Differential contributions of *BRCA1* and *BRCA2* to early-onset breast cancer. N Engl J Med 1997; 336: 1416-21.
43. Hartge P, Struewing JP, Wacholder S, Brody LC, Tucker MA. The prevalence of common *BRCA1* and *BRCA2* mutations among Ashkenazi Jews. Am J Hum Genet 1999; 64: 963-70.
44. Hopper JL, Jenkins MA. Modeling the probability that Ashkenazi Jewish women carry a founder mutation in *BRCA1* or *BRCA2*. Am J Hum Genet 1999; 65: 1771-6.
45. Foulkes WD, Brunet JS, Warner E, et al. The importance of a family history of breast cancer in predicting the presence of a *BRCA* mutation. Am J Hum Genet 1999; 65: 1776-9.
46. Li WF, Hu Z, Rao NY, et al. The prevalence of *BRCA1* and *BRCA2* germline mutations in high-risk breast cancer patients of Chinese Han nationality: two recurrent mutations were identified. Breast Cancer Res Treat 2008; 110: 99-109.
47. Zhang J, Pei R, Pang Z, et al. Prevalence and characterization of *BRCA1* and *BRCA2* germline mutations in Chinese women with familial breast cancer. Breast Cancer Res Treat 2012; 132: 421-8.
48. De Leon Matsuda ML, Liede A, Kwan E, et al. *BRCA1* and *BRCA2* mutations among breast cancer patients from the Philippines. Int J Cancer 2002; 98: 596-603.
49. Marcus JN, Watson P, Page DL, et al. Hereditary breast cancer: pathobiology, prognosis, and *BRCA1* and *BRCA2* gene linkage. Cancer 1996; 77: 697-709.
50. Johannsson OT, Ranstam J, Borg A, Olsson H. Survival of *BRCA1* breast and ovarian cancer patients: a population-based study from southern Sweden. J Clin Oncol 1998; 16: 397-404.
51. Robson M, Gilewski T, Haas B, et al. *BRCA*-associated breast cancer in young women. J Clin Oncol 1998; 16: 1642-9.
52. Noguchi S, Kasugai T, Miki Y, Fukutomi T, Emi M, Nomizu T. Clinicopathologic analysis of BRCA1- or BRCA2-associated hereditary breast carcinoma in Japanese women. Cancer 1999; 85: 2200-5.
53. Couch FJ, DeShano ML, Blackwood MA, et al. *BRCA1* mutations in women attending clinics that evaluate the risk of breast cancer. N Engl J Med 1997; 336: 1409-15.
54. Verhoog LC, Brekelmans CT, Seynaeve C, et al. Survival and tumour characteristics of breast-cancer patients with germline mutations of *BRCA1*. Lancet 1998; 351: 316-21.
55. Johannsson OT, Idvall I, Anderson C, et al. Tumour biological features of *BRCA1*-induced breast and ovarian cancer. Eur J Cancer 1997; 33: 362-71.
56. Armes JE, Egan AJ, Southey MC, et al. The histologic phenotypes of breast carcinoma occurring before age 40 years in women with and without *BRCA1* or *BRCA2* germline mutations: a population-based study. Cancer 1998; 83: 2335-45.
57. Garcia-Patiño E, Gomendio B, Provencio M, et al. Germ-line *BRCA1* mutations in women with sporadic breast cancer: clinical correlations. J Clin Oncol 1998; 16: 115-20.
58. Yu JH, Lee JW, Son BH, et al. Characteristics of *BRCA1/2* mutation-positive breast cancers in Korea: a comparison study based on multicenter data and the Korean Breast Cancer Registry. J Breast

Cancer 2014; 17: 129-35.
59. Foulkes WD, Wong N, Brunet JS, et al. Germ-line *BRCA1* mutation is an adverse prognostic factor in Ashkenazi Jewish women with breast cancer. Clin Cancer Res 1997; 3(12 Pt 1): 2465-9.
60. Verhoog LC, Brekelmans CT, Seynaeve C, et al. Survival in hereditary breast cancer associated with germline mutations of *BRCA2*. J Clin Oncol 1999; 17: 3396-402.
61. Wagner TM, Moslinger RA, Muhr D, et al. *BRCA1*-related breast cancer in Austrian breast and ovarian cancer families: specific *BRCA1* mutations and pathological characteristics. Int J Cancer 1998; 77: 354-60.
62. Eisinger F, Noguès C, Birnbaum D, Jacquemier J, Sobol H. Low frequency of lymph-node metastasis in *BRCA1*-associated breast cancer. Lancet 1998; 351: 1633-4.
63. Stoppa-Lyonnet D, Ansquer Y, Dreyfus H, et al. Familial invasive breast cancers: worse outcome related to *BRCA1* mutations. J Clin Oncol 2000; 18: 4053-9.
64. Robson ME, Chappuis PO, Satagopan J, et al. A combined analysis of outcome following breast cancer: differences in survival based on *BRCA1/BRCA2* mutation status and administration of adjuvant treatment. Breast Cancer Res 2004; 6: R8-17.
65. Ansquer Y, Gautier C, Fourquet A, Asselain B, Stoppa-Lyonnet D. Survival in early-onset *BRCA1* breast-cancer patients. Institut Curie Breast Cancer Group. Lancet 1998; 352: 541.
66. Moran MS, Yang Q, Harris LN, Jones B, Tuck DP, Haffty BG. Long-term outcomes and clinicopathologic differences of African-American versus white patients treated with breast conservation therapy for early-stage breast cancer. Cancer 2008; 113: 2565-74.
67. Foulkes WD, Chappuis PO, Wong N, et al. Primary node negative breast cancer in BRCA1 mutation carriers has a poor outcome. Ann Oncol 2000; 11: 307-13.
68. Nilsson MP, Hartman L, Idvall I, Kristoffersson U, Johannsson OT, Loman N. Long-term prognosis of early-onset breast cancer in a population-based cohort with a known *BRCA1/2* mutation status. Breast Cancer Res Treat 2014; 144: 133-42.
69. Nicoletto MO, Donach M, De Nicolo A, Artioli G, Banna G, Monfardini S. *BRCA-1* and *BRCA-2* mutations as prognostic factors in clinical practice and genetic counselling. Cancer Treat Rev 2001; 27: 295-304.
70. El-Tamer M, Russo D, Troxel A, et al. Survival and recurrence after breast cancer in *BRCA1/2* mutation carriers. Ann Surg Oncol 2004; 11: 157-64.
71. Albano WA, Recabaren JA, Lynch HT, et al. Natural history of hereditary cancer of the breast and colon. Cancer 1982; 50: 360-3.
72. Porter DE, Cohen BB, Wallace MR, et al. Breast cancer incidence, penetrance and survival in probable carriers of *BRCA1* gene mutation in families linked to *BRCA1* on chromosome 17q12-21. Br J Surg 1994; 81: 1512-5.
73. Rennert G, Bisland-Naggan S, Barnett-Griness O, et al. Clinical outcomes of breast cancer in carriers of *BRCA1* and *BRCA2* mutations. N Engl J Med 2007; 357: 115-23.
74. Bordeleau L, Panchal S, Goodwin P. Prognosis of *BRCA*-associated breast cancer: a summary of evidence. Breast Cancer Res Treat 2010; 119: 13-24.
75. Lee EH, Park SK, Park B, et al. Effect of *BRCA1/2* mutation on short-term and long-term breast cancer survival: a systematic review and meta-analysis. Breast Cancer Res Treat 2010; 122: 11-25.
76. Xu J, Wang B, Zhang Y, Li R, Wang Y, Zhang S. Clinical implications for *BRCA* gene mutation in breast cancer. Mol Biol Rep 2012; 39: 3097-102.
77. Lucassen A, Watson E, Eccles D. Evidence based case report: advice about mammography for a young woman with a family history of breast cancer. BMJ 2001; 322: 1040-2.
78. Chappuis PO, Nethercot V, Foulkes WD. Clinico-pathological characteristics of BRCA1- and BRCA2-related breast cancer. Semin Surg Oncol 2000; 18: 287-95.
79. Seynaeve C, Verhoog LC, van de Bosch LM, et al. Ipsilateral breast tumour recurrence in hereditary breast cancer following breast-conserving therapy. Eur J Cancer 2004; 40: 1150-8.
80. Haffty BG, Harrold E, Khan AJ, et al. Outcome of conservatively managed early-onset breast cancer by *BRCA1/2* status. Lancet 2002; 359: 1471-7.
81. Pathology of familial breast cancer: differences between breast cancers in carriers of *BRCA1* or *BRCA2* mutations and sporadic cases. Breast Cancer Linkage Consortium. Lancet 1997; 349: 1505-10.
82. Eisinger F, Jacquemier J, Charpin C, et al. Mutations at *BRCA1*: the medullary breast carcinoma revisited. Cancer Res 1998; 58: 1588-92.
83. Lakhani SR, Jacquemier J, Sloane JP, et al. Multifactorial analysis of differences between sporadic breast cancers and cancers involving *BRCA1* and *BRCA2* mutations. J Natl Cancer Inst 1998; 90: 1138-45.
84. Honrado E, Benítez J, Palacios J. The molecular pathology of hereditary breast cancer: genetic testing and therapeutic implications. Mod Pathol 2005; 18: 1305-20.
85. Lynch BJ, Holden JA, Buys SS, Neuhausen SL, Gaffney DK. Pathobiologic characteristics of hereditary breast cancer. Hum Pathol 1998; 29: 1140-4.
86. Eerola H, Heikkilä P, Tamminen A, Aittomäki K, Blomqvist C, Nevanlinna H. Histopathological features of breast tumours in *BRCA1*, *BRCA2* and mutation-negative breast cancer families. Breast Cancer Res 2005; 7: R93-100.
87. Agnarsson BA, Jonasson JG, Björnsdottir IB, Barkardottir RB, Egilsson V, Sigurdsson H. Inherited *BRCA2* mutation associated with high grade breast cancer. Breast Cancer Res Treat 1998; 47: 121-7.
88. Lakhani SR, Van De Vijver MJ, Jacquemier J, et al. The pathology of familial breast cancer: predictive value of immunohistochemical markers estrogen receptor, progesterone receptor, HER-2, and p53 in patients with mutations in *BRCA1* and *BRCA2*. J Clin Oncol 2002; 20: 2310-8.
89. Palacios J, Honrado E, Osorio A, et al. Immunohistochemical characteristics defined by tissue microarray of hereditary breast cancer not attributable to *BRCA1* or *BRCA2* mutations: differences from breast carcinomas arising in *BRCA1* and *BRCA2* mutation carriers. Clin Cancer Res 2003; 9(10 Pt 1): 3606-14.
90. Foulkes WD, Metcalfe K, Sun P, et al. Estrogen receptor status in *BRCA1*- and *BRCA2*-related breast cancer: the influence of age, grade, and histological type. Clin Cancer Res 2004; 10: 2029-34.
91. Osin PP, Lakhani SR. The pathology of familial breast cancer: immunohistochemistry and molecular analysis. Breast Cancer Res 1999; 1: 36-40.
92. Eisinger F, Jacquemier J, Charafe-Jauffret E, Rio MC, Birnbaum D, Sobol H. More about: multifactorial analysis of differences between sporadic breast cancers and cancers involving *BRCA1* and *BRCA2* mutations. J Natl Cancer Inst 1999; 91: 1421-2.

 https://doi.org/10.4132/jptm.2020.04.07

93. Armes JE, Trute L, White D, et al. Distinct molecular pathogeneses of early-onset breast cancers in *BRCA1* and *BRCA2* mutation carriers: a population-based study. Cancer Res 1999; 59: 2011-7.
94. Grushko TA, Blackwood MA, Schumm PL, et al. Molecular-cytogenetic analysis of *HER-2/neu* gene in BRCA1-associated breast cancers. Cancer Res 2002; 62: 1481-8.
95. Foulkes WD, Smith IE, Reis-Filho JS. Triple-negative breast cancer. N Engl J Med 2010; 363: 1938-48.
96. Mavaddat N, Barrowdale D, Andrulis IL, et al. Pathology of breast and ovarian cancers among *BRCA1* and *BRCA2* mutation carriers: results from the Consortium of Investigators of Modifiers of BRCA1/2 (CIMBA). Cancer Epidemiol Biomarkers Prev 2012; 21: 134-47.
97. Atchley DP, Albarracin CT, Lopez A, et al. Clinical and pathologic characteristics of patients with *BRCA*-positive and *BRCA*-negative breast cancer. J Clin Oncol 2008; 26: 4282-8.
98. Sharma P, Klemp JR, Kimler BF, et al. Germline BRCA mutation evaluation in a prospective triple-negative breast cancer registry: implications for hereditary breast and/or ovarian cancer syndrome testing. Breast Cancer Res Treat 2014; 145: 707-14.
99. Noh JM, Han BK, Choi DH, et al. Association between *BRCA* mutation status, pathological findings, and magnetic resonance imaging features in patients with breast cancer at risk for the mutation. J Breast Cancer 2013; 16: 308-14.
100. Claus EB, Petruzella S, Matloff E, Carter D. Prevalence of *BRCA1* and *BRCA2* mutations in women diagnosed with ductal carcinoma in situ. JAMA 2005; 293: 964-9.
101. Hoogerbrugge N, Bult P, de Widt-Levert LM, et al. High prevalence of premalignant lesions in prophylactically removed breasts from women at hereditary risk for breast cancer. J Clin Oncol 2003; 21: 41-5.
102. Kauff ND, Brogi E, Scheuer L, et al. Epithelial lesions in prophylactic mastectomy specimens from women with *BRCA* mutations. Cancer 2003; 97: 1601-8.
103. Adem C, Reynolds C, Soderberg CL, et al. Pathologic characteristics of breast parenchyma in patients with hereditary breast carcinoma, including *BRCA1* and *BRCA2* mutation carriers. Cancer 2003; 97: 1-11.

JPTM
Journal of Pathology and Translational Medicine 2020; 54: 276-289
https://doi.org/10.4132/jptm.2020.04.15

REVIEW

Evolving pathologic concepts of serrated lesions of the colorectum

Jung Ho Kim[1,2], Gyeong Hoon Kang[1,2]

[1]Department of Pathology, Seoul National University Hospital, Seoul National University College of Medicine, Seoul;
[2]Laboratory of Epigenetics, Cancer Research Institute, Seoul National University College of Medicine, Seoul, Korea

Here, we provide an up-to-date review of the histopathology and molecular pathology of serrated colorectal lesions. First, we introduce the updated contents of the 2019 World Health Organization classification for serrated lesions. The sessile serrated lesion (SSL) is a new diagnostic terminology that replaces sessile serrated adenoma and sessile serrated polyp. The diagnostic criteria for SSL were revised to require only one unequivocal distorted serrated crypt, which is sufficient for diagnosis. Unclassified serrated adenomas have been included as a new category of serrated lesions. Second, we review ongoing issues concerning the morphology of serrated lesions. Minor morphologic variants with distinct molecular features were recently defined, including serrated tubulovillous adenoma, mucin-rich variant of traditional serrated adenoma (TSA), and superficially serrated adenoma. In addition to intestinal dysplasia and serrated dysplasia, minimal deviation dysplasia and not otherwise specified dysplasia were newly suggested as dysplasia subtypes of SSLs. Third, we summarize the molecular features of serrated lesions. The critical determinant of CpG island methylation development in SSLs is patient age. Interestingly, there may be ethnic differences in *BRAF*/*KRAS* mutation frequencies in SSLs. The molecular pathogenesis of TSAs is divided into *KRAS* and *BRAF* mutation pathways. SSLs with *MLH1* methylation can progress into favorable prognostic microsatellite instability-positive (MSI+)/CpG island methylator phenotype-positive (CIMP+) carcinomas, whereas *MLH1*-unmethylated SSLs and *BRAF*-mutated TSAs can be precursors of poor-prognostic MSI–/CIMP+ carcinomas. Finally, based on our recent data, we propose an algorithm for stratifying risk subgroups of non-dysplastic SSLs.

Key Words: Adenoma; Colonic polyps; Colorectal neoplasms; Serrated pathway; Serrated polyp

Received: March 31, 2020 **Revised:** April 13, 2020 **Accepted:** April 15, 2020
Corresponding Author: Gyeong Hoon Kang, MD, PhD, Department of Pathology, Seoul National University College of Medicine, 103 Daehak-ro, Jongno-gu, Seoul 03080, Korea
Tel: +82-2-740-8263, Fax: +82-2-765-5600, E-mail: ghkang@snu.ac.kr

Serrated lesions and polyps of the colorectum include all non-malignant epithelial neoplastic lesions showing serrated morphology in the crypt epithelium. Until recently, serrated colorectal lesions were largely classified into three categories: hyperplastic polyp (HP), sessile serrated adenoma/polyp (SSA/P), and traditional serrated adenoma (TSA). However, since the publication of the previous 2010 World Health Organization (WHO) classification, many studies have improved our knowledge of serrated colorectal lesion pathology. In the recently updated 2019 WHO classification, there have been important changes in classification, terminology, and diagnostic criteria for serrated colorectal lesions. In this review, we briefly summarize three major components of the pathology of serrated lesions: (1) updates on the 2019 WHO classification of serrated lesions, (2) updates on morphologic variants and dysplasia of serrated lesions, and (3) the molecular pathology of serrated lesions.

UPDATES IN THE 2019 WHO CLASSIFICATION OF SERRATED COLORECTAL LESIONS

Classification, terminology, and diagnostic criteria for serrated lesions/polyps of the colorectum are being revised, and their clinical implications and molecular features have also been newly discovered or modified. The WHO classification of tumors of the digestive system was recently updated to the 5th edition [1]. Compared to the previous edition, the 5th edition has demonstrated several notable changes in the section on serrated colorectal lesions/polyps.

Changes in the terminology and categorization of serrated colorectal lesions

There are major and minor changes in the terminology and categorization of serrated colorectal lesions. Alterations in the

pISSN 2383-7837
eISSN 2383-7845

terminology and categorization of serrated colorectal lesions in the new WHO classification (5th edition) are summarized in Fig. 1. The most important change in terminology is the adoption of the new diagnostic term "sessile serrated lesion" (SSL), which refers to serrated premalignant lesions that were formerly called "sessile serrated adenomas" (SSAs) or "sessile serrated polyps" (SSPs) (Fig. 1) [1]. The rationale for replacing the term "adenoma" with "lesion" is based on the fact that a considerable number of SSLs do not show morphologic dysplasia, an essential component of classical "adenoma" in the colorectum [2]. Moreover, because some SSLs may not show a polypoid appearance, the term "polyp" is unsuitable [1]. There was also a minor change in the SSL category. Although SSLs (SSA/Ps) with cytologic dysplasia have already been described as an advanced subtype of SSL in the previous edition, the new WHO classification more clearly categorizes "SSL with dysplasia" (SSLD) as an established diagnostic terminology (Fig. 1) [1]. Another change in the new classification is the elimination of mucin-poor HP (MPHP) among the HP subtypes (Fig. 1) [1]. According to the previous WHO classification, HPs can be classified into three subtypes: microvesicular HP (MVHP), goblet cell-rich HP (GCHP), and a minor subtype, MPHP [3]. However, in the new WHO classification, only MVHP and GCHP remain among the HP subtypes. In fact, subtyping of HPs into MVHP or GCHP is practically unnecessary in pathologic diagnosis because the clinical significance of HP subtyping has not been proven [4]. The last change in terminology in the new WHO classification of serrated lesions introduces the new diagnostic entity "unclassified serrated adenoma" (or "serrated adenoma, unclassified") (Fig. 1) [1]. In fact, pathologists have occasionally encountered problematic colorectal polyp cases showing both dysplasia and serrated architecture, but these cannot be clearly classified as SSL, TSA, or conventional adenoma. Thus, these ambiguous adenomas with serrated morphology, including the recently suggested serrated tubulovillous adenoma (sTVA) category (described below), can be diagnosed as unclassified serrated adenoma (USA) according to the new WHO classification. Terminology and categorization of TSAs were maintained without revision from the 4th to the 5th edition of the WHO classification (Fig. 1).

Changes in the diagnostic criteria for SSLs

The diagnostic criteria for SSLs in the 5th WHO classification have become clearer than those of the previous edition. According to the 4th WHO classification, two or three typically distorted serrated crypts in a polyp might be necessary to diagnose SSL [3]. Because "two or three" was somewhat unclear for a cut-off value to establish definitive diagnosis, this suggestion occasionally induced confusion, especially when there were two distorted serrated crypts in a non-dysplastic serrated lesion. The criteria were occasionally interpreted as two contiguous or three dispersed typical crypts. After the publication of the 4th WHO classification in 2010, an American expert panel suggested that only one distorted serrated crypt might be sufficient for the diagnosis of SSL [5]. The updated 2019 WHO classification described this recommendation as the minimum requirement for SSL diagnosis [1]. Detailed diagnostic criteria for SSL based on the new WHO classification are summarized in Table 1. In detail, a serrated colorectal lesion must show an overall distorted crypt architecture to be diagnosed as an SSL. The architecturally distorted serrated crypt pathognomonic for SSL should satisfy one or more of the following morphologic features: (1) horizontally growing crypt along the muscularis mucosa, (2) dilated crypt base, (3)

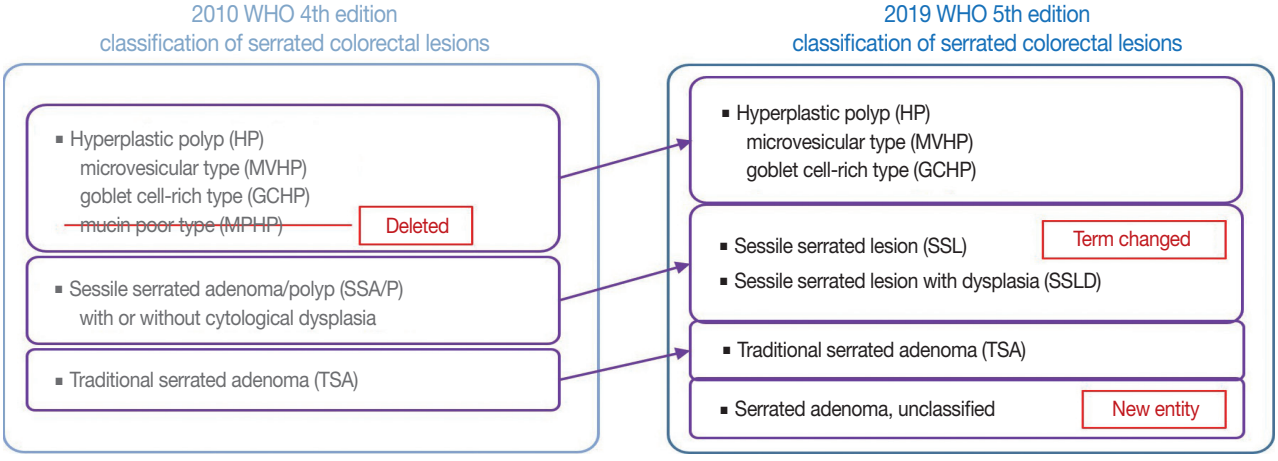

Fig. 1. Summary of changes in terminology and categorization of serrated colorectal lesions from the 4th to the 5th edition of the World Health Organization classification.

Table 1. Summary of the diagnostic criteria for colorectal sessile serrated lesions (SSLs) according to the 2019 WHO classification, 5th edition [1]

	Summary
Definition of an "architecturally distorted serrated crypt" that is typical in SSLs	A crypt showing at least one of the following histologic features: Horizontal growth along the muscularis mucosa (L-shaped or inverted T-shaped crypt) Dilation of the crypt base (basal one-third of the crypt) Serrations extending into the crypt base Asymmetrical proliferation (shift of the proliferation zone from the base to the lateral side)
Diagnostic criteria of SSL	The presence of at least one unequivocal "architecturally distorted serrated crypt" (defined above)

WHO, World Health Organization; SSL, sessile serrated lesion.

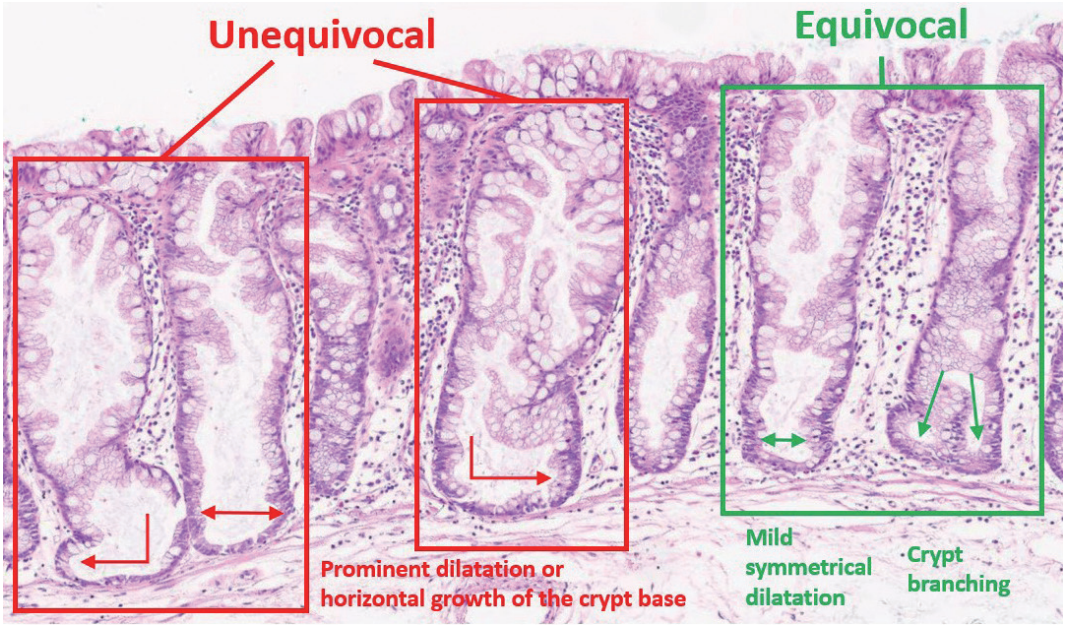

Fig. 2. Histologic features defining sessile serrated lesions (SSLs). Architecturally distorted serrated crypts defining SSLs. Although all five vertically well-sectioned crypts included in this photomicrograph show extended serration into the lower half of the crypt, crypt base serration is subtle in all the crypts. Instead, prominent dilatation or horizontal growth of the crypt base is definite in unequivocally distorted serrated crypts (red square and arrows). Note the equivocally distorted serrated crypts showing crypt branching or mild symmetrical dilatation of the crypt base (green square and arrows). These equivocal crypts must not be counted for the diagnosis of SSL.

serrated morphology throughout the crypt including the base, and (4) asymmetrical proliferative features of the crypt (Table 1) [1]. The 5th WHO classification exclusively introduced the presence of "one or more" unequivocal distorted serrated crypts as a diagnostic criterion for SSLs [1], which was suggested by an American expert panel [5], instead of the "two or three" criteria of the 4th WHO classification [3]. The authors of the new WHO classification also emphasized that a distorted serrated crypt should be morphologically "unequivocal" for the diagnosis of SSL [1]. Serrated crypts with equivocally distorted architecture, including crypt branching and mild symmetrical dilatation of the crypt base, should not be included in the count of distorted serrated crypts for SSL diagnosis [1]. Examples of unequivocal and equivocal architecturally distorted serrated crypts in SSLs are shown in Fig. 2.

Changes in the diagnostic criteria for TSAs

As mentioned above, there is no remarkable change in the terminology or categorization of TSAs. However, there is a minor revision in the description of essential morphologic components for the diagnosis of TSAs. Since the 4th edition of the WHO classification, it has been understood that TSAs have three morphologic characteristics that distinguish them from other serrated lesions or conventional adenomas: (1) unique cytological features, including intense eosinophilic cytoplasm with pencillate nuclei, (2) unique serrated morphology, including slit-like serrations, and (3) a unique crypt architecture, including ectopic crypt foci (ECFs) (Fig. 3A–C). Among these, the cytological and serration features are still recognized as defining factors of TSAs (Fig. 3B). Previous references, including the 4th edition of the WHO classification, described that the presence of ECF could be pathognomonic for TSAs [3]. However, recent investigations

https://doi.org/10.4132/jptm.2020.04.15

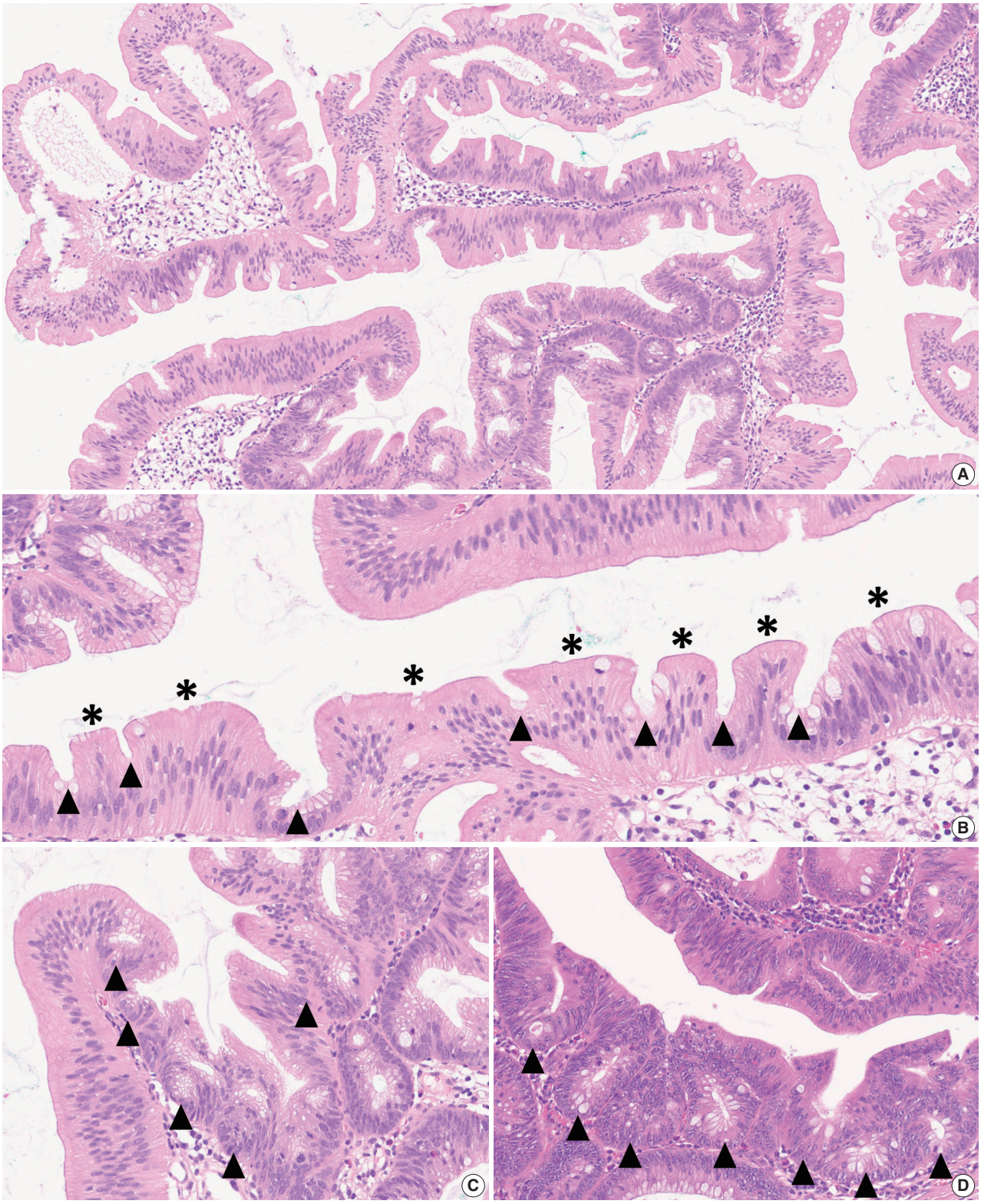

Fig. 3. Histologic features defining traditional serrated adenomas (TSAs). (A) A low power view of a TSA showing typical histologic features. (B) Morphologic features defining TSA. Note the centrally arranged, pencillate nuclei with abundant dense eosinophilic cytoplasm. Slit-like serrations indicate sharp invaginations (arrowheads) along the flat-topped, small intestine-like luminal border (asterisks). (C, D) Ectopic crypt formation (ECF) in a TSA (C) and in a serrated tubulovillous adenoma (D). Note the small, laterally budding crypt-like structures not reaching the muscularis mucosa (arrowheads). Although ECF is one of the morphologic characteristics of TSAs, it is not exclusive to or essential for TSAs.

have reported that ECFs can be found not only in TSAs but also in other adenomas, including tubulovillous adenomas (TVAs), villous adenomas (VAs), and sTVAs (Fig. 3C, D) [6,7]. Thus, ECF is currently not considered to be an exclusive feature of TSAs, and it is recommended that the diagnosis of TSAs based only on the presence of ECF should be avoided [1,4].

UPDATES ON MORPHOLOGIC VARIANTS AND DYSPLASTIC PATTERNS OF SERRATED LESIONS

In recent years, there have been several suggestions for novel morphologic variants of serrated colorectal lesions. Here, we review recently proposed morphologic variants including sTVA, mucin-rich variant of TSA (MrTSA), and superficially serrated adenoma (SuSA). These variants have not been widely accepted and are not officially included as diagnostic terms in the 2019 WHO classification. However, the molecular features and biological behaviors of these variants might be somewhat different from those of classic SSLs and TSAs. Therefore, to establish these variants as official subtypes of serrated lesions, clinicopathologic and molecular data of these variants should be further analyzed.

Serrated tubulovillous adenoma (sTVA)

sTVA was first defined by Bettington et al. [7], who stated that sTVA can be diagnosed when a polyp meets all the following criteria: (1) villous component in more than 25% of the polyp, (2) serrated morphology in more than 50% of the polyp, and (3) TSA-type cytological features and slit-like serrations in less than 10% of the polyp. Bettington et al. [7] found that sTVAs were larger and more likely to be proximal; they were also molecularly associated with CpG island methylation and *KRAS* mutations more than conventional TVAs. In addition, sTVAs were more likely to be proximal and were associated with less CpG island methylation and more frequent β-catenin nuclear expression than TSAs [7]. There were no cases showing MLH1 loss or *BRAF* mutation among the studied sTVAs [7]. These findings collectively indicate that sTVAs may be precursors of *KRAS*-mutated, microsatellite-stable (MSS) colorectal carcinomas (CRCs).

Mucin-rich TSA (MrTSA)

MrTSA was first described by Kalimuthu et al. [8]. MrTSA can be defined as a TSA showing ≥50% goblet cells or mucin-rich cells with a goblet cell/eosinophilic absorptive cell ratio of at least 1:1 [8]. Compared to classic TSAs, MrTSAs are characterized by variable growth patterns, a lower frequency of ECFs, and more intraepithelial lymphocytes [8]. Furthermore, the molecular characteristics of MrTSAs were also analyzed by Hiromoto et al. [9], who compared *KRAS*/*BRAF* mutation profiles and immunohistochemical expression statuses of MrTSAs to those of classic TSAs and sTVAs. In this study, MrTSAs demonstrated retained MLH1 expression, frequent *BRAF* mutations, and rare *KRAS* mutations [9]. These findings suggest that the majority of MrTSAs may be precursors of *BRAF*-mutated MSS CRCs, an aggressive molecular subtype of CRC.

Superficially serrated adenoma (SuSA)

SuSA was most recently suggested by Hashimoto et al. [10] as a polyp showing characteristic mixed adenomatous and serrated features, including straight adenomatous glands with serrations confined to the superficial portion. Molecularly, SuSAs display high frequencies of *KRAS* mutations and *RSPO* fusions [10]. Because concurrent *KRAS* mutations and *RSPO* fusions are distinct molecular features of a subset of TSAs [11], it is thought that SuSAs may be biologically connected to *KRAS*-mutated TSAs and, like sTVAs, may also be precursors of *KRAS*-mutated MSS CRC. Consistent with these findings, a case report recently described that a sigmoid colon carcinoma derived from SuSA molecularly demonstrated a *KRAS* mutation and a *RSPO2* fusion [12].

Unclassified serrated adenoma (USA)

Based on the updated 2019 WHO classification, both sTVAs and SuSAs may be included in the newly defined USA category. As mentioned above, the new WHO classification proposed that the USA can be defined as an unclassifiable dysplastic polyp with serrated architecture [1]. However, some of the newly defined serrated lesion variants including sTVAs and SuSAs demonstrate clinicopathologic and molecular features different from those of other classic serrated lesions; they may also be associated with transitional or mixed molecular profiles between serrated lesions and conventional adenomas. Although both sTVAs and SuSAs may be common precursors of *KRAS*-mutated MSS CRCs, there are also differences in detailed morphologic and molecular characteristics between sTVAs and SuSAs. These findings indicate that the USA category may need to include fairly heterogeneous serrated lesions. Therefore, to avoid using USA as a wastebasket diagnosis, it is expected that the USA category will be further subclassified into sTVA, SuSA, and other new variants based on their morphologic and molecular differences.

https://doi.org/10.4132/jptm.2020.04.15

Pathologic issues in morphologic dysplasia of serrated lesions

Although SSLs have been regarded as precursors to CRC, only a small proportion of overall SSLs show morphologic dysplasia (SSLDs). Moreover, some dysplasia patterns found in SSLDs differ considerably from the typical dysplastic features of colorectal conventional adenomas. It has been generally recognized that there are two distinct dysplasia subtypes in SSLDs: intestinal (adenomatous) and serrated [1,3,13]. Intestinal dysplasia in dysplastic serrated lesions is morphologically similar to the low-grade dysplasia found in conventional adenomas. Intestinal dysplasia in SSLDs is mainly characterized by typical cytological features including elongated, pseudostratified, hyperchromatic nuclei, and basophilic cytoplasm [1,3,13]. In contrast, serrated dysplasia in dysplastic serrated lesions is morphologically characterized by cuboidal cells, eosinophilic cytoplasm, increased mitoses, and nuclear atypia with vesicular nuclei and prominent nucleoli [1,3,13]. In both intestinal and serrated dysplasia, architectural complexity has not been considered as an essential factor for diagnosis, indicating that SSLDs can be diagnosed only based on cytological dysplasia within any portion of the crypt epithelium of SSLs. Of course, SSLDs can accompany various levels of architectural abnormalities; however, these architectural features generally do not change the simple diagnostic term "SSLD" because subtyping or grading of SSLDs has not yet been officially recommended.

In addition to the traditional dichotomous subtyping of dysplastic patterns in SSLDs, Liu et al. [14] proposed a novel classification of four different dysplastic patterns in SSLDs: (1) minimal deviation, (2) serrated, (3) adenomatous, and (4) not otherwise specified [14]. Minimal deviation dysplasia demonstrates only minor cytological and architectural changes but is mostly accompanied by loss of MLH1 expression (91%) [14]. Serrated dysplasia is architecturally characterized by tightly packed small glands with decreased serrations, and cytologically demonstrates frequent mitoses, atypical vesicular nuclei, and prominent nucleoli. Adenomatous dysplasia is similar to the dysplasia morphology of conventional adenomas. Liu et al. [14] reported that loss of MLH1 expression was rare in both serrated and adenomatous dysplasia (13% and 5%, respectively). Dysplasia not otherwise specified includes all dysplastic patterns not fulfilling the criteria of the above three dysplasia patterns and is the most common dysplasia subtype in SSLDs (79%) [14]. In contrast to serrated and adenomatous dysplasia, loss of MLH1 expression was frequently found in dysplasia not otherwise specified (83%) [14]. These four dysplasia subtypes have not yet been officially adopted by the WHO classification or other guidelines, and currently, there is little need to classify the four dysplasia patterns in the practical diagnosis of SSLDs. In future studies, the reproducibility of this dysplasia classification system should be further evaluated, and differential clinicopathologic and molecular implications of the four dysplasia patterns should be further elucidated.

As briefly mentioned above, grading of dysplasia (low-grade vs. high-grade), an essential component for the diagnostic description of conventional adenomas, is not recommended for dysplastic serrated lesions including SSLD, TSA, and USA [1]. This is because there are various issues related to morphologic heterogeneity, low reproducibility, and uncertain clinical implications. However, we believe that if a pathologist observes definite high-grade dysplastic (HGD) features or intramucosal carcinoma (IMC) components in a serrated lesion, based on the morphologic criteria applied in conventional adenomas, then this should be described in the diagnostic report. The new WHO classification also recommends that the HGD component should be reported separately when it is found in a TSA [1]. There is no consensus regarding the grading of dysplasia in serrated lesions. However, determination of HGD based on the traditional criteria for conventional adenomas may also be acceptable in serrated lesions because both morphologic characteristics and the risk of further invasive progression of advanced lesions may not differ significantly between the two. Conventional adenomas with HGD are characterized by combined cytological atypia (loss of polarity, marked enlargement of nuclei, prominent nucleoli, and occasional atypical mitoses) and architectural complexity (crowded, cribiforming, and irregularly branching glands with or without intraluminal necrosis) [1]. To determine HGD in conventional colorectal adenomas, architectural abnormalities are generally considered to be more critical than cytological features. Accompanying IMC can be diagnosed when there are atypical glands invading the lamina propria without invasion beyond the muscularis mucosa in an adenoma [1,15]. To establish surveillance and treatment strategies suitable for advanced serrated colorectal lesions, detailed differences in the morphologic, molecular, and prognostic features of HGD/IMC components between serrated lesions and conventional adenomas should be further investigated.

UPDATES ON THE MOLECULAR PATHOLOGY OF SERRATED LESIONS

Molecular pathogenesis of SSLs

It is hypothesized that most CRCs which develop through

SSLs molecularly display CpG island methylator phenotype-positivity (CIMP+ or CIMP-high), which is characterized by silencing of many cancer-related genes by extensive promoter CpG island hypermethylation [16,17]. The *MLH1* gene is a DNA mismatch repair (MMR) gene and is also frequently methylated under the CIMP+ condition [18]. *MLH1* silencing by promoter methylation causes high microsatellite instability (MSI-high), indicating an MSI-positive (MSI+) status that is characterized by genome-wide microsatellite sequence alterations and many consequential mutations [18]. CIMP+ with or without *MLH1* methylation is regarded as a major molecular hallmark of the transformation of SSLs to more advanced lesions (SSLDs or carcinomas) (Fig. 4A). If MSI-high is induced in an SSL by *MLH1* silencing, then this lesion will almost inevitably progress into an SSLD, which can rapidly transform into a carcinoma due to the high oncogenic pressure of high mutational burden (Fig. 4A). An interesting case report regarding the rapid malignant transformation of an SSL was recently published [19]. The rapid progression of SSLDs may explain why the detection rate of SSLDs among biopsied or resected colorectal polyps is generally very low; this may be one cause of interval cancers in the proximal colon [20].

Recent investigations including our previous study suggested that both *MLH1* methylation and CIMP+ occur almost exclu-

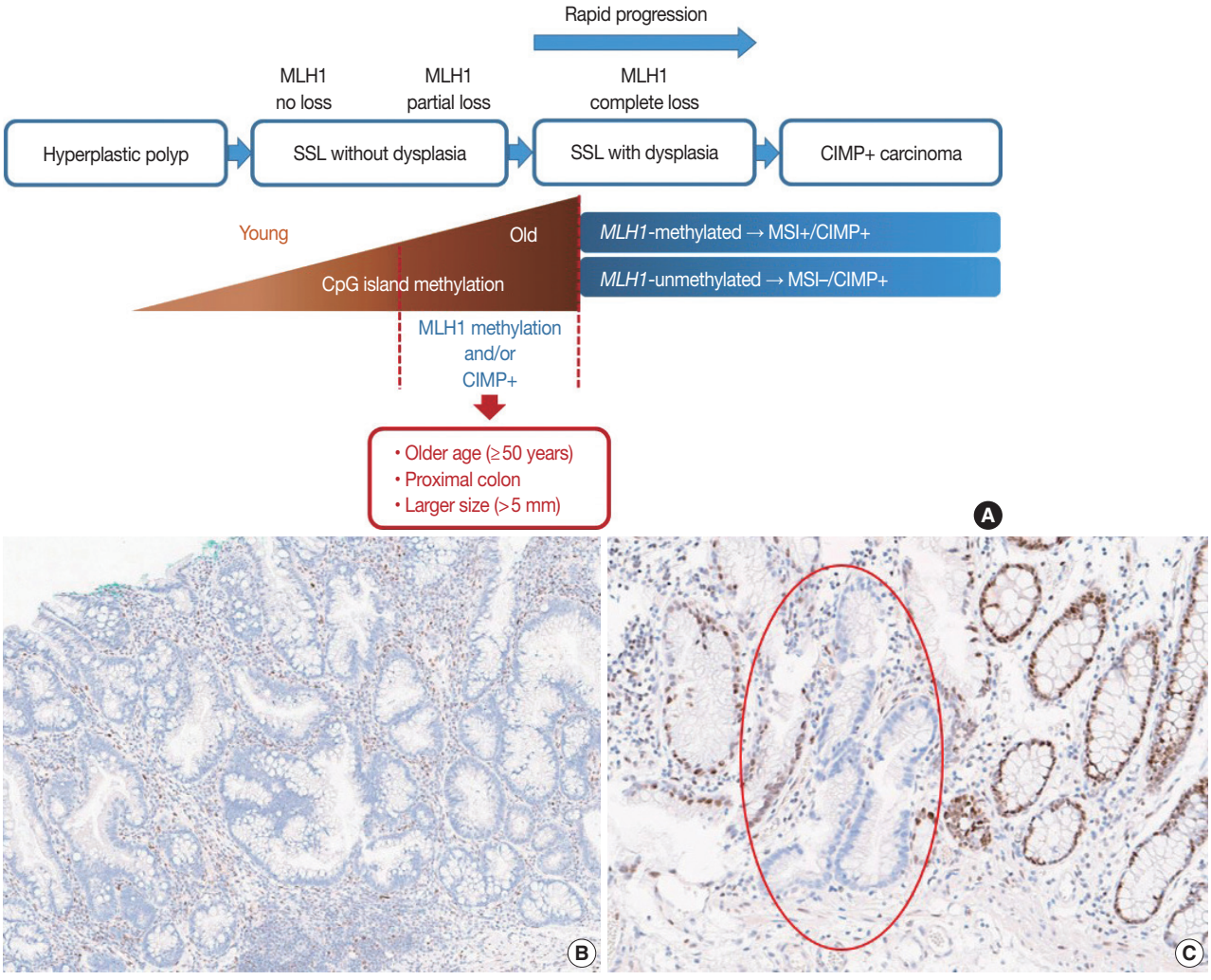

Fig. 4. Updated features of CpG island methylation and MLH1 alteration in the sessile serrated neoplasia pathway. (A) A sequence model of CpG island methylation and MLH1 alteration during the multistep sessile serrated lesion (SSL)-to-carcinoma pathway. Note that both *MLH1* promoter methylation and CpG island methylator phenotype-positivity (CIMP+) are late-step epigenetic events during the progression of non-dysplastic SSLs, and mainly occur in proximal, large (>5 mm) SSLs in older patients (≥50 years). (B) Complete loss of MLH1 expression in an SSL with dysplasia harboring the *MLH1* methylation. (C) Partial loss of MLH1 expression (involving a few non-dysplastic crypts; red ellipse) in a non-dysplastic SSL with *MLH1* methylation. Modified from Lee et al. J Pathol Transl Med 2019; 53: 225-35.

https://doi.org/10.4132/jptm.2020.04.15

sively in proximal, large SSLs in elderly patients (Fig. 4A) [21-23]. Liu et al. [22] examined 448 SSLs and found that the proportion of CIMP+ abruptly increased in SSL patients 51 or older compared to younger patients. According to the study, CIMP+ SSLs were significantly associated with older age and proximal colonic location, but were not correlated with patient sex or lesion size [22]. In our study, we tested 132 non-dysplastic SSLs and defined SSLs with CIMP+ and/or *MLH1* methylation as molecularly high-risk lesions. These high-risk SSLs were found exclusively in the older age group (≥50 years; 100%) and in the proximal colon (100%), which was statistically significant [21]. Although our findings were similar to the results of Liu et al. [22], we also found that histologically measured lesion size, but not endoscopically measured size, was significantly associated with CIMP+/*MLH1* methylation in non-dysplastic SSLs; the high-risk SSLs were found exclusively in SSLs which were >5 mm on histology [21]. Therefore, we concluded that SSLs with CIMP+ and/or *MLH1* methylation are concentrated in a specific subgroup of SSLs satisfying all the following conditions: older age (≥50 years), proximal colonic location (cecum, ascending colon, or transverse colon), and histologically larger polyp size (>5 mm) (Fig. 4A).

Most SSLDs harboring *MLH1* promoter methylation typically show complete loss of MLH1 immunohistochemical expression in their dysplastic crypts (Fig. 4B) [21,24]. Many non-dysplastic SSLs are *MLH1*-unmethylated and display retained expression of the MLH1 protein. However, we recently found that partial loss of MLH1 expression (involving a single or a few non-dysplastic crypts) can occasionally be observed in non-dysplastic SSLs (Fig. 4C) [21]. These unusual non-dysplastic SSLs with partial MLH1 loss demonstrated *MLH1* promoter methylation; however, they had lower levels of *MLH1* methylation than *MLH1*-methylated SSLDs with complete loss of MLH1 expression (Fig. 4B, C) [21]. This novel finding was supported by another recent study, which reported that 71 out of 400 (18%) cases demonstrated loss of MLH1 expression in their non-dysplastic crypts [25]. Collectively, partial loss of MLH1 expression in non-dysplastic SSLs can be a sign of impending dysplastic change and may be a biomarker to screen for molecularly advanced lesions among non-dysplastic SSLs.

The *BRAF* V600E mutation, along with CIMP+, is regarded as a molecular hallmark in the colorectal sessile serrated neoplasia pathway [26-28]. It is known that CIMP+ is tightly associated with the *BRAF* mutation in CRCs [29], indicating that both CIMP+ and the *BRAF* mutation originate from common premalignant lesions (SSLs) in the colon and rectum. Although it has been strongly suspected that the *BRAF* mutation and CIMP+ might synergistically impact carcinogenesis, the detailed mechanism underlying their interaction is unclear. Fang et al. [30,31] previously suggested that the BRAF oncoprotein might promote CpG island methylation in multiple gene promoters in CRC cells through increased promoter binding of MAFG, a transcriptional repressor. However, this finding has not yet been validated by other studies. Recently, Tao et al. [32] reported important clues for the relationship between the *BRAF* mutation and CIMP+ in colorectal carcinogenesis. In their experimental study, aging-related hypermethylation induced sensitivity of mouse colon organoids to *BRAF* mutation-induced oncogenic transformation [32]. This suggests that a *BRAF* mutation is not a prerequisite for CIMP development in SSLs. The finding is also consistent with the real-world observations that CIMP+ SSLs and subsequent CIMP+/*BRAF*-mutated CRCs occur almost exclusively in older patients.

According to data from Western countries including the United States, Canada, Australia, Germany, Austria, and Switzerland, frequencies of *BRAF* V600E mutations in SSLs range from 63% to 100% (Supplementary Table S1) [22,24,33-41]. However, in East Asian countries, including South Korea, Japan, and China, *BRAF* mutation frequencies in SSLs have been reported to be relatively lower, ranging from 14% to 86% (Supplementary Table S1) [42-55]. Using these data, we conducted a pooled analysis to directly compare the frequencies of *BRAF* mutations in SSLs between Western and Eastern countries (Table 2). Overall, *BRAF* mutations were found in 91% (932 of 1,028) of SSLs from Western countries and 76% (798 of 1,048) of SSLs in Eastern countries (Table 2). Interestingly, *KRAS* mutations, known to be mutually exclusive with *BRAF* mutations in tumors, were more frequently found in SSLs from Eastern countries (6%, 65 of 1,053 SSLs) compared to Western countries (2%, 22 of 988 SSLs) (Table 2). These regional differences

Table 2. Comparison of reported frequencies of *BRAF/KRAS* mutations in colorectal sessile serrated lesions (SSLs) between Western and Eastern countries: a pooled analysis using data published between 2006 and 2020[a]

	SSLs in Western countries[b]	SSLs in Eastern countries[c]	p-value
BRAF mutation	932/1,028 (91)	798/1,048 (76)	<.001
KRAS mutation	22/988 (2)	65/1,053 (6)	<.001

Values are presented as number (%).
[a]Detailed frequency data from individual studies are listed in Supplementary Table S1. [b]Western countries include United States, Canada, Australia, Germany, Austria, and Switzerland (total *BRAF*-tested samples n=1,028; total *KRAS*-tested samples n=988). [c]Eastern countries include South Korea, Japan, and China (total *BRAF*-tested samples n=1,048; total *KRAS*-tested samples n=1,053).

in *BRAF* and *KRAS* mutation frequencies in SSLs were all statistically significant (both $p < .001$) (Table 2). Although it is generally accepted that nearly all Western colorectal SSLs have *BRAF* mutations, there are likely ethnic differences in *BRAF* and *KRAS* mutation profiles in SSLs, based on the results of our pooled analysis. Unsurprisingly, the ethnic differences in *BRAF* mutation frequency in SSLs can be linked to a similar tendency in the molecular profiles of CRCs. In fact, we previously reported that CRCs from East Asian patients have lower *BRAF* mutation frequencies than those from Western populations [18]. In brief, it is reasonable to suggest that the lower frequency of *BRAF* mutations in SSLs from East Asian patients is directly reflected in the lower frequency of *BRAF* mutations in CRCs of the same regional population because SSLs are major precursors of *BRAF*-mutant CRCs (Fig. 5A).

Several previous studies analyzed RNA and/or protein expression profiles of SSLs. Caruso et al. [36] first found upregulation of cathepsin E (CTSE) and trefoil factor 1 in SSLs. It is also known that gastric-type mucins, including mucin 6 (MUC6) and mucin 5AC (MUC5AC), can be aberrantly expressed in SSLs and HPs [56-58]. Gonzalo et al. [59] suggested that annexin A10 (ANXA10) could be a potential marker of SSLs.

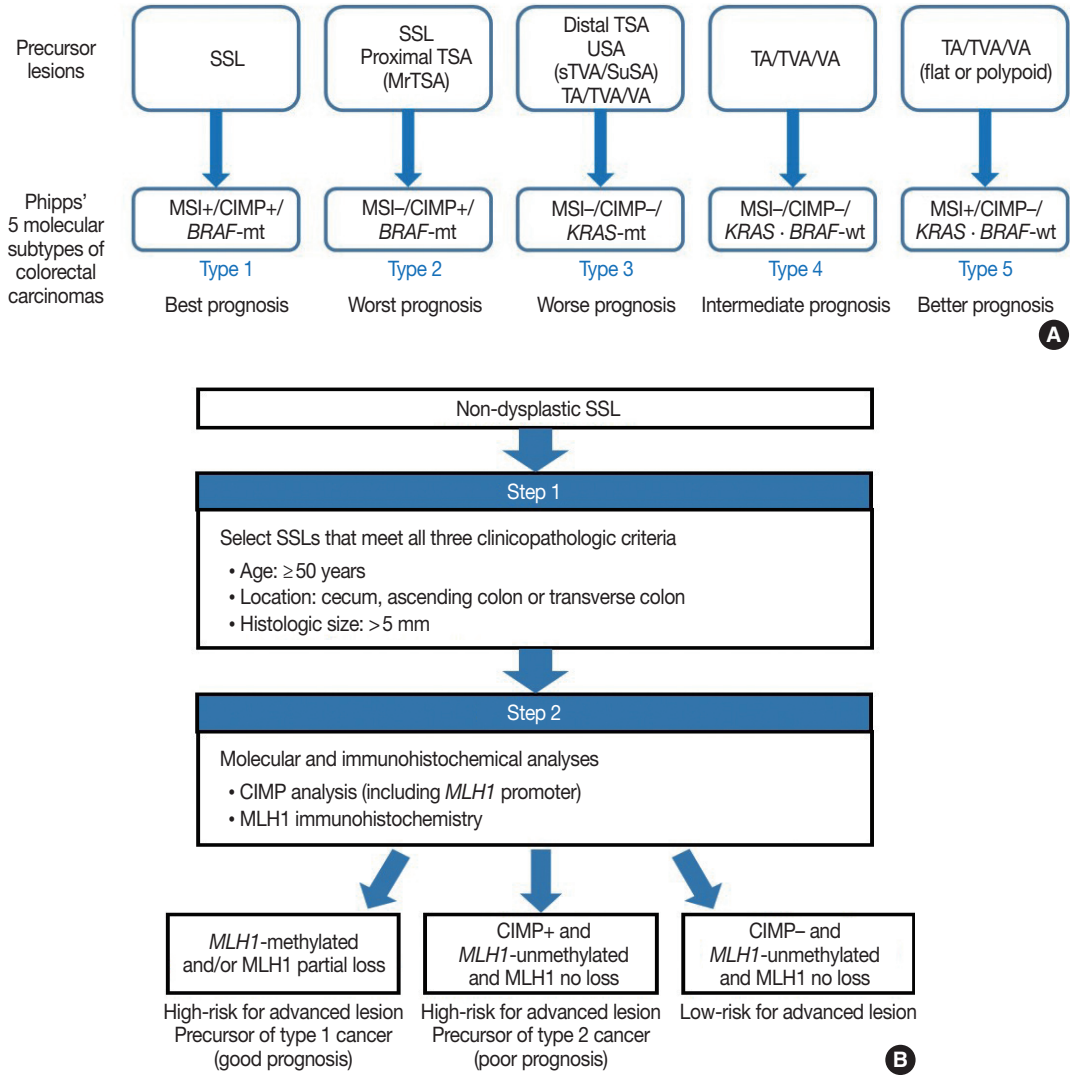

Fig. 5. Serrated lesions as precursors of different molecular subtypes of colorectal carcinoma (CRC). (A) Prognostically implicated molecular subtypes of CRCs and their conceptually matched precursor lesions. SSL, sessile serrated lesion; TSA, traditional serrated adenoma; MrTSA, mucin-rich traditional serrated adenoma; USA, unclassified serrated adenoma; sTVA, serrated tubulovillous adenoma; SuSA, superficially serrated adenoma; TA, tubular adenoma; TVA, tubulovillous adenoma; VA, villous adenoma; MSI, microsatellite instability; MSI+, MSI-positive; MSI–, MSI-negative; CIMP, CpG island methylator phenotype; CIMP+, CIMP-positive; CIMP–, CIMP-negative; mt, mutant-type; wt, wild-type. (B) An example of a two-step screening algorithm to stratify the risk subgroups of non-dysplastic SSLs.

https://doi.org/10.4132/jptm.2020.04.15

Various other proteins normally expressed in the gastric mucosa such as v-set and immunoglobulin domain containing 1 (VSIG1) and trefoil factor 2 (TFF2) were frequently overexpressed in SSLs [60,61]. However, the practical utility of these gastric-type proteins in the diagnosis of SSLs has been limited because these markers can also be expressed in subsets of other serrated lesions, including TSAs and HPs [61]. Recently, Rickelt and colleagues published interesting data regarding a potential biomarker of SSLs [62]. In their study, agrin (AGRN) expression in the muscularis mucosa is a specific feature of SSLs, which contrasts with the absence of AGRN expression in the muscularis mucosa of other types of serrated lesions and conventional adenomas [62]. The utility of AGRN immunohistochemistry in the differential diagnosis between SSLs and other colorectal polyps should be further validated by independent studies using large-scale samples.

Molecular pathogenesis of TSAs

During the past decade, there has been remarkable progress in understanding the molecular features of TSAs. The molecular pathogenesis of TSAs can be largely divided into two pathways: the *KRAS* mutation pathway and the *BRAF* mutation pathway [63,64]. *KRAS* or *BRAF* mutations are found in more than 80% of TSAs [41,64], and whether *KRAS* or *BRAF* mutations occur in a TSA is mainly dependent on the location of the TSA. Most *KRAS*-mutated TSAs are found in the distal colon (descending and sigmoid colon) and rectum, whereas *BRAF*-mutated TSAs are more frequently located in the proximal colon (cecum and the ascending and transverse colon) [64]. Because TSAs are generally more prevalent in the distal rather than proximal colon [11], *KRAS* mutations are also more prevalent than *BRAF* mutations in TSAs. It has been suggested that *BRAF*-mutated TSAs may be derived from proximal colonic SSLs or HPs based on morphologic connectivity and molecular similarity. SSLs or HPs are often found as precursor lesions around TSAs, especially proximal TSAs, indicating that proximally-located, *BRAF*-mutated TSAs can be transformed from preexisting SSLs or HPs [64-67]. In terms of molecular features, *BRAF*-mutated TSAs of the proximal colon frequently show CIMP+, whereas *KRAS*-mutated TSAs of the distal colorectum generally display CIMP-low or CIMP-negative status [63,64]. Because CIMP+ is an epigenetic hallmark of advanced SSLs as described above, proximal TSAs commonly share two major molecular features with SSLs, namely, *BRAF* mutation and CIMP+, and these findings support the theory of transition from SSLs to TSAs in the proximal colon. Although *MLH1* methylation is a frequent event in CIMP+ SSLDs, *MLH1* methylation or complete loss of MLH1 expression is rarely found in proximal TSAs, even in advanced TSAs [64]; this suggests that most proximal, *BRAF*-mutated TSAs may be precursors of CIMP+/MSI– CRCs but not CIMP+/MSI+ CRCs (Fig. 5A).

APC mutations are an initiating molecular hallmark and a main cause of Wnt signaling pathway activation in colorectal conventional adenomas; though these mutations are not frequent in TSAs, many TSAs show Wnt pathway activation, which can be confirmed by β-catenin expression in tumor cell nuclei [64,67,68]. Recent studies have identified that Wnt activation in TSAs may be caused more frequently by *RSPO* fusions or *RNF43* mutations than by *APC* mutations [69]. Sekine et al. [69] previously reported that *PTPRK-RSPO3* fusions and *RNF43* mutations were found almost exclusively in TSAs compared to other conventional adenomas or serrated lesions. In their study, genetic alterations associated with Wnt activation including *RSPO3* fusions, *RNF43* mutations, *APC* mutations, and *CTNNB1* mutations were mutually exclusive in TSAs [69]. Subsequent studies revealed that *RSPO* fusion-positive TSAs were significantly associated with distal location, larger size, and *KRAS* mutations, whereas *RNF43* mutations were frequently found in *BRAF*-mutated TSAs [67,70,71]. Although *PTPRK–RSPO3* fusions were a predominant form of *RSPO* fusions in TSAs, other minor fusions including *NRIP1–RSPO2*, *EIF3E–RSPO2*, and *PIEZO1–RSPO2* fusions were also found in TSAs [70,72]. Interestingly, in TSAs with adjacent precursor lesions (SSL or HP), Wnt activation-related genetic alterations including *RSPO* fusions, *RNF43* homozygous mutations, *APC* mutations, and *CTNNB1* mutations were found only in the TSA component but not in the precursor component, indicating that Wnt activation may be critical for the development of TSAs from precursor lesions [67].

Like SSLs, TSAs express gastric-type proteins including ANXA10, VSIG1, CTSE, TFF2, and MUC5AC, although their positivity rates and the intensity or extent of expression are generally lower than those of SSLs or MVHPs [61]. Specific biomarkers for the differential diagnosis of TSAs have not been established. However, Sohier et al. [73] performed proteomic analysis using formalin-fixed, paraffin-embedded tissues of various types of serrated lesions and conventional adenomas and found that LEFTY1, an inhibitory protein of the Nodal/transforming growth factor β pathway, was overexpressed specifically in TSAs. Although this may be promising, more studies will be necessary to validate whether LEFTY1 immunohistochemistry is practically useful in the diagnosis of TSAs.

Serrated lesions as precursors of different molecular subtypes of CRCs

Because SSLs, TSAs, and their variants are precursor lesions of CRCs, and each shows unique molecular features, serrated premalignant lesions can be matched to their consequential molecular subtypes of CRCs. Phipps et al. [74,75] recently classified CRCs into five molecular subtypes based on combined MSI, CIMP, and *KRAS*/*BRAF* mutation profiles and successfully validated the prognostic significance of CRC molecular subtyping in large-scale cohorts. The five molecular subtypes were defined as follows: (1) type 1: MSI+, CIMP+, *BRAF*-mutated, *KRAS*-wildtype; (2) type 2: MSI–, CIMP+, *BRAF*-mutated, *KRAS*-wildtype; (3) type 3: MSI–, CIMP–, *BRAF*-wildtype, *KRAS*-mutated; (4) type 4: MSI–, CIMP–, *BRAF*-wildtype, *KRAS*-wildtype; and (5) type 5: MSI+, CIMP–, *BRAF*-wildtype, *KRAS*-wildtype (Fig. 5A) [74,75]. This molecular subtyping proved to be useful in the prognostication of CRCs. The prognosis of the five molecular subtypes was ranked (best to worst) as follows: type 1–type 5–type 4–type 3–type 2 (Fig. 5A) [74,75]. Type 1 CRCs indicate sporadic MSI+ (MSI-high) tumors caused by promoter methylation-associated *MLH1* silencing, whereas the majority of type 5 CRCs are hereditary MSI+ tumors that arise in the setting of Lynch syndrome, which is genetically defined by germline mutations in one of the MMR genes. Because both type 1 and type 5 CRCs are molecularly MSI-high, which is well-established as a favorable prognostic factor in CRC [18], patients with these tumors generally show good survival. Sporadic *MLH1* methylation with CIMP+ and *BRAF* mutation occurs almost exclusively in SSLs among colorectal premalignant lesions. Thus, SSLs can be considered as unequivocal precursors of type 1 CRCs (Fig. 5A). Most precursor lesions in Lynch syndrome-associated CRCs are histologically conventional-type adenomas with grossly flat or polypoid appearance (Fig. 5A) [1]. Type 2 CRCs demonstrate the worst prognosis among the five molecular subtypes [74,75]. The molecular features of type 2 CRCs (CIMP+/MSI–/*BRAF* mutation) almost exactly match those of *MLH1*-unmethylated SSLs and proximal-located TSAs, and these serrated lesions can be precursors of type 2 CRCs (Fig. 5A). As described above, MrTSAs can also be considered precursors of type 2 CRCs. Type 3 CRCs are associated with poor prognosis, although their survival is slightly better than that of type 2 CRCs [74,75]. All subtypes of serrated lesions which frequently harbor *KRAS* mutations, including sTVAs and SuSAs (both can be classified as USA, as described above) as well as distally located TSAs, can be major precursors of type 3 CRCs (Fig. 5A). *KRAS* mutations are found in a subset of conventional adenomas, which can also be precursors of type 3 cancers (Fig. 5A). Type 4 carcinomas represent the most common CRC subtype developed through the classic adenoma-carcinoma sequence and are molecularly characterized by chromosomal instability. These cancers typically progress from conventional adenomas, including tubular adenoma, villous adenoma, or TVA (Fig. 5A).

Interestingly, SSLs are thought to be the main precursors of either the best or the worst prognostic CRCs (type 1 and type 2, respectively) (Fig. 5A). Although type 1 and type 2 CRCs commonly share CIMP+/*BRAF*-mutated status, obtained mainly through the SSL pathway, their contrasting survival rates critically depend on the presence or absence of MSI (that is to say, the presence or absence of *MLH1* methylation) [76]. If an SSL harbors *MLH1* methylation, the lesion is at a high risk of progressing into an advanced lesion, but an invasive carcinoma derived from the SSL will be expected to show a favorable prognosis. On the other hand, CIMP+ SSLs without *MLH1* methylation can be regarded as a potential high-risk precursor of poor-prognostic type 2 CRC. Thus, we believe that for early prevention of poor-prognostic CRCs, it will be helpful to screen CIMP+ SSLs without *MLH1* methylation (or CIMP+ SSLs without MLH1 loss) among non-dysplastic SSLs. Collectively, we propose a two-step screening method to stratify risk subgroups of non-dysplastic SSLs: first-step screening by combining age, location, and lesion size profiles, and second-step screening by combined molecular and immunohistochemical analyses. This screening approach can efficiently and differentially detect high-risk precursors of type 1 and type 2 CRCs (Fig. 5B). Using this approach, non-dysplastic SSLs at high risk for dysplastic/carcinomatous progression may be more precisely detected. Ultimately, the risk-subgrouping of non-dysplastic SSLs will help to prevent interval colon cancers arising from underestimated SSLs.

FUTURE DIRECTIONS

Although notable data refining the morphologic classification and molecular characterization of serrated colorectal lesions have accumulated during the last decade, several pathologic issues remain unresolved. First, overuse of the USA category should be avoided, and USAs should be more clearly divided into morphologic and/or molecular subtypes such as sTVAs and SuSAs. Second, in order to achieve personalized treatment and precision surveillance of serrated premalignant lesions, SSLs and TSAs should be further stratified into risk subgroups based on combined clinicopathologic and molecular profiles; our proposed

https://doi.org/10.4132/jptm.2020.04.15

algorithm for the risk-subgrouping of non-dysplastic SSLs is shown here (Fig. 5B). Third, immunohistochemical or molecular biomarkers should be further developed and validated to aid in the differential diagnosis or prognostic subgrouping of serrated colorectal lesions. Recently studied proteins such as AGRN and LEFTY1 are potential biomarkers which can aid in the differential diagnosis of serrated lesions [62,73].

Supplementary Information

The Data Supplement is available with this article at https://doi.org/10.4132/jptm.2020.04.15.

Ethics Statement

Not applicable.

ORCID

Jung Ho Kim https://orcid.org/0000-0002-6031-3629
Gyeong Hoon Kang https://orcid.org/0000-0003-2380-6675

Author Contributions

Conceptualization: JHK. Formal analysis: JHK. Funding acquisition: JHK. Investigation: JHK. Methodology: JHK. Project administration: JHK, GHK. Resources: JHK, GHK. Supervision: JHK, GHK. Validation: JHK, GHK. Visualization: JHK. Writing—original draft: JHK. Writing—review & editing: JHK, GHK. Approval of final manuscript: all authors.

Conflicts of Interest

J.H.K. and G.H.K., contributing editors of the *Journal of Pathology and Translational Medicine*, were not involved in the editorial evaluation or decision to publish this article.

Funding Statement

This study was supported by a grant from the SNUH Research Fund (04-2016-0680) as well as National Research Foundation of Korea grants funded by the Korean government (Ministry of Science and ICT) (NRF-2016R1C1B2010627 and NRF-2019R1F1A1059535).

References

1. WHO Classification of Tumours Editorial Board. WHO classification of tumors: digestive system tumours. 5th ed. Lyon: International Agency for Research on Cancer, 2019.
2. Bateman AC, Shepherd NA. UK guidance for the pathological reporting of serrated lesions of the colorectum. J Clin Pathol 2015; 68: 585-91.
3. World Health Organization., International Agency for Research on Cancer. WHO classification of tumours of the digestive system. 4th ed. Lyon: International Agency for Research on Cancer, 2010.
4. Pai RK, Bettington M, Srivastava A, Rosty C. An update on the morphology and molecular pathology of serrated colorectal polyps and associated carcinomas. Mod Pathol 2019; 32: 1390-415.
5. Rex DK, Ahnen DJ, Baron JA, et al. Serrated lesions of the colorectum: review and recommendations from an expert panel. Am J Gastroenterol 2012; 107: 1315-29.
6. Hafezi-Bakhtiari S, Wang LM, Colling R, Serra S, Chetty R. Histological overlap between colorectal villous/tubulovillous and traditional serrated adenomas. Histopathology 2015; 66: 308-13.
7. Bettington M, Walker N, Rosty C, et al. Serrated tubulovillous adenoma of the large intestine. Histopathology 2016; 68: 578-87.
8. Kalimuthu SN, Serra S, Hafezi-Bakhtiari S, Colling R, Wang LM, Chetty R. Mucin-rich variant of traditional serrated adenoma: a distinct morphological variant. Histopathology 2017; 71: 208-16.
9. Hiromoto T, Murakami T, Akazawa Y, et al. Immunohistochemical and genetic characteristics of a colorectal mucin-rich variant of traditional serrated adenoma. Histopathology 2018; 73: 444-53.
10. Hashimoto T, Tanaka Y, Ogawa R, et al. Superficially serrated adenoma: a proposal for a novel subtype of colorectal serrated lesion. Mod Pathol 2018; 31: 1588-98.
11. McCarthy AJ, Serra S, Chetty R. Traditional serrated adenoma: an overview of pathology and emphasis on molecular pathogenesis. BMJ Open Gastroenterol 2019; 6: e000317.
12. Mizuguchi Y, Sakamoto T, Hashimoto T, et al. Identification of a novel PRR15L-RSPO2 fusion transcript in a sigmoid colon cancer derived from superficially serrated adenoma. Virchows Arch 2019; 475: 659-63.
13. Cenaj O, Gibson J, Odze RD. Clinicopathologic and outcome study of sessile serrated adenomas/polyps with serrated versus intestinal dysplasia. Mod Pathol 2018; 31: 633-42.
14. Liu C, Walker NI, Leggett BA, Whitehall VL, Bettington ML, Rosty C. Sessile serrated adenomas with dysplasia: morphological patterns and correlations with MLH1 immunohistochemistry. Mod Pathol 2017; 30: 1728-38.
15. Amin MB, Edge S, Greene F, et al. AJCC cancer staging manual. Chicago: Springer, 2017.
16. Kang GH. Four molecular subtypes of colorectal cancer and their precursor lesions. Arch Pathol Lab Med 2011; 135: 698-703.
17. Bae JM, Kim JH, Kang GH. Molecular subtypes of colorectal cancer and their clinicopathologic features, with an emphasis on the serrated neoplasia pathway. Arch Pathol Lab Med 2016; 140: 406-12.
18. Kim JH, Kang GH. Molecular and prognostic heterogeneity of microsatellite-unstable colorectal cancer. World J Gastroenterol 2014; 20: 4230-43.
19. Amemori S, Yamano HO, Tanaka Y, et al. Sessile serrated adenoma/polyp showed rapid malignant transformation in the final 13 months. Dig Endosc 2019 Nov 1 [Epub]. https://doi.org/10.1111/den.13572.
20. Burgess NG, Tutticci NJ, Pellise M, Bourke MJ. Sessile serrated adenomas/polyps with cytologic dysplasia: a triple threat for interval cancer. Gastrointest Endosc 2014; 80: 307-10.
21. Lee JA, Park HE, Yoo SY, et al. CpG island methylation in sessile serrated adenoma/polyp of the colorectum: implications for differential diagnosis of molecularly high-risk lesions among non-dysplastic sessile serrated adenomas/polyps. J Pathol Transl Med 2019; 53: 225-35.
22. Liu C, Bettington ML, Walker NI, et al. CpG island methylation in sessile serrated adenomas increases with age, indicating lower risk of malignancy in young patients. Gastroenterology 2018; 155: 1362-5.
23. Bettington M, Brown I, Rosty C, et al. Sessile serrated adenomas in young patients may have limited risk of malignant progression. J Clin Gastroenterol 2019; 53: e113-6.
24. Bettington M, Walker N, Rosty C, et al. Clinicopathological and molecular features of sessile serrated adenomas with dysplasia or carcinoma. Gut 2017; 66: 97-106.
25. Yozu M, Kem M, Cenaj O, Mino-Kenudson M, Odze RD, Misdraji J. Loss of expression of MLH1 in non-dysplastic crypts is a harbin-

ger of neoplastic progression in sessile serrated adenomas/polyps. Histopathology 2019; 75: 376-84.
26. Bettington M, Walker N, Clouston A, Brown I, Leggett B, Whitehall V. The serrated pathway to colorectal carcinoma: current concepts and challenges. Histopathology 2013; 62: 367-86.
27. O'Brien MJ, Zhao Q, Yang S. Colorectal serrated pathway cancers and precursors. Histopathology 2015; 66: 49-65.
28. Rhee YY, Kim KJ, Kang GH. CpG island methylator phenotype-high colorectal cancers and their prognostic implications and relationships with the serrated neoplasia pathway. Gut Liver 2017; 11: 38-46.
29. Weisenberger DJ, Siegmund KD, Campan M, et al. CpG island methylator phenotype underlies sporadic microsatellite instability and is tightly associated with BRAF mutation in colorectal cancer. Nat Genet 2006; 38: 787-93.
30. Fang M, Ou J, Hutchinson L, Green MR. The BRAF oncoprotein functions through the transcriptional repressor MAFG to mediate the CpG island methylator phenotype. Mol Cell 2014; 55: 904-15.
31. Fang M, Hutchinson L, Deng A, Green MR. Common *BRAF* (V600E)-directed pathway mediates widespread epigenetic silencing in colorectal cancer and melanoma. Proc Natl Acad Sci U S A 2016; 113: 1250-5.
32. Tao Y, Kang B, Petkovich DA, et al. Aging-like spontaneous epigenetic silencing facilitates Wnt activation, stemness, and *BRAF*(V600E)-induced tumorigenesis. Cancer Cell 2019; 35: 315-28.
33. Jass JR, Baker K, Zlobec I, et al. Advanced colorectal polyps with the molecular and morphological features of serrated polyps and adenomas: concept of a 'fusion' pathway to colorectal cancer. Histopathology 2006; 49: 121-31.
34. Chung SM, Chen YT, Panczykowski A, Schamberg N, Klimstra DS, Yantiss RK. Serrated polyps with "intermediate features" of sessile serrated polyp and microvesicular hyperplastic polyp: a practical approach to the classification of nondysplastic serrated polyps. Am J Surg Pathol 2008; 32: 407-12.
35. Kim YH, Kakar S, Cun L, Deng G, Kim YS. Distinct CpG island methylation profiles and BRAF mutation status in serrated and adenomatous colorectal polyps. Int J Cancer 2008; 123: 2587-93.
36. Caruso M, Moore J, Goodall GJ, et al. Over-expression of cathepsin E and trefoil factor 1 in sessile serrated adenomas of the colorectum identified by gene expression analysis. Virchows Arch 2009; 454: 291-302.
37. Sandmeier D, Benhattar J, Martin P, Bouzourene H. Serrated polyps of the large intestine: a molecular study comparing sessile serrated adenomas and hyperplastic polyps. Histopathology 2009; 55: 206-13.
38. Yachida S, Mudali S, Martin SA, Montgomery EA, Iacobuzio-Donahue CA. Beta-catenin nuclear labeling is a common feature of sessile serrated adenomas and correlates with early neoplastic progression after BRAF activation. Am J Surg Pathol 2009; 33: 1823-32.
39. Mesteri I, Bayer G, Meyer J, et al. Improved molecular classification of serrated lesions of the colon by immunohistochemical detection of *BRAF* V600E. Mod Pathol 2014; 27: 135-44.
40. Rau TT, Agaimy A, Gehoff A, et al. Defined morphological criteria allow reliable diagnosis of colorectal serrated polyps and predict polyp genetics. Virchows Arch 2014; 464: 663-72.
41. Rau TT, Atreya R, Aust D, et al. Inflammatory response in serrated precursor lesions of the colon classified according to WHO entities, clinical parameters and phenotype-genotype correlation. J Pathol Clin Res 2016; 2: 113-24.
42. Fujita K, Yamamoto H, Matsumoto T, et al. Sessile serrated adenoma with early neoplastic progression: a clinicopathologic and molecular study. Am J Surg Pathol 2011; 35: 295-304.
43. Kim KM, Lee EJ, Ha S, et al. Molecular features of colorectal hyperplastic polyps and sessile serrated adenoma/polyps from Korea. Am J Surg Pathol 2011; 35: 1274-86.
44. Maeda T, Suzuki K, Togashi K, et al. Sessile serrated adenoma shares similar genetic and epigenetic features with microsatellite unstable colon cancer in a location-dependent manner. Exp Ther Med 2011; 2: 695-700.
45. Kwon HJ, Cho NY, Chang MS, Kim YS, Kang GH. Intermediate serrated polyp as an intermediate lesion of hyperplastic polyp and sessile serrated polyp/adenoma in terms of morphological and molecular features. Hum Pathol 2014; 45: 1759-65.
46. Morimoto T, Mitomi H, Saito T, et al. Distinct profile of HIF1α, PTCH, EphB2, or DNA repair protein expression and *BRAF* mutation in colorectal serrated adenoma. J Gastroenterol Hepatol 2014; 29: 1192-9.
47. Naito T, Nosho K, Ito M, et al. IGF2 differentially methylated region hypomethylation in relation to pathological and molecular features of serrated lesions. World J Gastroenterol 2014; 20: 10050-61.
48. Qiu Y, Fu X, Zhang W, et al. Prevalence and molecular characterisation of the sessile serrated adenoma in a subset of the Chinese population. J Clin Pathol 2014; 67: 491-8.
49. Lee H, Lee JH, Kim DK, et al. *PIK3CA* amplification is common in left side-tubular adenomas but uncommon sessile serrated adenomas exclusively with *KRAS* mutation. Int J Med Sci 2015; 12: 349-53.
50. Murakami T, Mitomi H, Saito T, et al. Distinct WNT/beta-catenin signaling activation in the serrated neoplasia pathway and the adenoma-carcinoma sequence of the colorectum. Mod Pathol 2015; 28: 146-58.
51. Nosho K, Igarashi H, Ito M, et al. Clinicopathological and molecular characteristics of serrated lesions in Japanese elderly patients. Digestion 2015; 91: 57-63.
52. Tanaka Y, Yamano HO, Yamamoto E, et al. Endoscopic and molecular characterization of colorectal sessile serrated adenoma/polyps with cytologic dysplasia. Gastrointest Endosc 2017; 86: 1131-8.
53. Hashimoto T, Yamashita S, Yoshida H, et al. WNT pathway gene mutations are associated with the presence of dysplasia in colorectal sessile serrated adenoma/polyps. Am J Surg Pathol 2017; 41: 1188-97.
54. Cho H, Hashimoto T, Yoshida H, et al. Reappraisal of the genetic heterogeneity of sessile serrated adenoma/polyp. Histopathology 2018; 73: 672-80.
55. Chan AW, Pan Y, Tong JH, et al. Receptor tyrosine kinase fusions act as a significant alternative driver of the serrated pathway in colorectal cancer development. J Pathol 2020; 251: 74-86.
56. Mochizuka A, Uehara T, Nakamura T, Kobayashi Y, Ota H. Hyperplastic polyps and sessile serrated 'adenomas' of the colon and rectum display gastric pyloric differentiation. Histochem Cell Biol 2007; 128: 445-55.
57. Fujita K, Hirahashi M, Yamamoto H, et al. Mucin core protein expression in serrated polyps of the large intestine. Virchows Arch 2010; 457: 443-9.
58. Gibson JA, Hahn HP, Shahsafaei A, Odze RD. MUC expression in hyperplastic and serrated colonic polyps: lack of specificity of MUC6. Am J Surg Pathol 2011; 35: 742-9.

59. Gonzalo DH, Lai KK, Shadrach B, et al. Gene expression profiling of serrated polyps identifies annexin A10 as a marker of a sessile serrated adenoma/polyp. J Pathol 2013; 230: 420-9.
60. Delker DA, McGettigan BM, Kanth P, et al. RNA sequencing of sessile serrated colon polyps identifies differentially expressed genes and immunohistochemical markers. PLoS One 2014; 9: e88367.
61. Kim JH, Kim KJ, Rhee YY, et al. Gastric-type expression signature in serrated pathway-associated colorectal tumors. Hum Pathol 2015; 46: 643-56.
62. Rickelt S, Condon C, Mana M, et al. Agrin in the muscularis mucosa serves as a biomarker distinguishing hyperplastic polyps from sessile serrated lesions. Clin Cancer Res 2020; 26: 1277-87.
63. Tsai JH, Liau JY, Lin YL, et al. Traditional serrated adenoma has two pathways of neoplastic progression that are distinct from the sessile serrated pathway of colorectal carcinogenesis. Mod Pathol 2014; 27: 1375-85.
64. Bettington ML, Walker NI, Rosty C, et al. A clinicopathological and molecular analysis of 200 traditional serrated adenomas. Mod Pathol 2015; 28: 414-27.
65. Kim MJ, Lee EJ, Suh JP, et al. Traditional serrated adenoma of the colorectum: clinicopathologic implications and endoscopic findings of the precursor lesions. Am J Clin Pathol 2013; 140: 898-911.
66. Chetty R, Hafezi-Bakhtiari S, Serra S, Colling R, Wang LM. Traditional serrated adenomas (TSAs) admixed with other serrated (so-called precursor) polyps and conventional adenomas: a frequent occurrence. J Clin Pathol 2015; 68: 270-3.
67. Hashimoto T, Ogawa R, Yoshida H, et al. Acquisition of WNT pathway gene alterations coincides with the transition from precursor polyps to traditional serrated adenomas. Am J Surg Pathol 2019; 43: 132-9.
68. Borowsky J, Dumenil T, Bettington M, et al. The role of APC in WNT pathway activation in serrated neoplasia. Mod Pathol 2018; 31: 495-504.
69. Sekine S, Yamashita S, Tanabe T, et al. Frequent PTPRK-RSPO3 fusions and RNF43 mutations in colorectal traditional serrated adenoma. J Pathol 2016; 239: 133-8.
70. Sekine S, Ogawa R, Hashimoto T, et al. Comprehensive characterization of RSPO fusions in colorectal traditional serrated adenomas. Histopathology 2017; 71: 601-9.
71. Tsai JH, Liau JY, Yuan CT, et al. RNF43 is an early and specific mutated gene in the serrated pathway, with increased frequency in traditional serrated adenoma and its associated malignancy. Am J Surg Pathol 2016; 40: 1352-9.
72. Hashimoto T, Ogawa R, Yoshida H, et al. EIF3E-RSPO2 and PIEZO1-RSPO2 fusions in colorectal traditional serrated adenoma. Histopathology 2019; 75: 266-73.
73. Sohier P, Sanson R, Leduc M, et al. Proteome analysis of formalin-fixed paraffin-embedded colorectal adenomas reveals the heterogeneous nature of traditional serrated adenomas compared to other colorectal adenomas. J Pathol 2020; 250: 251-61.
74. Phipps AI, Limburg PJ, Baron JA, et al. Association between molecular subtypes of colorectal cancer and patient survival. Gastroenterology 2015; 148: 77-87.
75. Phipps AI, Alwers E, Harrison T, et al. Association between molecular subtypes of colorectal tumors and patient survival, based on pooled analysis of 7 international studies. Gastroenterology 2020; 158: 2158-68.
76. Kim JH, Bae JM, Cho NY, Kang GH. Distinct features between MLH1-methylated and unmethylated colorectal carcinomas with the CpG island methylator phenotype: implications in the serrated neoplasia pathway. Oncotarget 2016; 7: 14095-111.

JPTM
Journal of Pathology and Translational Medicine 2020; 54: 290-299
https://doi.org/10.4132/jptm.2020.05.04

ORIGINAL ARTICLE

Peripheral type squamous cell carcinoma of the lung: clinicopathologic characteristics in comparison to the central type

Yeoun Eun Sung[1], Uiju Cho[2], Kyo Young Lee[1]

[1]Department of Hospital Pathology, Seoul St. Mary's Hospital, College of Medicine, The Catholic University of Korea, Seoul;
[2]Department of Hospital Pathology, St. Vincent's Hospital, College of Medicine, The Catholic University of Korea, Seoul, Korea

Background: Squamous cell carcinomas (SqCCs) of the lung are known to arise more often in a central area but reports of peripheral SqCCs have increased, with a pathogenesis that is obscured. In this study, the clinicopathologic characteristics of peripheral lung SqCCs were studied and compared with those of the central type. **Methods:** This study included 63 peripheral lung SqCCs and 48 randomly selected central cases; hematoxylin and eosin-stained slides of surgically resected specimens were reviewed in conjunction with radiologic images and clinical history. Cytokeratin-7 immunohistochemical staining of key slides and epidermal growth factor receptor (*EGFR*)/*KRAS* mutations tested by DNA sequencing were also included. **Results:** Stages of peripheral SqCCs were significantly lower than central SqCCs (p=.016). Cystic change of the mass (p=.007), presence of interstitial fibrosis (p=0.007), and anthracosis (p=.049) in the background lung were significantly associated with the peripheral type. Cytokeratin-7 positivity was also higher in peripheral SqCCs with cutoffs of both 10% and 50% (p=.011). Pathogenic mutations in *EGFR* and *KRAS* were observed in only one case out of the 72 evaluated. The Cox proportional hazard model indicated a significantly better disease-free survival (p=.009) and the tendency of better overall survival (p=.106) in the peripheral type. **Conclusions:** In peripheral type, lower stage is a favorable factor for survival but more frequent interstitial fibrosis and older age are unfavorable factors. Multivariate Cox analysis revealed that peripheral type is associated with better disease-free survival. The pathogenesis of peripheral lung SqCCs needs further investigation, together with consideration of the background lung conditions.

Key Words: Squamous cell carcinoma; Lung neoplasms; Peripheral; Cytokeratin-7

Received: December 24, 2019 **Revised:** April 10, 2020 **Accepted:** May 4, 2020
Corresponding Author: Kyo Young Lee, MD, Department of Hospital Pathology, Seoul St. Mary's Hospital, College of Medicine, The Catholic University of Korea, 222 Banpo-daero, Seocho-gu, Seoul 06591, Korea
Tel: +82-2-2258-1618, Fax: +82-2-2258-1627, E-mail: leekyoyo@catholic.ac.kr

Lung cancer is known to be the leading cause of cancer fatalities worldwide, in both developed and less developed countries [1]. Squamous cell carcinoma (SqCC) is one of the major non-small cell lung carcinomas and can be classified according to the location of the tumor into either a central or peripheral type [2]. About one-third of SqCCs are known to arise from the periphery, while the majority of SqCCs are associated with the central portion of the lung [2]. More recently, the peripheral type of SqCCs has been reported to increase, and now comprise approximately one-half of the SqCCs of the lung [3,4]. Multistage pathogenesis of SqCC arising in the central airway epithelium is known, with several sequential molecular abnormalities; starting at the normal epithelium, through squamous metaplasia, dysplasia, and carcinoma in situ [5]. Several sequential molecular abnormalities are recognized, including 3p loss of heterozygosity, 9p loss of heterozygosity, telomerase activation, methylation of tumor suppressor gene, and 5q loss of heterozygosity, that contribute to the development of invasive carcinoma [5]. On the other hand, the exact etiology of peripheral SqCCs remains unknown, with only a few studies of molecular events associated with peripheral SqCCs using animal models [6,7]. Although peripheral lung SqCCs have been investigated [3,8-10], the studies are limited in number with partly inconsistent results. In this study, we tried to reveal the clinicopathologic, immunohistochemical (cytokeratin-7), and molecular (epidermal growth factor receptor [*EGFR*] and *KRAS*) characteristics of the peripheral type of SqCCs, and compared them to the central type. Not only the tumor but also the background lung condition was in-

pISSN 2383-7837
eISSN 2383-7845

cluded as the object of research. Furthermore, this study aimed to see if any of the findings suggested some indication of the pathogenesis or associated factors of peripheral SqCCs.

MATERIALS AND METHODS

Study subjects

Patients with surgically resected specimens of lung SqCC from January 2011 to December 2013 at Seoul St. Mary's Hospital were reviewed. Specimens of patients who had received neoadjuvant chemotherapy or radiotherapy for SqCC or had a previous malignancy at other sites were excluded. In total, 63 cases of peripheral SqCC, with clinical history, radiologic data, and immunohistochemical study available, were included. As well as these 63 peripheral SqCCs, 48 randomly selected non-peripheral SqCCs (central SqCC) were also included in this study, for comparison. Peripheral SqCC was defined as SqCC located at or distal to subsegmental bronchi [3,11], based on both radiologic images and pathologic findings. The survival length was defined as the interval in months between the day of surgical resection and the date of either the last follow-up or death. Each cause of death was reviewed to exclude death due to any other cause.

Pathological studies

The surgically resected specimens for SqCCs were fixed routinely in 10% formalin, followed by embedding in paraffin, 4-micron sectioning, and hematoxylin and eosin (H&E) staining. The determination of histological classification and TNM classification was based on the World Health Organization classification (2015) [5]; Verhoeff-Van Gieson Elastic staining was additionally done with the cases in need for pleural status evaluation. The presence of the adenocarcinoma component was evaluated by morphological features of adenocarcinoma, in conjunction with immunohistochemical studies of thyroid transcription factor-1 (TTF-1) (Fig. 1A–C). Adenosquamous carcinoma, which requires at least 10% of both an adenocarcinoma and SqCC component, was excluded. Cystic change in the mass was defined as a definite presence of cystic space inside the mass lesion, revealed in computed tomography (CT) images and/or gross examination of the resected specimens (Fig. 1D–F). Interstitial fibrosis, including usual interstitial pneumonia (idiopathic pulmonary fibrosis) (Fig. 1G–I), emphysema, bronchiectasis, and anthracosis (Fig. 1J) were decided by characteristic histologic findings, with or without concomitant radiological evidence. The occupational history of the patients was reviewed for evaluation of pneumoconiosis, with applicable CT images and evidence of histological findings (Fig. 1K, L). History of tuberculosis was also reviewed with radiologic and/or pathologic evidence of tuberculous scars.

Antibodies and immunohistochemical studies with evaluation

Among the 111 cases, immunohistochemical studies were available for 105 cases (94.6%); 61 peripheral SqCCs (61 out of 63, 96.8%) and 44 central SqCCs (44 out of 48, 91.7%). Six cases were excluded due to the absence of preexisting informed consent for the further use of their human-derived materials. Immunohistochemical staining was performed with antibodies of TTF-1 (1:200, clone SPT24, Novo, Newcastle upon Tyne, UK) and cytokeratin-7 (CK7; 1:50, clone OV-TL 12/30, Dako, Glostrup, Denmark). TTF-1 analysis was integrated as part of evaluating glandular component of SqCCs, as previously described. Each glandular morphology by H&E staining was confirmed by TTF-1 positivity. Representative sections of each SqCC were stained for CK7, which were interpreted and categorized as negative (0%), focally positive (+1, < 10%; +2, 10%–50%), and positive (+3, ≥ 50%). For SqCC cases containing a focal glandular (adenocarcinoma) component, CK7 positivity was evaluated only in the SqCC component.

Molecular studies

Among the 111 cases, molecular studies. including assessment of *EGFR* and *KRAS*, were performed in 72 (64.9%) of the patients, who consented to the test performance: 44 peripheral SqCCs (44 out of 63, 69.8%) and 28 central SqCCs (28 out of 48, 58.3%). DNA was extracted from formalin-fixed paraffin-embedded specimens by using a Maxwell 16 Tissue DNA Purification Kit (Promega, Madison, WI, USA) following the manual. Polymerase chain reaction (PCR) was performed by using Qiagen HotStar Taq DNA Polymerase (Qiagen, Hilden, Germany). The forward sequencing primers used were 5'-ACTGCTTTCCAGCATGGTGAGG-3' for *EGFR* exon 18, 5'-GTGGCACCATCTCACAATTGCC-3' for *EGFR* exon 19, 5'-ATGCGTCTTCACCTGGAAGG-3' for *EGFR* exon 20, 5'-CCTGAATTCGGATGCAGAGCTTC-3' for *EGFR* exon 21, 5'-GGTGAGTTTGTATTAAAAGG-3' for *KRAS* exon 2 and 5'-GGTGCACTGTAATAATCCAGAC-3' for *KRAS* exon 3. PCR conditions consisted of initial denaturing at 95°C for 5 minutes, 40 cycles at 94°C for 30 seconds, at 60°C (*EGFR* exon 18) or 57°C (*EGFR* exon 19, 20, and 21) or 50°C (*KRAS* exon 2 and 3) for 30 seconds, at 72°C for 30 seconds and a final extension at 72°C for 7 minutes. The PCR products were sequenced using the BigDye Terminator v3.1 Cycle Sequencing kit (Applied

Biosystems, Foster City, CA, USA), according to the manufacturer's instructions.

Statistical analysis

IBM SPSS ver. 22.0 (IBM Corp., Armonk, NY, USA) and R ver. 3.6.2 [12] was used for statistical analysis in this study. The correlation between each type of lung SqCC and clinicopatho-

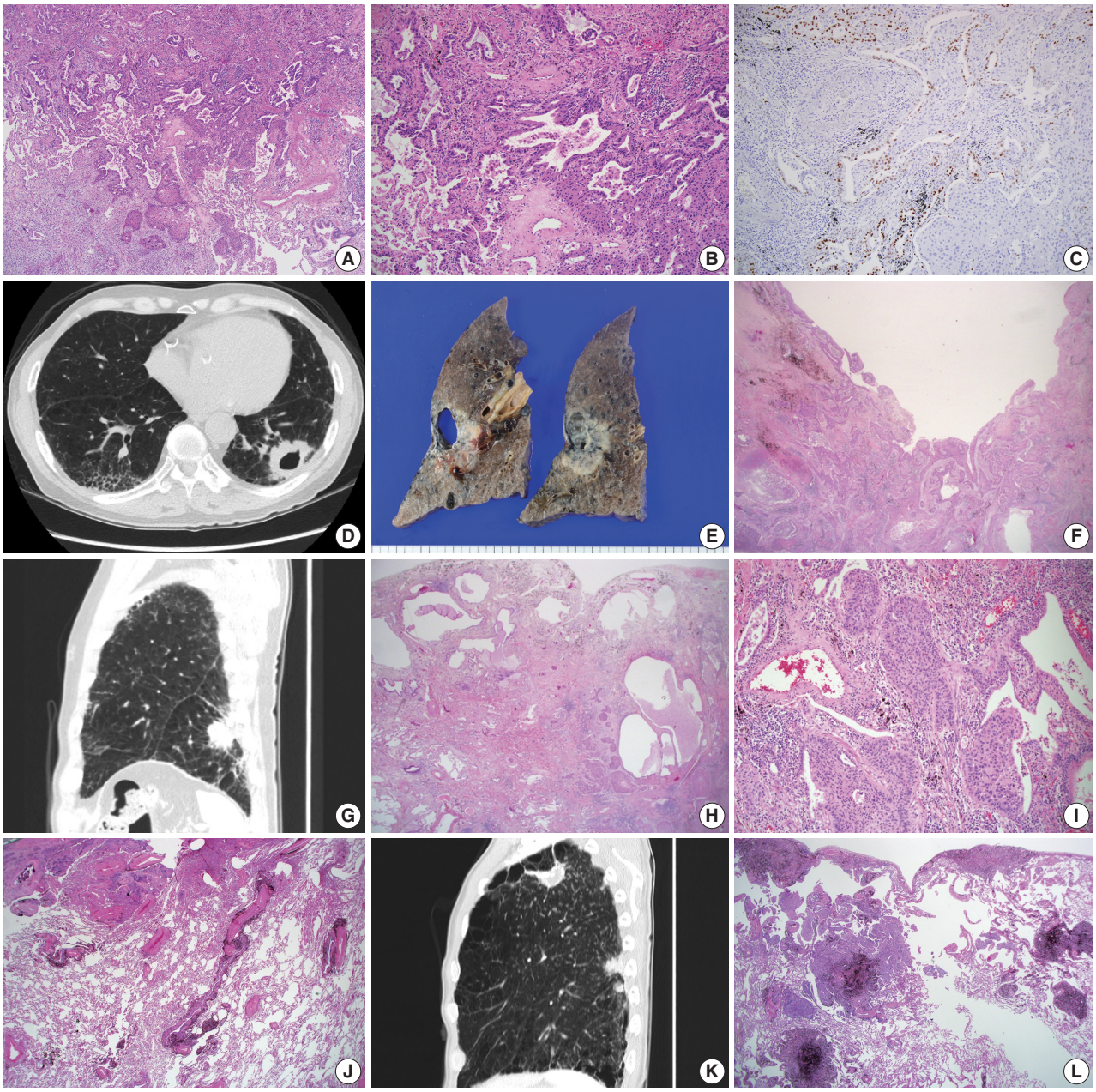

Fig. 1. Clinicopathologic characteristics of peripheral lung squamous cell carcinoma. (A–C) Microscopic findings of the glandular component (adenocarcinoma component) in peripheral squamous cell carcinoma of the lung: H&E staining (A, B) and thyroid transcription factor-1 immunohistochemical staining (C). (D–F) Radiologic and pathologic images of cystic change of the mass: computed tomography (CT) image of the chest (D), gross examination (E), and H&E staining (F). (G–I) Interstitial fibrosis, especially usual interstitial pneumonia with squamous cell carcinoma in the peripheral lung; CT image showing coarse reticulation with honeycombing and mass in the lower lobe of the lung (G), H&E staining (H, I). (J) Overall anthracosis coexisting with squamous cell carcinoma in the left upper area of the image. (K, L) Peripheral squamous cell carcinoma in pneumoconiosis lung: CT image (K) and H&E staining (L) showing progressive massive fibrosis with irregular mass at the subpleural portion of the left lower lobe.

https://doi.org/10.4132/jptm.2020.05.04

logic data was evaluated by the chi-square test for discrete variables. For variables having an expected count of less than 5, Fisher exact test was used. The continuous variables including age and smoking history (pack years) were first tested by the Shapiro-Wilk normality test, and analyzed by the Wilcoxon rank-sum test. Immunohistochemical study with CK7 was finally categorized as 0%–10% versus ≥10% and <50% versus ≥50%, both analyzed by the chi-square test. The length of survival was defined as the interval between the day of surgical resection and the date of death or the last follow-up, in months; 40 deaths occurred and the median follow-up period was 35.3 months. Survival analysis was done by Kaplan-Meier curve and Cox proportional hazard model. Every factor and feature was analyzed individually, followed by the analysis of selected factors using the Cox proportional hazard model. In all instances, a $p \leq .05$ was considered statistically significant.

RESULTS

The clinicopathologic characteristics of the 63 peripheral and 48 central lung SqCCs are summarized in Table 1. The median age of patients with peripheral or central SqCC was 70 (range, 65 to 74) and 68 (range, 58 to 72), respectively, with male predominance in both types (93.7% and 97.9%). The age of pe-

Table 1. Clinicopathologic characteristics of peripheral and central squamous cell carcinoma of the lung

Characteristic	Peripheral (n=63)	Central (n=48)	p-value
Age (yr)	70 (65–74)	68 (58.5–72)	.037[a]
Sex			.387
Male	59 (93.7)	47 (97.9)	
Female	4 (6.3)	1 (2.1)	
Smoking (pack year)	35 (20–50)	40 (28–50)	.629[a]
T category			.412
T1	25 (39.7)	21 (43.7)	
T2	31 (49.2)	25 (52.1)	
≥T3	7 (11.1)	2 (4.2)	
N category			<.001
N0	52 (82.5)	22 (45.8)	
≥N1	11 (17.5)	26 (54.2)	
Stage			.016
I	41 (65.1)	19 (39.6)	
II	18 (28.6)	20 (41.7)	
≥III	4 (6.3)	9 (18.8)	
Pathologic features			
Adenocarcinoma component	6 (9.5)	2 (4.2)	.462
Cystic change of the mass	16 (25.4)	3 (6.3)	.007
Interstitial fibrosis	22 (32.9)	6 (12.5)	.007
Emphysema	37 (58.7)	24 (50)	.360
Bronchiectasis	3 (4.8)	0	.257
Anthracosis	35 (55.6)	18 (37.5)	.049
Pneumoconiosis	5 (7.9)	1 (2.1)	.232
Tuberculosis history and/or lung scar	18 (28.6)	9 (18.8)	.232
Cytokeratin-7 (%)			.011
0–10	30/61 (49.2)	32/44 (72.7)	
10–50	12/61 (19.7)	8/44 (18.2)	
50–100	19/61 (31.1)	4/44 (9.1)	
Metastasis and/or recur and/or death			.063[b]
Event	23 (36.5)	27 (56.2)	
Disease-free survival	25.0 (11.0–50.5)	35.0 (22.0–48.5)	
Death			.487[b]
Event	21 (33.3)	19 (39.6)	
Overall survival	37.0 (29.0–49.0)	33.5 (19.5–53.5)	

Values are presented as median (interquartile range) or number (%).
Statistical analysis method: Pearson chi-square test and Fisher exact test.
[a]Wilcoxon rank-sum test; [b]Kaplan-Meier method.

ripheral SqCC patients was significantly older than that of the central type (p = .037), with no difference in sex ratio between the two groups (p = .387). Among the 111 patients included, 96 were smokers, with a median smoking history of 35 pack year (range, 20 to 50) in peripheral SqCC and 40 pack year (range, 28 to 50) in central SqCC. Neither the ratio of smokers to nonsmokers nor the period of smoking was associated with SqCC lung location (p = .629). Although T category did not show any difference between the two types, the frequency of lymph node metastases (N category, ≥N1) was lower in the peripheral type than in the central type (17.5% vs. 54.2%, p < .001; odds ratio, 0.179; 95% confidence interval [CI], 0.075 to 0.424). The overall stage evaluated by T, N, and M of each case showed differences between the two types, with a low-stage more frequent in patients with the peripheral type (p = .016).

Among the pathologic features studied, peripheral SqCC was associated with a more frequent cystic change of the mass (25.4% vs. 6.3%, p = .007; odds ratio, 5.217; 95% CI, 1.422 to 19.140). For evaluation of interstitial fibrosis, not only pathologic findings but also clinical aspects were considered. Cases with definite histologic features of interstitial fibrosis showing various or uniform stages were included, but some cases with characteristic radiologic findings including honeycomb pattern were also considered to be in the 'interstitial fibrosis' group if they had consistent pathologic findings. Most of the interstitial fibrosis cases were usual interstitial pneumonia and the presence or absence of interstitial fibrosis was significantly different between the two groups (32.9% vs. 12.5%, p = .007; odds ratio, 3.756; 95% CI, 1.382 to 10.210). Anthracosis was also more frequently found in peripheral type SqCCs (55.6% vs. 3.5%, p = .049; odds ratio, 2.160; 95% CI, 1.000 to 4.668), compared to central SqCCs. TTF-1 immunohistochemical studies were interpreted in conjunction with glandular morphologic features, to evaluate the adenocarcinoma component. The presence of the adenocarcinoma component was analyzed for each case and the difference was found to be statistically insignificant between the peripheral and central type. The remaining features, including the presence of emphysema, bronchiectasis, pneumoconiosis, and tuberculosis history were also statistically unrelated to either type of lung SqCCs.

CK7 immunohistochemical results were categorized as 0%–10%, 10%–50%, and 50%–100%, according to the proportion of positive tumor cells out of the total number of tumor cells, as summarized in Table 1. Representative images of each proportional group are shown in Fig. 2. The proportion of each group was significantly different between peripheral and central SqCCs (p = .011), with higher CK7 expression in peripheral SqCC. The result was the same when dividing cases of each location into two subgroups with different cutoffs; with 10% cutoff (0%–10% vs. 10%–100%, p=.036); with 50% cutoff (0%–5% vs. 50%–100%, p = .007). Furthermore, we analyzed if there was any correlation between CK7 positivity and survival in each group. For peripheral SqCCs, there existed no difference in overall survival according to CK7 expression (p = .912 in the 10%–50% group and p = .915 in the 50%–100% group). However, for central SqCCs, higher CK7 positivity was associated with worse overall survival (p = .041 in the 10%–50% group and p = .022 in the 50%–100% group).

Molecular changes in *EGFR* existed in four out of 44 evaluated peripheral SqCCs and four out of 28 evaluated central peripheral SqCCs; seven out of eight cases harbored silent mutations, mostly the exon 20 Gln787Gln (c.2361G > A) polymorphism (Table 2). Only one case (case No. 3) showed pathogenic mutation; exon 18 Glu709Gly (c.2126A > G) mutation with concomitant exon 19 Leu747_Thr751del (c.2240_2254del) (Table 2). *KRAS* mutation was detected in 1 out of 28 central

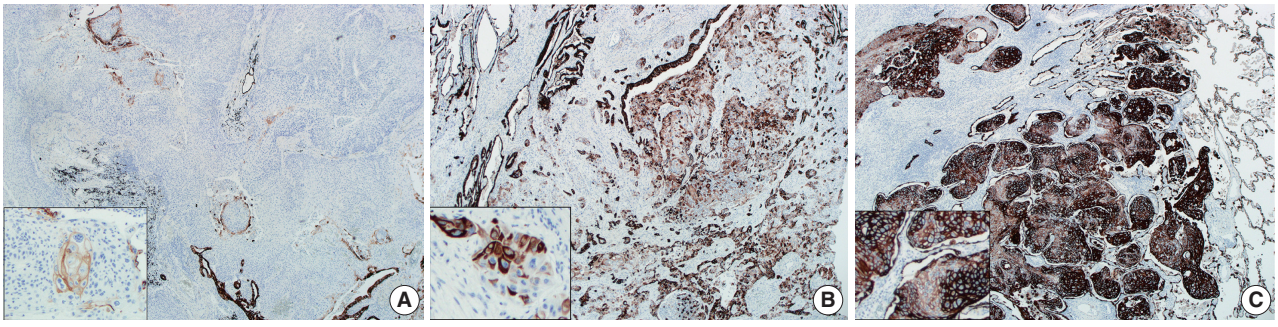

Fig. 2. Cytokeratin-7 (CK7) immunohistochemical staining of squamous cell carcinoma of the lung. (A) Less than 10% positivity of tumor cells. Entrapped normal bronchial cells (right lower area) are excluded from the evaluation. (B) Between 10%–50% CK7 positivity of tumor cells, with entrapped normal bronchial cells and pneumocytes in the left and upper area. (C) More than 50% CK7 positivity of tumor cells, with strong intensity.

https://doi.org/10.4132/jptm.2020.05.04

Table 2. Molecular studies for *EGFR* and *KRAS* of peripheral and central squamous cell carcinoma of the lung

	Peripheral	Central
EGFR mutation		
Case No. 1	Exon 20 Gln787Gln (c.2361G>A) polymorphism	-
Case No. 3	- Exon 18 Glu709Gly (c.2126A>G) mutation - Exon 19 Leu747_Thr751del (c.2240_2254del)	-
Case No. 7	-	Exon 20 Gln787Gln (c.2361G>A) polymorphism
Case No. 57	-	Exon 20 Gln787Gln (c.2361G>A) polymorphism
Case No. 60	-	Exon 20 Gln787Gln (c.2361G>A) polymorphism
Case No. 61	Exon 18 Thr725Thr (c.2175G>A) polymorphism	-
Case No. 80	Exon 20 Gln787Gln (c.2361G>A) polymorphism	-
Case No. 97	-	Exon 20 Gln787Gln (c.2361G>A) polymorphism Intron 19 (c.2284-60T>C) polymorphism
KRAS mutation		
Case No. 56	-	Gly12Val (c.35G>T) mutation

EGFR, epidermal growth factor receptor.

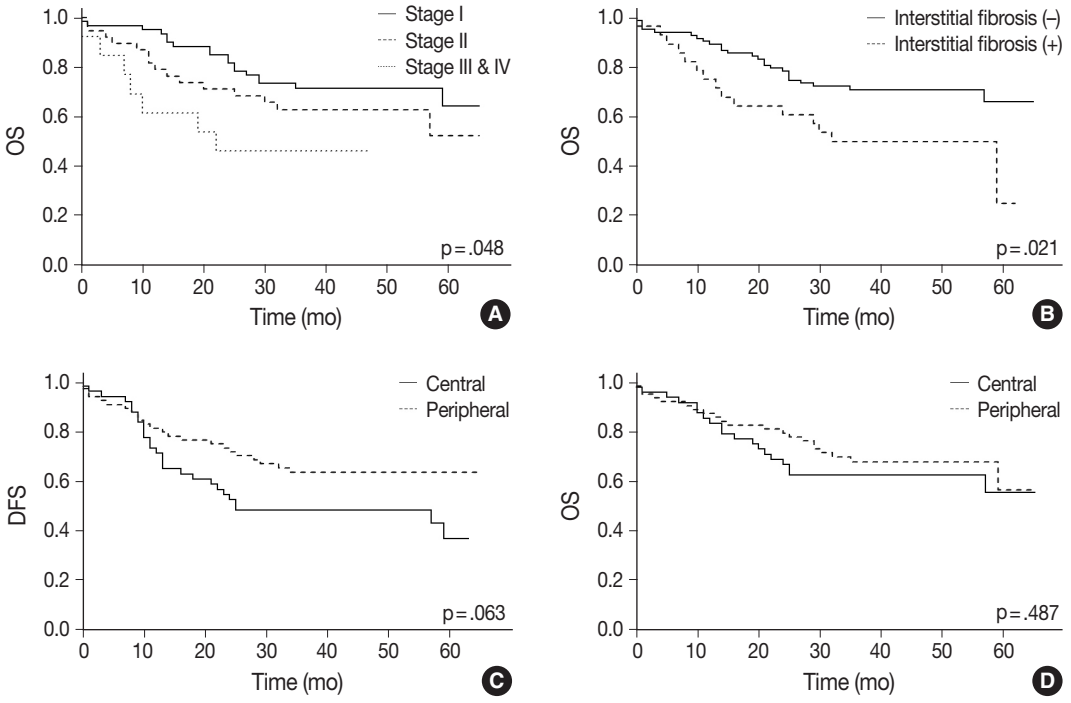

Fig. 3. Survival analysis by Kaplan-Meier curves (A) Overall survival of each stage; stage I, including stage IA and IB; sage II, including stage IIA and IIB; stage III & IV, including IIIA, IIIB, and IV. (B) Overall survival according to the presence or absence of interstitial fibrosis; the presence of interstitial fibrosis was significantly associated with poor survival (p=.021). (C, D) Disease-free survival (DFS) (C) and overall survival (OS) (D) according to the peripheral or central type of lung squamous cell carcinoma (SqCC); peripheral SqCC had a tendency of better DFS, but the result was statistically not significant (p=.063); there was no significant difference in OS (p=.487).

SqCCs and not found in peripheral SqCCs; the mutated case (case No. 56) harbored a Gly12Val (c.35G>T) mutation (Table 2).

A Kaplan-Meier curve of overall survival according to stages is shown in Fig. 3A. Sex and smoking history were not significantly associated with survival. Among the pathologic features listed in Table 1, only interstitial fibrosis revealed to be a significant prognosticator of overall survival; patients having interstitial fibrosis showed worse overall survival compared to those without it (p=.021) (Fig. 3B). Patients with peripheral SqCC had a tendency of better disease-free survival (Fig. 3C) but the result was not statistically significant (p=.063). There was no difference in overall survival between peripheral and central lung SqCCs (p=.487) (Fig. 3D).

Based on the results obtained, the Cox proportional hazard procedure was used for further analysis. The included variables were age and stage, as well-known prognosticators, the variables

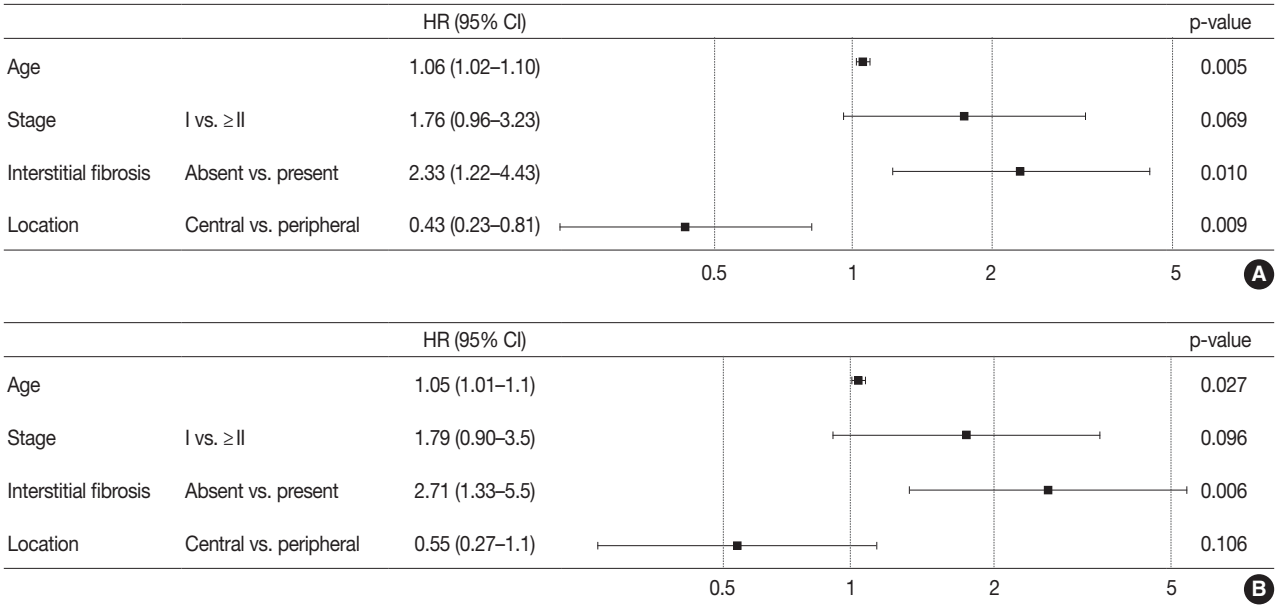

Fig. 4. Hazard ratio by Cox proportional hazard model analyzed for disease-free survival (DFS) (A) and overall survival (OS) (B). Peripheral lung squamous cell carcinoma (SqCC) was significantly associated with a better prognosis (hazard ratio [HR], 0.43; 95% confidence interval [95% CI], 0.23 to 0.81; p = .009). It also had a tendency of better OS (HR, 0.55; 95% CI, 0.27 to 1.10) but was not statistically significant (p = .106).

revealed to be different between the two groups, and interstitial fibrosis. Patients with peripheral lung SqCC showed a tendency of better overall survival (hazard ratio, 0.55; 95% CI, 0.27 to 1.1) but this was not statistically significant (p = .106) (Fig. 4). However, in disease-free survival, peripheral lung SqCC was significantly associated with better prognosis (hazard ratio 0.43; 95% CI, 0.23 to 0.81; p = .009) (Fig. 4).

DISCUSSION

In the current study, we first investigated clinicopathologic features of peripheral and central lung SqCC (Table 1). The age of patients was significantly different between the two groups (p = .037), which is consistent with two previous studies that found patients with peripheral lung SqCC were older [3,10]. T categories were not significantly different between the two types, whereas the N category of the peripheral type was significantly lower than the central type (p < .001). The tendency of lower lymph node metastases in the peripheral type was previously confirmed in one study by Funai et al. [3]; however, another study revealed no difference in metastases between the peripheral and central type [10]. In this study, the overall stage, evaluated from the T, N, and M category, was also different between the two types, probably due to lower lymph node metastasis in peripheral lung SqCC. The possibility cannot be ruled out that a lower N category, in the setting of the same T category, is caused by a greater physical distance from the main mass to mediastinal lymph nodes, in the peripheral SqCC.

Adenosquamous carcinoma is known to typically arise in the peripheral pulmonary parenchyma, with some cases reported to be located centrally [5]. We evaluated all the cases to determine there was a glandular component (adenocarcinoma component) in up to 10% of the tumors (Fig. 1A–C). An adenocarcinoma component was observed in 9.5% (6 out of 63 cases) and 4.2% (2 out of 48 cases) in peripheral and central lung SqCCs, respectively (Table 1). However, statistical analysis with Fisher's exact test revealed no significant difference, probably due to the limited number of cases.

There existed more frequent cystic change of the mass in peripheral type SqCCs than in central type (25.4% vs. 6.3%, p = .007), which was confirmed by both CT images and gross examination, along with microscopic findings in each case (Fig. 1D–F). Cystic change of lung cancers has been studied by several researchers of radiology [13,14]. The majority of the data consisted of adenocarcinoma. The cystic lesions were considered to include emphysematous bullae, congenital or fibrotic cysts, bronchiectatic airways, and distended distal airspaces [13]. In the current study, microscopic findings of the masses with cystic change revealed an empty space lined by SqCC cells or partly suspicious for SqCC in situ (Fig. 1F). With gross examination and CT images of some cases, the cystic lesion was suspected to have been previously bronchiolar airway, of which the proximal portion was

https://doi.org/10.4132/jptm.2020.05.04

blocked by a mass effect. Cystic change due to necrosis was scarce in this study. It is possible to assume that the lower proportion of cystic change in central lung SqCCs might be due to a relatively larger airway diameter obstructed by the mass. It might be noteworthy that differential diagnoses of solid masses with cystic change in the lung should include SqCC, especially those located in the peripheral area of the lung.

In the investigation of pathologic features of background lung, we focused on the diffuse and overall change of lung, in conjunction with CT images. Among those reviewed, the presence of interstitial fibrosis (Fig. 1G–I) and anthracosis (Fig. 1J) were more associated with the peripheral type than the central type of SqCCs (32.9% vs. 12.5%, p = .007; 55.6% vs. 37.5%, p = .049) (Table 1). Interstitial fibrosis cases included in this study were mostly of the usual interstitial pneumonia pattern. With the established multistage pathogenesis of SqCCs, which includes morphological changes from normal epithelium through to squamous metaplasia, dysplasia, and carcinoma in situ in the central bronchial area [5], it is possible to assume that similar pathogenic events may occur in the peripheral area of the lung parenchyma if it has undergone bronchial metaplasia. In the peripheral SqCC cases with simultaneous interstitial fibrosis, SqCCs usually coexisted with interstitial fibrosis and bronchial metaplasia (Fig. 1H, I), although the sequential morphologic change from dysplasia or carcinoma in situ to SqCC was not sufficient to be verified microscopically.

Some authors have proposed several growth patterns for the peripheral SqCC of the lung, including pushing patterns, infiltrative patterns, alveolar filling patterns, and pseudoalveolar filling patterns [15] or an alveolar space-filling type, expanding type, and combined type [3]. These previous studies suggest that the alveolar filling growth pattern might be associated with a better prognosis [3,15]. However, in the current study, it seemed reasonable to consider the presence of diffuse interstitial fibrosis, including usual interstitial pneumonia, in evaluating peripheral SqCC of the lung for the following two reasons: (1) interstitial fibrosis might be more frequently associated with the peripheral type of SqCC than the central type and (2) for the cases of background fibrotic lung, certain growth patterns such as the alveolar filling pattern may be impossible.

In regards to the background condition of the lung, we also investigated the presence of emphysema, bronchiectasis, pneumoconiosis, and histologic evidence of past tuberculosis with or without a clinical history of tuberculosis, all of which revealed to be of no significant relevance with either type of lung SqCC (Table 1). Among these, the presence of emphysema, which was reported to be relevant to peripheral type SqCC in one previous study [9], did not show significant association in the current study (p = .360). Especially, patients with pneumoconiosis whose lungs show multiple scattered fibrotic nodules were hypothesized initially to have an association with peripheral type SqCCs, as interstitial fibrosis or anthracosis. There were five pneumoconiosis cases out of 63 peripheral SqCCs (7.9%) and one case out of 48 central SqCCs (2.1%). The statistical results may be due to the limited number of pneumoconiosis cases included as well as rare epidemiology. A further large-scale study with a greater number of patients might be necessary.

CK7 expression is usually considered a characteristic feature of adenocarcinoma of various origin sites, including lung, biliary tract, pancreas, salivary gland, breast, ovary, and endometrium [16-18]. Relatively less studied in SqCC, CK7 is known to be positive in more than 20% of lung SqCCs according to a previous study [19]. In esophageal SqCCs, a group of researchers revealed an association between CK7 expression and poor prognosis [20]. No such study was found for the prognostic significance of CK7 positivity in lung SqCC. However, the difference in immunohistochemical staining between the peripheral and central type of lung SqCCs was included in a few previous studies; CK7 expression was more frequently observed in the peripheral type in one study [10], while there was no difference between the two types in another study [9]. In both studies, tissue microarrays were evaluated. In the current study, whole slides of each key block in all tumors were stained with CK7 and overall a heterogenous staining pattern was obtained. Therefore, we interpreted CK7 staining with categorization according to the proportion of positive tumor cells out of the entire number of tumor cells as 0%–10%, 10%–50%, and 50%–100% (Fig. 2). With cutoffs of both 10% and 50%, significantly more CK7 positivity in peripheral type lung SqCC was confirmed (Table 1). It was notable that with a cutoff of 10%, 47.5% of peripheral type lung SqCC showed CK7 positivity.

As CK7 expression was evaluated in only SqCC, even in the cases containing a focal adenocarcinoma component, the difference of CK7 expression between peripheral and central groups was not associated with the glandular component. Additionally, the presence of the focal adenocarcinoma component was not significantly different between the two groups, as shown in Table 1. CK7 expression was observed not only in various percentages but also with various intensity, as shown in Fig. 2. The fact that adenosquamous carcinoma frequently arises in the peripheral area [5] and that an adenocarcinoma component of up to 10% was observed in a proportion of peripheral SqCC in this study,

although not significant, suggests some association. A weak to moderate, and even strong, expression of CK7 in peripheral SqCC might suggest a different biologic and/or molecular aspect from central SqCC. This possible difference needs further study and probably needs to be separated from the cases accompanying interstitial fibrosis. Furthermore, the survival analysis according to CK7 expression in each location revealed high CK7 expression was associated with worse overall survival in central SqCC, with no survival difference in peripheral SqCC. Although this finding might suggest a new prognostic aspect of CK7 in central SqCC, it is limited by a relatively small number of samples (44 central SqCCs) and the fact that there was no difference in disease-free survival in both central and peripheral SqCCs.

According to previous studies, the *EGFR* and *KRAS* mutation in lung SqCC is sparse and reported in less than 5% of all patients [5]. In the current study, though some polymorphism was observed in several cases, only one case in the peripheral type harbored the *EGFR* mutation and another case in the central type had a *KRAS* mutation (Table 2). Until now, the molecular difference between the two types of SqCC has not been studied. This study has limitations in that only a portion of the cases collected were the object of molecular tests. For further investigation, studies with a much larger number of cases might be necessary, opening the possibility of assessing novel molecular events of peripheral type SqCCs of the lung other than *EGFR* or *KRAS* mutations.

With Kaplan-Meier curves, peripheral lung SqCC did not show a significant difference in survival, although the slight tendency of a better DFS was suggested (Fig. 3C, D). We hypothesized that a lower TNM stage in peripheral SqCC is a favorable factor, but more frequent interstitial fibrosis and older age are counteracting factors. This could be verified by the Cox proportional hazard model, which revealed an association with better survival after adjustment for age, stage, and the presence of interstitial fibrosis (Fig. 4).

In conclusion, the current study suggests that peripheral type lung SqCC is possibly different from the central type in clinicopathologic aspects, with lower lymph node metastasis but more frequently accompanying interstitial fibrosis and anthracosis in the background lung. In addition, a cystic change in the mass is more commonly observed in the peripheral type, which can be evaluated by CT images preoperatively and also with gross examination after surgery. Immunohistochemically, the peripheral type shows more tendency of CK7 staining, which has been known to be positive in only a minority of SqCC. Some of the cases in our study revealed rare *EGFR* and *KRAS* mutations in both types. The peripheral type of lung SqCCs may have different pathogenic events from that of the central type, which needs further investigation with a larger set of cases. We believe the current study could be considered with further investigation and expect the information to be reflected eventually in patient care.

Ethics Statement

All procedures performed in the current study were approved by the Institutional Review Boards (IRB) of the Catholic Medical Center Office of Human Research Protection Program (KC15SISI0146) in accordance with the 1964 Helsinki declaration and its later amendments. Formal written informed consent was not required with a waiver by the appropriate IRB and/or national research ethics committee.

ORCID

Yeoun Eun Sung https://orcid.org/0000-0002-9408-0085
Uiju Cho https://orcid.org/0000-0002-6229-8418
Kyo Young Lee https://orcid.org/0000-0001-9954-8583

Author Contributions

Conceptualization: KYL. Data curation: UC, YES. Formal analysis: UC, YES. Investigation: UC, YES, KYL. Methodology: KYL. Project administration: UC, YES. Resources: UC, YES. Supervision: KYL. Validation: KYL. Visualization: YES. Writing—original draft: YES. Writing—review & editing: UC, YES, KYL. Approval of final manuscript: all authors.

Conflicts of Interest

The authors declare that they have no potential conflicts of interest.

Funding Statement

No funding to declare.

References

1. Torre LA, Bray F, Siegel RL, Ferlay J, Lortet-Tieulent J, Jemal A. Global cancer statistics, 2012. CA Cancer J Clin 2015; 65: 87-108.
2. Colby TV, Koss KM, Travis WD. Tumors of the lower respiratory tract, fascicle 13. Washington, DC: Armed Forces Institute of Pathology, 1995.
3. Funai K, Yokose T, Ishii G, et al. Clinicopathologic characteristics of peripheral squamous cell carcinoma of the lung. Am J Surg Pathol 2003; 27: 978-84.
4. Brooks DR, Austin JH, Heelan RT, et al. Influence of type of cigarette on peripheral versus central lung cancer. Cancer Epidemiol Biomarkers Prev 2005; 14: 576-81.
5. Travis WD, Brambilla E, Burke AP, Marx A, Nicholson AG. WHO classification of tumours of the lung, pleura, thymus and heart. Lyon: International Agency for Research on Cancer (IARC), 2015.
6. Yamano S, Gi M, Tago Y, et al. Role of deltaNp63(pos)CD44v(pos) cells in the development of N-nitroso-tris-chloroethylurea-induced peripheral-type mouse lung squamous cell carcinomas. Cancer Sci 2016; 107: 123-32.
7. Dai YB, Miao YF, Wu WF, et al. Ablation of Liver X receptors alpha and beta leads to spontaneous peripheral squamous cell lung cancer in mice. Proc Natl Acad Sci U S A 2016; 113: 7614-9.
8. Sakurai H, Asamura H, Watanabe S, Suzuki K, Tsuchiya R. Clinicopathologic features of peripheral squamous cell carcinoma of the lung. Ann Thorac Surg 2004; 78: 222-7.

9. Hayashi T, Sano H, Egashira R, et al. Difference of morphology and immunophenotype between central and peripheral squamous cell carcinomas of the lung. Biomed Res Int 2013; 2013: 157838.
10. Saijo T, Ishii G, Nagai K, et al. Differences in clinicopathological and biological features between central-type and peripheral-type squamous cell carcinoma of the lung. Lung Cancer 2006; 52: 37-45.
11. Shimosato Y, Suzuki A, Hashimoto T, et al. Prognostic implications of fibrotic focus (scar) in small peripheral lung cancers. Am J Surg Pathol 1980; 4: 365-73.
12. R Core Team. R: a language and environment for statistical computing [Internet]. Vienna: R Foundation for Statistical Computing, 2018 [cited 2019 Dec 24]. Available from: https://www.R-project.org/.
13. Sheard S, Moser J, Sayer C, Stefanidis K, Devaraj A, Vlahos I. Lung cancers associated with cystic airspaces: underrecognized features of early disease. Radiographics 2018; 38: 704-17.
14. Mascalchi M, Attina D, Bertelli E, et al. Lung cancer associated with cystic airspaces. J Comput Assist Tomogr 2015; 39: 102-8.
15. Yousem SA. Peripheral squamous cell carcinoma of lung: patterns of growth with particular focus on airspace filling. Hum Pathol 2009; 40: 861-7.
16. van de Molengraft FJ, van Niekerk CC, Jap PH, Poels LG. OV-TL 12/30 (keratin 7 antibody) is a marker of glandular differentiation in lung cancer. Histopathology 1993; 22: 35-8.
17. Baars JH, De Ruijter JL, Smedts F, et al. The applicability of a keratin 7 monoclonal antibody in routinely Papanicolaou-stained cytologic specimens for the differential diagnosis of carcinomas. Am J Clin Pathol 1994; 101: 257-61.
18. van Niekerk CC, Jap PH, Ramaekers FC, van de Molengraft F, Poels LG. Immunohistochemical demonstration of keratin 7 in routinely fixed paraffin-embedded human tissues. J Pathol 1991; 165: 145-52.
19. Johansson L. Histopathologic classification of lung cancer: relevance of cytokeratin and TTF-1 immunophenotyping. Ann Diagn Pathol 2004; 8: 259-67.
20. Xu Y, Wang W, Li L, et al. FOXA1 and CK7 expression in esophageal squamous cell carcinoma and its prognostic significance. Neoplasma 2018; 65: 469-76.

JPTM
Journal of Pathology and Translational Medicine 2020; 54: 300-309
https://doi.org/10.4132/jptm.2020.06.08

ORIGINAL ARTICLE

Analysis of PAX8 immunohistochemistry in lung cancers: a meta-analysis

Jae Han Jeong[1], Nae Yu Kim[2], Jung-Soo Pyo[3]

[1]Department of Thoracic and Cardiovascular Surgery, Chosun University Hospital, Chosun University School of Medicine, Gwangju; Departments of [2]Internal Medicine and [3]Pathology, Daejeon Eulji University Hospital, Eulji University School of Medicine, Daejeon, Korea

Background: In this meta-analysis, we aimed to evaluate the PAX8 immunohistochemical expressions in primary lung cancers and metastatic cancers to the lung. **Methods:** We identified and reviewed relevant articles from the PubMed databases. Ultimately, 18 articles were included in this meta-analysis. PAX8 expression rates were analyzed and compared between primary and metastatic lung cancers. **Results:** The PAX8 expression rate in primary lung cancers was 0.042 (95% confidence interval [CI], 0.025 to 0.071). PAX8 expression rates of small cell (0.129; 95% CI, 0.022 to 0.496) and non-small cell carcinomas of the lung (0.037; 95% CI, 0.022 to 0.061) were significantly different (p = .049 in a meta-regression test). However, the PAX8 expression rates of adenocarcinoma (0.013; 95% CI, 0.006 to 0.031) and squamous cell carcinoma (0.040; 95% CI, 0.016 to 0.097) were not significantly different. PAX8 expression rates of metastatic carcinomas to the lung varied, ranging from 1.8% to 94.9%. Metastatic carcinomas from the lung to other organs had a PAX8 expression rate of 6.3%. The PAX8 expression rates of metastatic carcinomas from the female genital organs, kidneys, and thyroid gland to the lung were higher than those of other metastatic carcinomas. **Conclusions:** Primary lung cancers had a low PAX8 expression rate regardless of tumor subtype. However, the PAX8 expression rates of metastatic carcinomas from the female genital organs, kidneys, and thyroid were significantly higher than those of primary lung cancers.

Key Words: PAX8; Immunohistochemistry; Lung; Primary; Metastatic; Meta-analysis

Received: April 10, 2020 **Revised:** May 24, 2020 **Accepted:** June 8, 2020
Corresponding Author: Nae Yu Kim, MD, Department of Internal Medicine, Daejeon Eulji University Hospital, Eulji University School of Medicine, 95 Dunsanseo-ro, Seo-gu, Daejeon 35233, Korea
Tel: +82-42-611-3043, Fax: +82-42-611-3853, E-mail: naeyu46@eulji.ac.kr
Corresponding Author: Jung-Soo Pyo, MD, Department of Pathology, Daejeon Eulji University Hospital, Eulji University School of Medicine, 95 Dunsanseo-ro, Seo-gu, Daejeon 35233, Korea
Tel: +82-42-611-3895, Fax: +82-42-611-3459, E-mail: anapyojs@gmail.com

Although various targeted therapies have been developed and applied in lung cancers, a detailed diagnosis of tumor type is important to identify precise treatment [1]. Primary lung tumors includes small and non-small cell lung cancers (20% and 80%, respectively) [2]. However, the lung is a common metastatic site for metastatic extrapulmonary carcinomas [3]. Differential diagnosis between primary lung cancers and metastatic carcinomas to the lung is challenging in some cases due to similar histologic findings or poorly differentiated tumors [4]. Although thyroid transcription factor 1 (TTF-1) and Napsin A are useful markers for primary lung adenocarcinoma [4-7], complete differentiation between primary lung cancers and metastatic carcinomas to the lung may be limited. Additional precise markers are needed in daily practice.

The paired box transcription factor PAX8 has long been studied in malignant tumors of the lung [4,7-24]. PAX8, which includes a family of cell-lineage transcription factors, is involved in the organogenesis of the thyroid gland and kidney as well as the Müllerian system. PAX8 can be expressed in the neoplastic cells of associated organs and is expressed both in the normal tissues and tumors from these organs [25-29]. In previous studies, high PAX8 expression levels have been shown in kidney, thyroid, ovarian, endometrial, and endocervical carcinomas [25-32]. Although PAX8 expression of primary lung cancers was absent in some reports, variable PAX8 expression rates in primary lung cancers has been reported [4,7-24]. PAX8 expression in normal lung tissue is unclear. In normal lung tissue, various cell types are present, including bronchial epithelium,

pISSN 2383-7837
eISSN 2383-7845

pneumocytes, submucosal glands, neuroendocrine cells, and lymphocytes, and each has a different PAX8 expression pattern. Moreover, studies have reported PAX8 expression in normal B lymphocytes [14,18]. These results make interpretation of PAX8 expression in the lung difficult, necessitating a meta-analysis to obtain conclusive information.

Because various malignant tumors including metastatic tumors can occur in the lung, a comparison of PAX8 expression between primary lung cancers and metastatic carcinomas to the lung is needed. In addition, detailed information based on tumor subtypes is not available. In this meta-analysis, we investigated PAX8 immunohistochemical expression rates in primary lung cancers and metastatic carcinomas to the lung as well as in various tumor subtypes of primary lung cancers. Subgroup analysis for PAX8 expression based on the origin of the metastatic carcinomas was also performed.

MATERIALS AND METHODS

Database search and selection criteria

Relevant articles were extracted from the PubMed database through January 31, 2020 using the following keywords: "PAX8," "immunohistochemistry or immunohistochemical," and "cancer or carcinoma." The titles and abstracts of all searched articles were screened. The included articles had information for PAX8 immunohistochemistry of primary lung cancers and metastatic cancers to the lung and metastatic carcinomas from the lung. Additionally, studies on metastatic lung cancers in other organs were included. However, case reports, non-original articles, or articles written in non-English were excluded. We followed PRISMA guidelines.

Data extraction

Data on the PAX8 immunohistochemical expressions of primary lung cancers and metastatic cancers to the lung and metastatic carcinomas from the lung were extracted from each eligible study [4,8-24]. All data were extracted by two independent authors. The extracted data included the authors' information, study location, number of patients analyzed, antibody information (manufacturer and clonality), tumor subtypes and PAX8 expression rates.

Statistical analyses

The meta-analysis was performed using the Comprehensive Meta-Analysis software package (Biostat, Englewood, NJ, USA). The PAX8 expression rates of various primary lung cancers and metastatic cancers to the lung and the metastatic carcinomas from the lung were investigated. In addition, subgroup analysis was performed based on tumor subtypes of the primary lung cancers and the metastatic carcinoma from the lung. Heterogeneity between studies was checked using Q and I^2 statistics and is expressed as p-values. Additionally, sensitivity analysis was conducted to assess the heterogeneity of eligible studies and the impact of each study on the combined effects. In the meta-analysis, because the eligible studies used various evaluation criteria and PAX8 antibodies, a random-effect model was more suitable than a fixed-effect model. To assess publication bias, Begg's funnel plot and Egger's test were used. If significant publication bias was found, the fail-safe N and trim-fill tests were additionally used to confirm the degree of publication bias. The results were considered statistically significant at $p < .05$.

RESULTS

Selection and characteristics of the studies

In this study, 457 relevant articles were extracted from the PubMed database and reviewed for meta-analysis. Of these, 265 articles with no or insufficient information for a meta-analysis and 122 non-original articles were excluded. Furthermore, 52 articles were excluded for the following reasons: in a language other than English (n = 24), on other diseases (n = 19), and involving non-human subjects (n = 9) (Fig. 1). Finally, 18 eligible articles were selected and included in this meta-analysis. These studies included 3,238 patients with primary and metastatic lung cancers (Table 1).

PAX8 expression in primary lung cancers and metastatic cancers to the lung

PAX8 expression rates were estimated in primary lung cancers, including small cell and non-small cell carcinomas. The PAX8 expression rate of overall primary lung cancers was 0.042 (95% confidence interval [CI], 0.025 to 0.071). The PAX8 expression rates were 0.129 (95% CI, 0.022 to 0.496) and 0.037 (95% CI, 0.022 to 0.061) in small cell and non-small cell carcinomas, respectively (Table 2, Fig. 2). There was a significant difference in PAX8 expression between small cell and non-small cell carcinomas by the meta-regression test (p = .049). Detailed subgroup analysis was performed based on tumor subtypes of non-small cell carcinomas. PAX8 expression rates were 0.013 (95% CI, 0.006 to 0.031), 0.040 (95% CI, 0.016 to 0.097), and 0.113 (95% CI, 0.059 to 0.205) in adenocarcinoma, squamous cell carcinoma, and large cell carcinoma, respectively. The PAX8

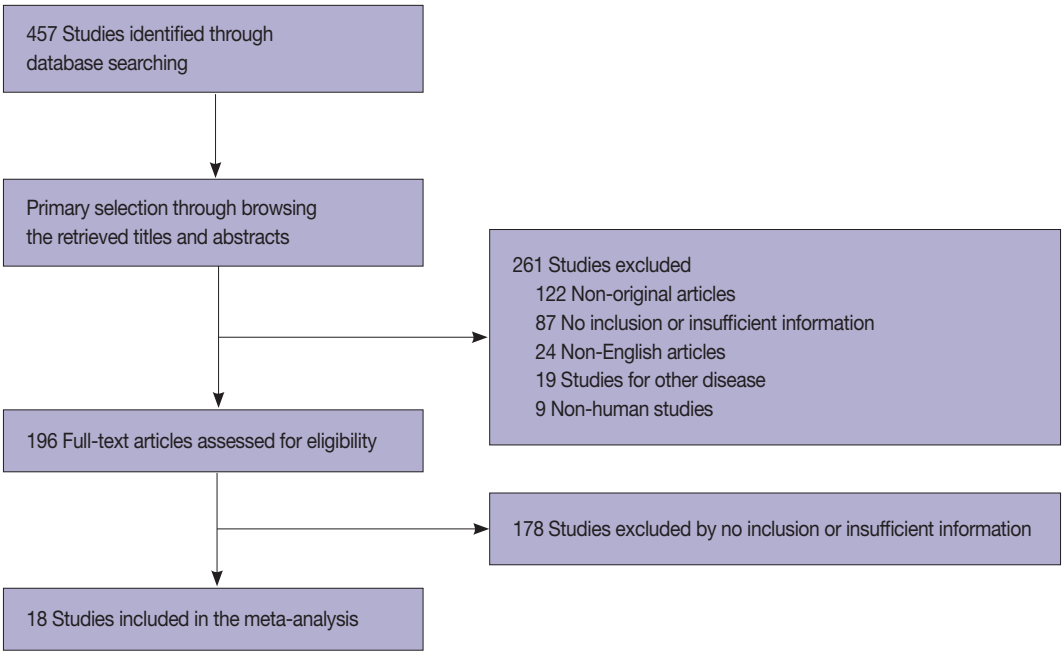

Fig. 1. Flow chart of study search and selection methods.

expression rate was 0.071 (95% CI, 0.004 to 0.577) in micropapillary carcinoma and 0.050 (95% CI, 0.007 to 0.272) in large cell neuroendocrine carcinoma. Moreover, the PAX8 expression rate of metastatic cancers from the lung to other organs was investigated; the estimated PAX8 expression rates were similar to those of primary lung cancers. The PAX8 expression rates in metastatic lung adenocarcinoma and squamous cell carcinoma were 0.050 (95% CI, 0.003 to 0.475) and 0.071 (95% CI, 0.004 to 0.577), respectively (Table 3). In addition, the PAX8 expression rate of metastatic small cell carcinomas from the lungs was 0.067 (95% CI, 0.009 to 0.352).

PAX8 expression in metastatic carcinomas from various organs

The PAX8 expression rates of metastatic carcinomas to the lung were investigated to elucidate the differential role of PAX8 immunohistochemistry. Metastatic carcinomas to the lung showed different PAX8 expression rates, ranging from 1.8% to 94.9% (Table 4, Fig. 3). Among metastatic carcinomas to the lung, PAX8 expression rates in metastatic carcinomas from the female genital organs, kidney, and thyroid were 0.746 (95% CI, 0.501 to 0.895), 0.876 (95% CI, 0.796 to 0.928), and 0.879 (95% CI, 0.697 to 0.959), respectively. There were significant differences in PAX8 expression rates between primary lung cancers and metastatic carcinomas from the female genital organs, kidneys, and thyroid gland.

DISCUSSION

Because PAX8 expression can differ by tumor origin, PAX8 may be useful in differentiating malignant tumors of various origins. Some studies reported that PAX8 expression was absent or very low in primary lung cancers [4,8-24], whereas others reported high PAX8 expressions of up to 66.7% [8,14,16,21-24]; thus detailed information on PAX8 expression according to tumor subtypes of lung cancer was unclear. In this meta-analysis, we evaluated the diagnostic roles of PAX8 immunohistochemical expression in primary lung cancers and metastatic carcinomas to the lung.

It is difficult to obtain conclusive data from individual studies because of the small sample size and difference in evaluation methods. PAX8 expression was found in 0%–66.7%, 0%–12.5%, and 0%–33.3% cases of small cell lung carcinoma, adenocarcinoma, and squamous cell carcinoma of the lung, respectively [4,8-24]. Unlike previous studies, estimated PAX8 expression rates were 12.9% and 3.6% in small cell and non-small cell carcinomas, respectively. However, the cause for discrepancy in the results between the present meta-analysis and previous studies could not be determined. Based on our results, the PAX8 expression was significantly higher in small cell carcinoma than in non-small cell carcinoma ($p = .049$ in the meta-regression test). Clinically, the usefulness of differentiation between small cell and non-small cell carcinomas is limited, regardless of statistical sig-

https://doi.org/10.4132/jptm.2020.06.08

Table 1. Main characteristics of the eligible studies

Study	Location	Antibody manufacturer clonality	Clonality organ	Tumor subtype	PAX8 IHC	
					Positive	Negative
Asirvatham et al. (2014) [8]	USA	Polyclonal	Lung	ND	1	14
Bi et al. (2019) [9]	China	Monoclonal	Metastatic		0	7
Bi et al. (2016) [10]	China	Polyclonal	Lung	NEC	0	20
El-Maqsoud et al. (2016) [11]	Egypt	Monoclonal	Lung	Adenocarcinoma	0	30
		Monoclonal	Lung	Squamous cell carcinom	0	15
		Monoclonal	Lung	Large cell carcinoma	0	5
		Monoclonal	Metastatic		88	55
Gailey et al. (2013) [12]	USA	Polyclonal	Lung	Squamous cell carcinoma	0	12
Heidarpour et al. (2014) [13]	Iran	Polyclonal	Lung	ND	0	5
Laury et al. (2011) [14]	USA	Polyclonal	Lung	Adenocarcinoma	0	120
		Polyclonal	Lung	squamous cell carcinoma	4	8
		Polyclonal	Lung	Adenosquamous carcinoma	0	3
		Polyclonal	Lung	Small cell carcinoma	0	9
Lotan et al. (2009) [15]	USA	Polyclonal	Lung	Micropapillary carcinoma	0	6
Mentrikoski et al. (2014) [16]	USA	Polyclonal	Lung	Adenocarcinoma	1	7
		Polyclonal	Lung	Squamous cell carcinoma	0	3
Nonaka et al. (2008) [17]	USA	Polyclonal	Lung	Adenocarcinoma	0	114
		Polyclonal	Lung	Squamous cell carcinoma	0	29
		Polyclonal	Lung	Large cell carcinoma	0	4
Ozcan et al. (2011) [18]	USA	Polyclonal	Lung	Squamous cell carcinoma	0	4
		Polyclonal	Lung	Adenocarcinoma	0	7
		Polyclonal	Lung	Small cell carcinoma	0	12
		Polyclonal	From lung	Small cell carcinoma	1	14
		Polyclonal	From lung	Adenocarcinoma	0	9
		Polyclonal	From lung	Squamous cell carcinoma	0	6
Suzuki et al. (2015) [19]	Japan	Polyclonal	Lung	Squamous cell carcinoma	0	5
Tacha et al. (2013) [20]	USA	Monoclonal	Lung	ND	0	50
Tacha et al. (2011) [21]	USA	Polyclonal	Lung	Squamous cell carcinoma	1	48
		Polyclonal	Lung	Adenosquamous carcinoma	0	11
		Polyclonal	Lung	Adenocarcinoma	0	15
Toriyama et al. (2014) [22]	Japan	Polyclonal	Lung	Adenocarcinoma	6	247
		Polyclonal	Lung	Squamous cell carcinoma	3	155
		Polyclonal	Lung	LCNEC	17	89
		Polyclonal	Lung	Small cell carcinoma	27	40
		Polyclonal	Lung	Pleomorphic carcinoma	0	41
		Polyclonal	Lung	Large cell carcinoma	2	9
		Monoclonal	Lung	Adenocarcinoma	0	253
		Monoclonal	Lung	Squamous cell carcinoma	0	158
		Monoclonal	Lung	LCNEC	0	106
		Monoclonal	Lung	Small cell carcinoma	0	67
		Monoclonal	Lung	Pleomorphic carcinoma	0	41
		Monoclonal	Lung	Large cell carcinoma	0	11
Vidarsdottir et al. (2019) [23]	Sweden	Monoclonal	Lung	Adenocarcinoma	2	429
		Monoclonal	Lung	Squamous cell carcinom	4	198
		Monoclonal	Lung	Large cell carcinoma	2	7
		Monoclonal	Lung	Sarcomatoid carcinoma	0	6
		Monoclonal	Lung	Small cell carcinoma	2	1
		Monoclonal	Lung	Large cell NEC	1	19
		Monoclonal	Metastatic		55	251
Weissferdt et al. (2013) [24]	USA	Polyclonal	Lung	NEC	2	23
Ye et al. (2012) [4]	USA	ND	Lung	Adenocarcinoma	0	120
		ND	Metastatic		45	56

ND, no description; NEC, neuroendocrine carcinoma; LCNEC, large cell neuroendocrine carcinoma.

Table 2. The estimated rates of PAX8 immunohistochemical expressions in primary lung cancers

	No. of subsets	Fixed effect (95% CI)	Heterogeneity test p-value	Random effect (95% CI)	Egger's test p-value
Lung, primary	45	0.092 (0.075–0.114)	<.001	0.042 (0.025–0.071)	<.001
Small cell carcinoma	5	0.350 (0.254–0.461)	.002	0.129 (0.022–0.496)	.185
Non-small cell carcinoma	3,537	0.054 (0.042–0.071) 0.055 (0.042–0.071)	<.001	0.036 (0.021–0.061) 0.037 (0.022–0.061)	.022 .018
Adenocarcinoma	10	0.016 (0.009–0.027)	.113	0.013 (0.006–0.031)	.493
Micropapillary carcinoma	1	0.071 (0.004–0.577)	>.99	0.071 (0.004–0.577)	-
Squamous cell carcinoma	11	0.041 (0.025–0.067)	.004	0.040 (0.016–0.097)	.907
Large cell carcinoma	8	0.139 (0.094–0.199)	.216	0.113 (0.059–0.205)	.101
Large cell NEC	3	0.136 (0.087–0.205)	.020	0.050 (0.007–0.272)	.192
Sarcomatoid carcinoma	1	0.071 (0.004–0.577)	>.99	0.071 (0.004–0.577)	-
Pleomorphic carcinoma	2	0.012 (0.002–0.080)	>.99	0.012 (0.002–0.080)	-
Adenosquamous carcinoma	2	0.071 (0.010–0.373)	.569	0.071 (0.010–0.373)	-

CI, confidence interval; NEC, neuroendocrine carcinoma.

nificance. This may be due to the low expression rates of PAX8 in both small cell and non-small cell lung carcinomas. In addition, a significant difference in PAX8 expression between tumor subtypes of primary lung cancers was not identified in the meta-regression tests. Therefore, the usefulness of PAX8 expression in the differentiation of tumor subtypes of primary lung cancer is limited.

In daily practice, pathologists have to diagnose various metastatic cancers to the lung, which is a common metastatic site for extrapulmonary carcinomas [3]. The histologic diagnosis of some metastatic cancers of unknown origin is challenging, especially when the metastatic cancer to the lung has histologic findings similar to a primary lung cancer. In previous studies, tumors that originated from the female genital organs, kidney, and thyroid gland were found to have high PAX8 expressions. PAX8 expression rates of metastatic carcinoma from these organs were 62.9%–94.9%. However, metastatic carcinomas from other organs showed lower PAX8 expression than the metastatic carcinoma from the female genital organs, kidney, and thyroid gland (1.8%–16.7% vs. 62.9%–94.9%). Taken together, these results indicate that metastatic carcinomas from the female genital organs, kidney, and thyroid gland can be differentiated from primary lung cancers based on different PAX8 expression rates.

Because lung cancer can metastasize to other organs, PAX8 expression levels were investigated in metastatic lung cancers [33]. In this study, there was no significant difference in PAX8 expression between primary lung cancers and metastatic cancers to the lung. For example, lung adenocarcinoma metastasizes to the ovary at an extremely low rate [33]. The metastatic lung cancers can be easily differentiated from the primary ovarian cancers using immunohistochemistry for TTF-1, Napsin A, and PAX8 [7].

The most common site of distant metastasis for thyroid carcinomas is the lung [34]. In addition, some lung cancers, up to 3.1%, can metastasize to the thyroid glands [35,36]. Thus, the need for differentiating between lung and thyroid carcinomas may be common in daily practice. The histologic findings of papillary thyroid carcinoma can overlap with some non-mucinous bronchioloalveolar and papillary types of lung adenocarcinoma [17]. Because TTF-1 is expressed in both thyroid and lung cancers, other specific markers are needed for differentiation in daily practice. In our results, PAX8 was highly expressed in metastatic thyroid cancer of the lung, similar to primary thyroid cancers [23]. According to these findings, cases with TTF-1 and PAX8 expressions theoretically can be considered as metastatic thyroid cancer. On the other hand, cases with only TTF-1 expression can be considered as primary lung cancer. The PAX8 expression rates of anaplastic thyroid carcinomas were reported to be 50.0%–100.0% [22,37]. In addition, the histologic findings, such as anaplastic spindle and giant cells, can overlap between pleomorphic carcinoma of the lung and anaplastic thyroid carcinoma [1,38]. The TTF-1 expression rates were higher in lung pleomorphic carcinoma than in anaplastic thyroid carcinoma [39,40]. Because TTF-1 expression can be lower in anaplastic thyroid carcinoma than in other types of thyroid carcinoma, the histologic findings of the original tumor are important for differentiation. Therefore, the immunohistochemical markers, including PAX8, can be useful for the differential diagnosis of malignant tumors of the lung.

PAX8 expression was evaluated by monoclonal or polyclonal antibodies. However, the difference in clonality of the primary PAX8 antibody is not clear in primary lung cancers. This point may be necessary for defining PAX8 expression because PAX8

https://doi.org/10.4132/jptm.2020.06.08

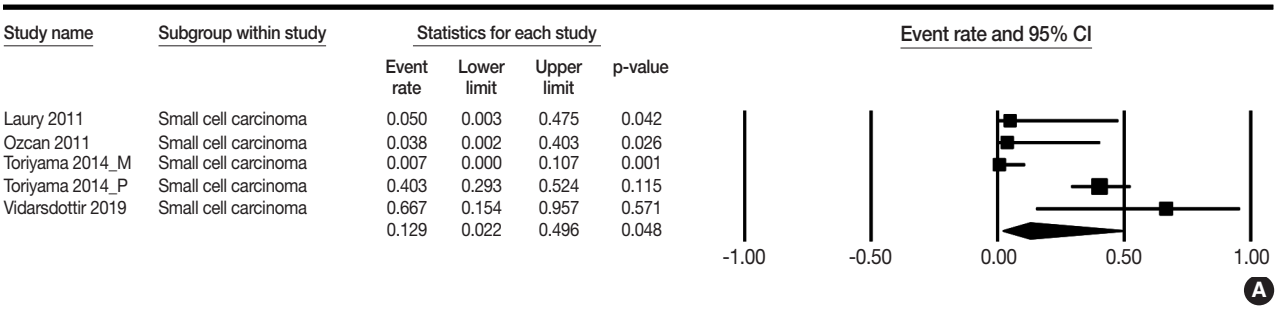

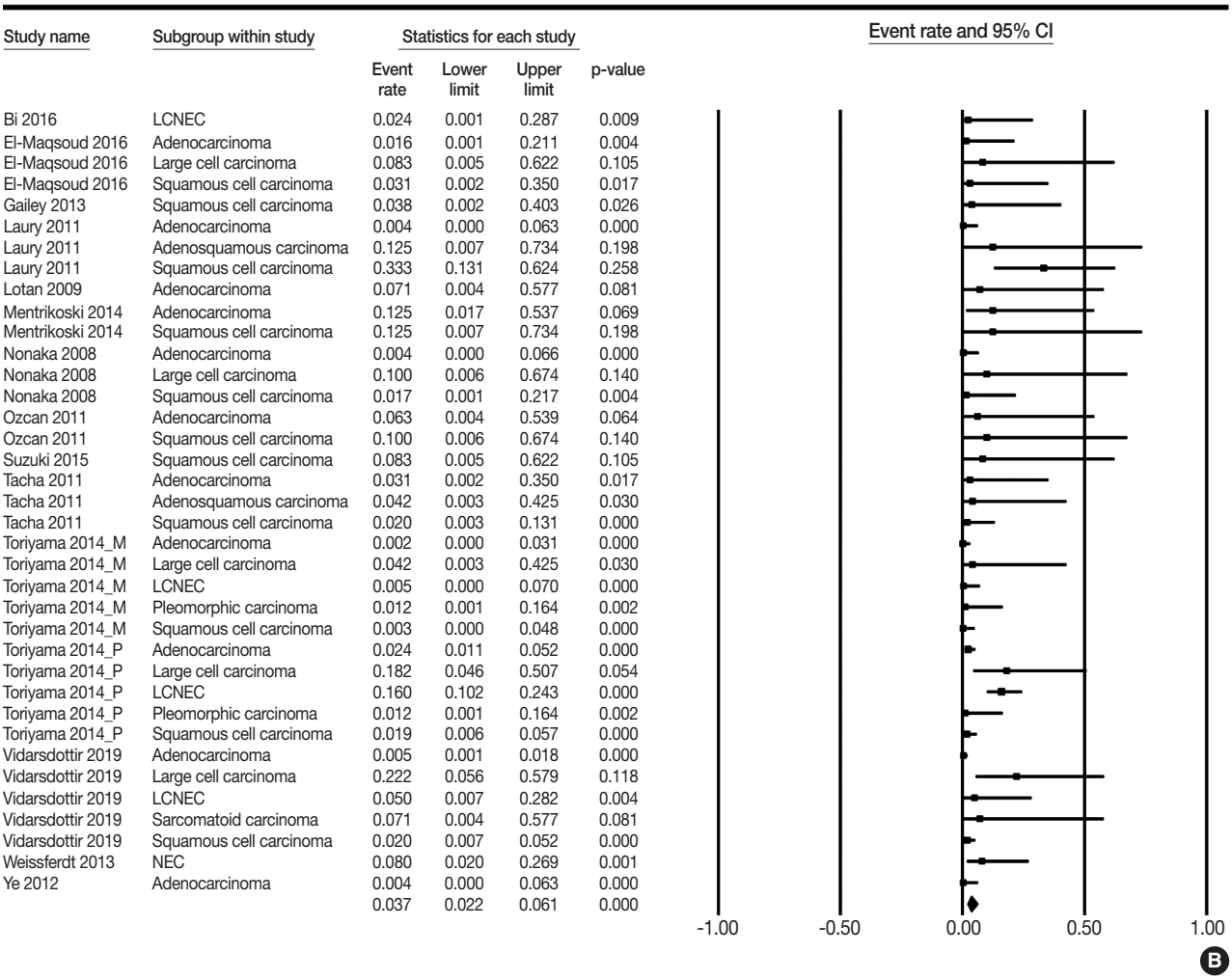

Fig. 2. Forest plots for PAX8 expression rates in small cell lung cancer (A) and non-small cell lung cancer (B) [4,10-12,14-19,21-24]. CI, confidence interval; LCNEC, large cell neuroendocrine carcinoma; NEC, neuroendocrine carcinoma.

expression in primary lung cancers was low or absent. In previous studies, the immunohistochemistry using PAX8 polyclonal antibody showed cross-reactivity with other PAX families and detected immunoreactivity in normal tissues and tumors represented by B lymphocytes [41-43]. Some studies reported different PAX8 expression rates according to the clonality of antibodies in the same tissues [22,23]. Toriyama et al. (2014) [22] reported that PAX8 expression was only detected in immunohistochemistry with polyclonal antibody but not with a monoclonal antibody. However, Vidarsdottir et al. (2019) [23] detected PAX8 expression in primary lung cancers using a monoclonal antibody. In our results, PAX8 expression rates of small cell car-

Table 3. The estimated rates of PAX8 immunohistochemical expressions in metastatic lung cancer

	No. of subsets	Fixed effect (95% CI)	Heterogeneity test p-value	Random effect (95% CI)	Egger's test p-value
Lung, metastatic	3	0.063 (0.016–0.220)	.980	0.063 (0.016–0.220)	.755
Adenocarcinoma	1	0.050 (0.003–0.475)	>.99	0.050 (0.003–0.475)	-
Squamous cell carcinoma	1	0.071 (0.004–0.577)	>.99	0.071 (0.004–0.577)	-
Small cell carcinoma	1	0.067 (0.009–0.352)	>.99	0.067 (0.009–0.352)	-

CI, confidence interval.

Table 4. The estimated rates of PAX8 immunohistochemical expressions in metastatic carcinoma to the lung

	No. of subsets	Fixed effect (95% CI)	Heterogeneity test p-value	Random effect (95% CI)	Egger's test p-value
Metastatic carcinoma	39	0.492 (0.412–0.573)	<.001	0.337 (0.191–0.523)	.005
Adrenal cortex	1	0.167 (0.010–0.806)	>.99	0.167 (0.010–0.806)	-
Appendix	1	0.100 (0.006–0.674)	>.99	0.100 (0.006–0.674)	-
Breast	3	0.039 (0.010–0.142)	.991	0.039 (0.010–0.142)	.701
Colorectum	3	0.018 (0.006–0.056)	.468	0.018 (0.006–0.056)	.049
Esophagus	1	0.125 (0.007–0.734)	>.99	0.125 (0.007–0.734)	-
Female genital organ[a]	7	0.717 (0.571–0.828)	.042	0.746 (0.501–0.895)	.570
Ovary	4	0.641 (0.423–0.813)	.038	0.629 (0.243–0.899)	.908
Mucinous carcinoma	1	0.600 (0.297–0.842)	>.99	0.600 (0.297–0.842)	-
Serous carcinoma	1	0.955 (0.552–0.997)	>.99	0.955 (0.552–0.997)	-
Uterine endometrium	2	0.949 (0.713–0.993)	.615	0.949 (0.713–0.993)	-
Kidney-RCC	5	0.876 (0.796–0.928)	.884	0.876 (0.796–0.928)	.213
Clear cell RCC	1	0.923 (0.609–0.989)	>.99	0.923 (0.609–0.989)	-
Chromophobe RCC	1	0.833 (0.369–0.977)	>.99	0.833 (0.369–0.977)	-
Papillary RCC	1	0.958 (0.575–0.997)	>.99	0.958 (0.575–0.997)	-
Liver	3	0.063 (0.013–0.260)	.914	0.063 (0.013–0.260)	.048
Pancreatobiliary	2	0.133 (0.026–0.466)	.472	0.133 (0.026–0.466)	-
Prostate	2	0.072 (0.014–0.290)	.678	0.072 (0.014–0.290)	-
Salivary gland	2	0.071 (0.010–0.370)	>.99	0.071 (0.010–0.370)	-
Small bowel	1	0.167 (0.010–0.806)	>.99	0.167 (0.010–0.806)	-
Stomach	1	0.083 (0.005–0.622)	>.99	0.083 (0.005–0.622)	-
Testis	1	0.125 (0.007–0.734)	>.99	0.125 (0.007–0.734)	-
Thyroid	4	0.879 (0.697–0.959)	.421	0.879 (0.697–0.959)	.839
Papillary carcinoma	1	0.938 (0.665–0.991)	>.99	0.938 (0.665–0.991)	-
Follicular carcinoma	1	0.967 (0.634–0.998)	>.99	0.967 (0.634–0.998)	-
Urinary system	2	0.171 (0.032–0.564)	.261	0.165 (0.024–0.613)	-

CI, confidence interval; RCC, renal cell carcinoma.
[a]Included uterine corpus and cervix and ovary.

cinoma were 0.113 (95% CI, 0.001 to 0.968) and 0.141 (95% CI, 0.019 to 0.585) in monoclonal and polyclonal antibodies, respectively (data not shown). In addition, in non-small cell lung carcinoma, PAX8 expression rates were 0.020 (95% CI, 0.009 to 0.044) and 0.057 (95% CI, 0.033 to 0.095) in monoclonal and polyclonal antibodies, respectively (data not shown). However, the difference in PAX8 expression between clonalities of PAX8 antibody was significant in non-small cell lung carcinoma but not in small cell lung carcinoma ($p = .030$ and $p = .993$ in the meta-regression test, respectively). Therefore, the difference in PAX8 expression rates as detected by monoclonal and polyclonal antibodies is uncertain. However, regardless of these differences, both monoclonal and polyclonal antibodies can be useful for differentiating between metastatic carcinomas with high expression rates of PAX8 and primary lung cancers with low expression rates of PAX8. From previous studies, the high expression rate of PAX8 immunohistochemistry using a polyclonal antibody can be considered a highly sensitive method. Conversely, the low expression rate of PAX8 immunohistochemistry using a monoclonal antibody can be considered a highly specific method. As described above, the possibility of misinterpretation for other components, including normally

https://doi.org/10.4132/jptm.2020.06.08

Study name	Subgroup within study	Statistics for each study			
		Event rate	Lower limit	Upper limit	p-value
Bi 2016	Adenocarcinoma	0.063	0.004	0.539	0.064
El-Maqsoud 2016	Breast cancer	0.045	0.003	0.448	0.035
El-Maqsoud 2016	Chromophobe RCC	0.833	0.369	0.977	0.142
El-Maqsoud 2016	Clear cell RCC	0.923	0.609	0.989	0.017
El-Maqsoud 2016	Colon cancer	0.045	0.003	0.448	0.035
El-Maqsoud 2016	Endometrium	0.969	0.650	0.998	0.017
El-Maqsoud 2016	Esophagus	0.125	0.007	0.734	0.198
El-Maqsoud 2016	Follicular thyroid carcinoma	0.967	0.634	0.998	0.019
El-Maqsoud 2016	Gastric cancer	0.083	0.005	0.622	0.105
El-Maqsoud 2016	Liver	0.045	0.003	0.448	0.035
El-Maqsoud 2016	Ovary_Mucinous carcinoma	0.600	0.297	0.842	0.530
El-Maqsoud 2016	Ovary_serous carcinoma	0.955	0.552	0.997	0.035
El-Maqsoud 2016	Papillary RCC	0.958	0.575	0.997	0.030
El-Maqsoud 2016	Papillary thyroid carcinoma	0.938	0.665	0.991	0.009
El-Maqsoud 2016	Prostate	0.045	0.003	0.448	0.035
Vidarsdottir 2019	Adenoid cystic carcinom	0.071	0.004	0.577	0.081
Vidarsdottir 2019	Appendix	0.100	0.006	0.674	0.140
Vidarsdottir 2019	Breast	0.037	0.005	0.221	0.001
Vidarsdottir 2019	Colorectum	0.011	0.003	0.044	0.000
Vidarsdottir 2019	Female genital tract	0.706	0.458	0.872	0.100
Vidarsdottir 2019	HCC	0.100	0.006	0.674	0.140
Vidarsdottir 2019	Pancreas	0.200	0.027	0.691	0.215
Vidarsdottir 2019	Prostate	0.091	0.013	0.439	0.028
Vidarsdottir 2019	RCC	0.857	0.717	0.934	0.000
Vidarsdottir 2019	Small bowel	0.167	0.010	0.806	0.299
Vidarsdottir 2019	Thyroid	0.667	0.154	0.957	0.571
Vidarsdottir 2019	UC	0.056	0.003	0.505	0.052
Ye 2012	Adrenal cortex	0.167	0.010	0.806	0.299
Ye 2012	Breast	0.036	0.002	0.384	0.022
Ye 2012	Colon	0.056	0.003	0.505	0.052
Ye 2012	Endometrium	0.917	0.378	0.995	0.105
Ye 2012	Liver	0.056	0.003	0.505	0.052
Ye 2012	Ovary	0.750	0.377	0.937	0.178
Ye 2012	Pancreatobiliary	0.063	0.004	0.539	0.064
Ye 2012	RCC	0.879	0.718	0.954	0.000
Ye 2012	Salivary gland	0.071	0.004	0.577	0.081
Ye 2012	Testis	0.125	0.007	0.734	0.198
Ye 2012	Thyroid	0.800	0.309	0.973	0.215
Ye 2012	Urinary tract	0.333	0.043	0.846	0.571
		0.337	0.191	0.523	0.084

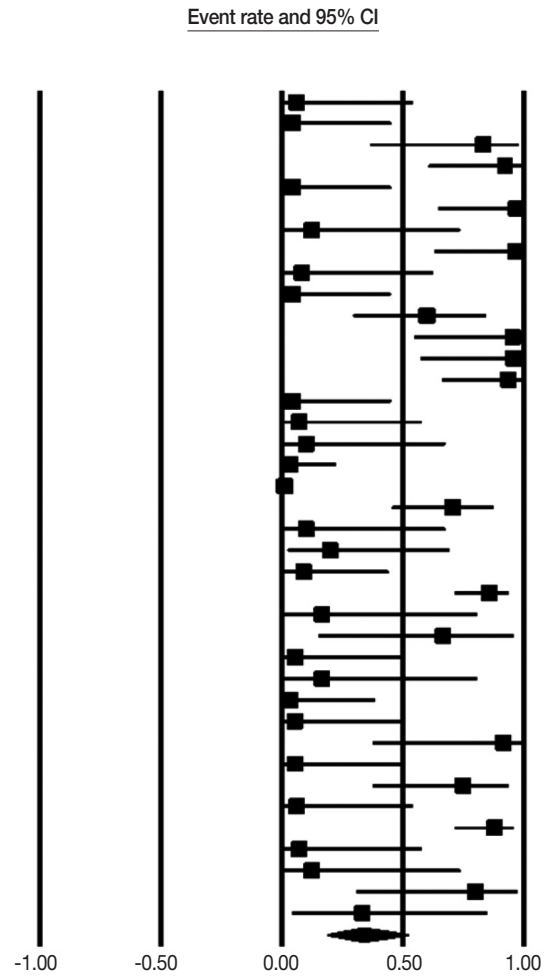

Fig. 3. Forest plot for PAX8 expression rate in metastatic carcinomas to the lung from other organs [4,10,11,23]. CI, confidence interval; RCC, renal cell carcinoma; HCC, hepatocellular carcinoma.

placed components, should be considered. In addition, immunohistochemical staining techniques can affect the positive rates of PAX8, regardless of the clonality of antibody.

This study has some limitations. First, subgroup analysis based on clonality of antibody could not be performed for metastatic carcinomas from other organs due to insufficient information. Second, the detailed information for PAX8 expression of metastatic lung cancer based on metastatic organs could not be obtained due to insufficient information. Third, although the pleura is the most common metastatic site of lung cancer, a comparison of PAX8 expressions between the primary and metastatic tumors of the pleura could not be performed due to a lack of information. Fourth, subgroup analysis based on differentiation of tumors and subtypes of adenocarcinoma could not be performed due to insufficient information on eligible studies. Fifth, detailed analyses for some uncommon subtypes of the primary lung cancer with low incidence were not performed due to the small sample size of patients with these cancers. Lastly, the impact of changed diagnostic criteria of primary lung cancers could not be investigated because we did not include cases applying revised diagnostic criteria in eligible studies.

In conclusion, our results showed that PAX8 expression was lower in primary lung cancer than in metastatic carcinoma of the lung. However, the diagnostic role of PAX8 expression in differentiating tumor subtypes of primary lung cancers is limited due to low rates of PAX8 immunohistochemistry. In daily practice, PAX8 immunohistochemistry can be useful for the diagnosis of metastatic cancer from the female genital organs, kidney, and thyroid gland.

Ethics Statement

Not applicable.

ORCID

Jae Han Jeong https://orcid.org/0000-0003-1112-7405
Nae Yu Kim https://orcid.org/0000-0002-0461-6385
Jung-Soo Pyo https://orcid.org/0000-0003-0320-8088

Author Contributions

Conceptualization: JHJ, JSP. Data curation: JSP. Formal analysis: JHJ, NYK. Funding acquisition: JHJ. Investigation: JHJ, JSP. Methodology: JSP. Supervision: NYK. Validation: NYK. Writing—original draft: JHJ, JSP. Writing—review & editing: NYK. Approval of final manuscript: all authors.

Conflicts of Interest

The authors declare that they have no potential conflicts of interest.

Funding Statement

This study was supported by research fund from Chosun University Hospital, 2019.

References

1. Travis WD, Brambilla E, Burke AP, Marx A, Nicholson AG. WHO classification of tumours of the lung, pleura, thymus and heart. 4th ed. Lyon: International Agency for Research on Cancer, 2015.
2. Brown AF, Sirohi D, Fukuoka J, et al. Tissue-preserving antibody cocktails to differentiate primary squamous cell carcinoma, adenocarcinoma, and small cell carcinoma of lung. Arch Pathol Lab Med 2013; 137: 1274-81.
3. Travis WD. Pathology of lung cancer. Clin Chest Med 2002; 23: 65-81.
4. Ye J, Hameed O, Findeis-Hosey JJ, et al. Diagnostic utility of PAX8, TTF-1 and napsin A for discriminating metastatic carcinoma from primary adenocarcinoma of the lung. Biotech Histochem 2012; 87: 30-4.
5. Bishop JA, Sharma R, Illei PB. Napsin A and thyroid transcription factor-1 expression in carcinomas of the lung, breast, pancreas, colon, kidney, thyroid, and malignant mesothelioma. Hum Pathol 2010; 41: 20-5.
6. Boggaram V. Thyroid transcription factor-1 (TTF-1/Nkx2.1/TITF1) gene regulation in the lung. Clin Sci (Lond) 2009; 116: 27-35.
7. Ye J, Findeis-Hosey JJ, Yang Q, et al. Combination of napsin A and TTF-1 immunohistochemistry helps in differentiating primary lung adenocarcinoma from metastatic carcinoma in the lung. Appl Immunohistochem Mol Morphol 2011; 19: 313-7.
8. Asirvatham JR, Esposito MJ, Bhuiya TA. Role of PAX-8, CD5, and CD117 in distinguishing thymic carcinoma from poorly differentiated lung carcinoma. Appl Immunohistochem Mol Morphol 2014; 22: 372-6.
9. Bi R, Bai Q, Zhu X, et al. *ALK* rearrangement: a high-frequency alteration in ovarian metastasis from lung adenocarcinoma. Diagn Pathol 2019; 14: 96.
10. Bi Y, Deng Y, Li S, et al. Immunophenotypic and prognostic analysis of PAX8 and TTF-1 expressions in neuroendocrine carcinomas of thymic origin: A comparative study with their pulmonary counterparts. J Surg Oncol 2016; 114: 697-702.
11. El-Maqsoud NM, Tawfiek ER, Abdelmeged A, Rahman MF, Moustafa AA. The diagnostic utility of the triple markers Napsin A, TTF-1, and PAX8 in differentiating between primary and metastatic lung carcinomas. Tumour Biol 2016; 37: 3123-34.
12. Gailey MP, Bellizzi AM. Immunohistochemistry for the novel markers glypican 3, PAX8, and p40 (DeltaNp63) in squamous cell and urothelial carcinoma. Am J Clin Pathol 2013; 140: 872-80.
13. Heidarpour M, Tavanafar Z. Diagnostic utility of PAX8 in differentiation of mullerian from non-mullerian tumors. Adv Biomed Res 2014; 3: 96.
14. Laury AR, Perets R, Piao H, et al. A comprehensive analysis of PAX8 expression in human epithelial tumors. Am J Surg Pathol 2011; 35: 816-26.
15. Lotan TL, Ye H, Melamed J, Wu XR, Shih Ie M, Epstein JI. Immunohistochemical panel to identify the primary site of invasive micropapillary carcinoma. Am J Surg Pathol 2009; 33: 1037-41.
16. Mentrikoski MJ, Wendroth SM, Wick MR. Immunohistochemical distinction of renal cell carcinoma from other carcinomas with clear-cell histomorphology: utility of CD10 and CA-125 in addition to PAX-2, PAX-8, RCCma, and adipophilin. Appl Immunohistochem Mol Morphol 2014; 22: 635-41.
17. Nonaka D, Tang Y, Chiriboga L, Rivera M, Ghossein R. Diagnostic utility of thyroid transcription factors Pax8 and TTF-2 (FoxE1) in thyroid epithelial neoplasms. Mod Pathol 2008; 21: 192-200.
18. Ozcan A, Shen SS, Hamilton C, et al. PAX 8 expression in non-neoplastic tissues, primary tumors, and metastatic tumors: a comprehensive immunohistochemical study. Mod Pathol 2011; 24: 751-64.
19. Suzuki A, Hirokawa M, Takada N, et al. Diagnostic significance of PAX8 in thyroid squamous cell carcinoma. Endocr J 2015; 62: 991-5.
20. Tacha D, Qi W, Zhou D, Bremer R, Cheng L. PAX8 mouse monoclonal antibody [BC12] recognizes a restricted epitope and is highly sensitive in renal cell and ovarian cancers but does not cross-react with b cells and tumors of pancreatic origin. Appl Immunohistochem Mol Morphol 2013; 21: 59-63.
21. Tacha D, Zhou D, Cheng L. Expression of PAX8 in normal and neoplastic tissues: a comprehensive immunohistochemical study. Appl Immunohistochem Mol Morphol 2011; 19: 293-9.
22. Toriyama A, Mori T, Sekine S, Yoshida A, Hino O, Tsuta K. Utility of PAX8 mouse monoclonal antibody in the diagnosis of thyroid, thymic, pleural and lung tumours: a comparison with polyclonal PAX8 antibody. Histopathology 2014; 65: 465-72.
23. Vidarsdottir H, Tran L, Nodin B, et al. Immunohistochemical profiles in primary lung cancers and epithelial pulmonary metastases. Hum Pathol 2019; 84: 221-30.
24. Weissferdt A, Tang X, Wistuba, II, Moran CA. Comparative immunohistochemical analysis of pulmonary and thymic neuroendocrine carcinomas using PAX8 and TTF-1. Mod Pathol 2013; 26: 1554-60.
25. Bowen NJ, Logani S, Dickerson EB, et al. Emerging roles for PAX8 in ovarian cancer and endosalpingeal development. Gynecol Oncol 2007; 104: 331-7.
26. Kobel M, Kalloger SE, Boyd N, et al. Ovarian carcinoma subtypes are different diseases: implications for biomarker studies. PLoS Med 2008; 5: e232.
27. Nonaka D, Chiriboga L, Soslow RA. Expression of pax8 as a useful marker in distinguishing ovarian carcinomas from mammary carcinomas. Am J Surg Pathol 2008; 32: 1566-71.
28. Tong GX, Weeden EM, Hamele-Bena D, et al. Expression of PAX8 in nephrogenic adenoma and clear cell adenocarcinoma of the lower urinary tract: evidence of related histogenesis? Am J Surg Pathol 2008; 32: 1380-7.
29. Tong GX, Yu WM, Beaubier NT, et al. Expression of PAX8 in nor-

mal and neoplastic renal tissues: an immunohistochemical study. Mod Pathol 2009; 22: 1218-27.
30. Albadine R, Schultz L, Illei P, et al. PAX8 (+)/p63 (-) immunostaining pattern in renal collecting duct carcinoma (CDC): a useful immunoprofile in the differential diagnosis of CDC versus urothelial carcinoma of upper urinary tract. Am J Surg Pathol 2010; 34: 965-9.
31. Fabbro D, Di Loreto C, Beltrami CA, Belfiore A, Di Lauro R, Damante G. Expression of thyroid-specific transcription factors TTF-1 and PAX-8 in human thyroid neoplasms. Cancer Res 1994; 54: 4744-9.
32. Fujiwara M, Taube J, Sharma M, McCalmont TH, Kim J. PAX8 discriminates ovarian metastases from adnexal tumors and other cutaneous metastases. J Cutan Pathol 2010; 37: 938-43.
33. Niu FY, Zhou Q, Yang JJ, et al. Distribution and prognosis of uncommon metastases from non-small cell lung cancer. BMC Cancer 2016; 16: 149.
34. Mazzaferri EL. Thyroid carcinoma: papillary and follicular. In: Mazzaferri EL, Samaan N, eds. Endocrine tumors. Cambridge: Blackwell Scientific Publications Inc., 1993; 278-333.
35. Lin JD, Weng HF, Ho YS. Clinical and pathological characteristics of secondary thyroid cancer. Thyroid 1998; 8: 149-53.
36. Nakhjavani MK, Gharib H, Goellner JR, van Heerden JA. Metastasis to the thyroid gland: a report of 43 cases. Cancer 1997; 79: 574-8.
37. Kuhn E, Ragazzi M, Ciarrocchi A, et al. Angiosarcoma and anaplastic carcinoma of the thyroid are two distinct entities: a morphologic, immunohistochemical, and genetic study. Mod Pathol 2019; 32: 787-98.
38. Colby T, Koss M, Travis W. Carcinoma of the lung; clinical, radiographic aspects, spread, staging, management, and prognosis. In: Colby T, Koss M, Travis W, eds. Tumors of the lower respiratory tract, 3rd series edition. Washington, DC: Armed Forces Institute of Pathology, 1995; 107-34.
39. Miettinen M, Franssila KO. Variable expression of keratins and nearly uniform lack of thyroid transcription factor 1 in thyroid anaplastic carcinoma. Hum Pathol 2000; 31: 1139-45.
40. Rossi G, Cavazza A, Sturm N, et al. Pulmonary carcinomas with pleomorphic, sarcomatoid, or sarcomatous elements: a clinicopathologic and immunohistochemical study of 75 cases. Am J Surg Pathol 2003; 27: 311-24.
41. Moretti L, Medeiros LJ, Kunkalla K, Williams MD, Singh RR, Vega F. N-terminal PAX8 polyclonal antibody shows cross-reactivity with N-terminal region of PAX5 and is responsible for reports of PAX8 positivity in malignant lymphomas. Mod Pathol 2012; 25: 231-6.
42. Morgan EA, Pozdnyakova O, Nascimento AF, Hirsch MS. PAX8 and PAX5 are differentially expressed in B-cell and T-cell lymphomas. Histopathology 2013; 62: 406-13.
43. Lorenzo PI, Jimenez Moreno CM, Delgado I, et al. Immunohistochemical assessment of Pax8 expression during pancreatic islet development and in human neuroendocrine tumors. Histochem Cell Biol 2011; 136: 595-607.

JPTM
Journal of Pathology and Translational Medicine 2020; 54: 310-317
https://doi.org/10.4132/jptm.2020.05.12

ORIGINAL ARTICLE

Highly prevalent *BRAF* V600E and low-frequency *TERT* promoter mutations underlie papillary thyroid carcinoma in Koreans

Sue Youn Kim[1], Taeeun Kim[2], Kwangsoon Kim[3], Ja Seong Bae[3], Jeong Soo Kim[3], Chan Kwon Jung[1,4]

[1]Department of Hospital Pathology, College of Medicine, The Catholic University of Korea, Seoul;
[2]Molecular Pathology Unit, Pathology Laboratory, Seoul St. Mary's Hospital, College of Medicine, The Catholic University of Korea, Seoul;
[3]Department of Surgery, College of Medicine, The Catholic University of Korea, Seoul;
[4]Cancer Research Institute, College of Medicine, The Catholic University of Korea, Seoul, Korea

Background: The presence of telomerase reverse transcriptase (*TERT*) promoter mutations have been associated with a poor prognosis in patients with papillary thyroid carcinomas (PTC). The frequency of *TERT* promoter mutations varies widely depending on the population and the nature of the study. **Methods:** Data were prospectively collected in 724 consecutive patients who underwent thyroidectomy for PTC from 2018 to 2019. Molecular testing for *BRAF* V600E and *TERT* promoter mutations was performed in all cases. **Results:** *TERT* promoter alterations in two hotspots (C228T and C250T) and C216T were found in 16 (2.2%) and 4 (0.6%) of all PTCs, respectively. The hotspot mutations were significantly associated with older age at diagnosis, larger tumor size, extrathyroidal extension, higher pathologic T category, lateral lymph node metastasis, and higher American Thyroid Association recurrence risk. The patients with C216T variant were younger and had a lower American Thyroid Association recurrence risk than those with hotspot mutations. Concurrent *BRAF* V600E was found in 19 of 20 cases with *TERT* promoter mutations. Of 518 microcarcinomas measuring ≤1.0 cm in size, hotspot mutations and C216T variants were detected in five (1.0%) and three (0.6%) cases, respectively. **Conclusions:** Our study indicates a low frequency of *TERT* promoter mutations in Korean patients with PTC and supports previous findings that *TERT* promoter mutations are more common in older patients with unfavorable clinicopathologic features and *BRAF* V600E. *TERT* promoter mutations in patients with microcarcinoma are uncommon and may have a limited role in risk stratification. The C216T variant seems to have no clinicopathologic effect on PTC.

Key Words: Papillary thyroid carcinoma; *TERT* promoter; *BRAF*; Molecular typing; Mutation rate

Received: March 31, 2020 **Revised:** May 4, 2020 **Accepted:** May 12, 2020
Corresponding Author: Chan Kwon Jung, MD, PhD, Department of Pathology, Seoul St. Mary's Hospital, College of Medicine, The Catholic University of Korea, 222 Banpo-daero, Seocho-gu, Seoul 06591, Korea
Tel: +82-2-2258-1622, Fax: +82-2-2258-1627, E-mail: ckjung@catholic.ac.kr

The incidence of thyroid cancer has dramatically increased over the past several decades [1,2]. The highest incidence of thyroid cancer in the world has been observed in Korea [3,4]. The increase in the incidence of thyroid cancer was responsible for the increase in papillary thyroid carcinoma (PTC), which accounts for over 95% of all thyroid cancer cases in Korea [3,5,6]. Despite the increased incidence of thyroid cancer, the thyroid cancer mortality rate has not changed significantly over the last three decades [3,5]. A multicenter cohort study reported a disease-specific 10-year survival rate of 98% in Korean patients with well-differentiated thyroid carcinoma [6].

Independent prognostic factors related to survival in patients with PTC include elements of cancer staging, such as patient age at diagnosis, tumor size, extensive extrathyroidal extension, and distant metastasis [7]. There have been many studies demonstrating the prognostic value of molecular markers for tumor recurrence and survival. Telomerase reverse transcriptase (*TERT*) promoter mutation is one of the most evident molecular factors related to poor prognosis of patients with PTC [8-11]. The cancer-specific *TERT* promoter mutations occur in two mutually exclusive hotspots in chromosome 5, g.1 295 228 C > T (C228T) and g.1 295 250 C > T (C250T) which correspond to 124 bp (c.–124C > T) and 146 bp (c.–146C > T), upstream from the translation start codon of the *TERT* gene promoter sequence [10-16]. The pooled prevalence of *TERT* promoter mutations in PTC was 11.3% (95% confidence interval, 9.3 to 13.5) in a

pISSN 2383-7837
eISSN 2383-7845

previous meta-analysis of 13 studies [14]. However, the retrospective data may overestimate the mutation frequency because of potential patient selection bias. Patients with microcarcinoma ≤ 1.0 cm were more easily excluded from the molecular studies [8-10,15,17-19]. Furthermore, old archival paraffin blocks may have suboptimal DNA quality that results in molecular test failures and analytical errors.

The *BRAF* V600E mutation is the most common genetic alteration in PTC and remains controversial as an independent prognostic factor [7]. The coexistence of *BRAF* V600E and *TERT* promoter mutations, however, could more accurately indicate the highest mortality risk for patients with PTC [8,19].

The present study aimed to evaluate the real-world frequency of *TERT* promoter mutations in prospectively-collected consecutive cases of PTC and assess the relationship between *TERT* promoter mutations and clinicopathological features in Korean patients with PTC and a high frequency of *BRAF* V600E mutations.

MATERIALS AND METHODS

Patients

We reviewed the prospectively collected data from 724 consecutive patients who underwent thyroidectomy for PTC and molecular testing at Seoul St. Mary's Hospital of the Catholic University of Korea from 2018 to 2019. Molecular tests for *BRAF* and *TERT* promoter mutations were performed in all patients who agreed to allow molecular analysis of their surgical specimens. In cases of multifocal PTCs, the largest tumor was defined as the primary lesion and was chosen for evaluation. The histologic variants of PTC were classified following the diagnostic criteria and terminology of the World Health Organization [7]. The tall cell variant was defined using 30% of tall cell area as a criterion. The PTCs were further classified as classic PTC with tall cell features if it harbored between 10%–30% tall cells and as classic PTC if it contained less than 10% of tall cell area and any well-formed papillae. Cancer staging was done using the 8th edition of the American Joint Committee on Cancer (AJCC) staging system [20]. Minimal extrathyroidal extension was defined as extrathyroidal invasion that was restricted to the perithyroidal soft tissues detected only on microscopic examination (including microscopic strap muscle invasion). When strap muscle invasion was found on preoperative imaging and/or at the time of surgery, the case was considered as gross extrathyroidal extension. Risk stratification of patients for tumor recurrence was done using the 2015 American Thyroid Association (ATA) guidelines [21].

Mutational analyses for *TERT* promoter and *BRAF* V600E mutations

Genomic DNA was extracted from 10 μm-thick formalin-fixed paraffin-embedded (FFPE) tissue blocks using a Maxwell 16 FFPE Tissue LEV Purification Kit (Promega, Fitchburg, WI, USA). Tumor areas were manually dissected with a scalpel under a microscope.

The *TERT* promoter was amplified using the nested polymerase chain reaction (PCR) method. The first-round 235-bp PCR amplicon was amplified using forward 5'-AGTGGATTCGCGGGCACAGA-3' and reverse 5'-CAGCGCTGCCTGAAACTC-3' primers. Then, the second-round 163-bp PCR amplicon was amplified using forward 5'-GTCCTGCCCCTTCACCTT-3' and reverse 5'-CAGCGCTGCCTGAAACTC-3' primers. Bidirectional Sanger sequencing was performed in both directions using the same primers that were used for the second-round PCR. *BRAF* V600E mutation was analyzed using the real-time PCR clamping technology of PNAClampTM BRAF kit (Panagene, Daejeon, Korea) [22]. Each test had a positive control of mutation-holding human genomic DNA and a negative control of distilled water.

Statistical analysis

Categorical variables were analyzed using the Pearson's chi-square, Fisher exact test, or linear-by-linear association when appropriate. Continuous variables were compared using the Student's t-test or Mann-Whitney test when appropriate. The statistical significance threshold was defined as a p-value less than 0.05. All statistical analyses were done using SPSS Statistics program, ver. 21.0 (IBM Corp., Armonk, NY, USA).

RESULTS

Demographic and clinicopathologic characteristics

Table 1 summarizes the baseline clinicopathologic characteristics of the 724 patients with PTC. The median age of the patients at the time of diagnosis was 46 years (interquartile range [IQR], 36 to 56 years). The female to male ratio was 2.7:1. The median tumor size was 0.7 cm (IQR, 0.5 to 1.1 cm). The proportion of microcarcinomas (≤1.0 cm in size) was 71.5% (518/724). Lobectomy was done in 504 (69.6%) and total thyroidectomy in 191 patients (26.4%). The numbers of patients with minimal and gross extrathyroidal extension were 405 (55.9%) and 41 (5.7%), respectively. Cervical lymph node metastases were found in 409 patients (56.5%).

Table 1. Baseline characteristics

Characteristic	No. (%) (n = 724)
Age at diagnosis (yr)	45.9 ± 13.0
< 55	531 (73.3)
≥ 55	193 (26.7)
Sex	
Female	528 (72.9)
Male	196 (27.1)
Tumor size (cm)	
≤ 1.0	518 (71.5)
> 1.0	206 (28.5)
Surgical procedure	
Lobectomy	504 (69.6)
Total thyroidectomy	191 (26.4)
Isthmusectomy	29 (4.0)
Histologic types	
Classic	490 (67.7)
Classic with tall cell features	83 (11.5)
Classic encapsulated	46 (6.4)
Tall cell variant	49 (6.8)
Warthin-like variant	15 (2.1)
Infiltrative follicular variant	10 (1.4)
Invasive encapsulated follicular variant	6 (0.8)
Diffuse sclerosing variant	8 (1.1)
Oncocytic variant	8 (1.1)
Solid variant	5 (0.7)
Hobnail variant	3 (0.4)
Cribriform-morular variant	1 (0.1)
Extrathyroidal extension[a]	
Absent	278 (38.4)
Minimal (microscopic)	405 (55.9)
Gross (strap muscle invasion, pT3b)	30 (4.1)
Gross (tracheal, esophageal or recurrent laryngeal nerve invasion, pT4a)	11 (1.5)
Pathologic T category[a]	
pT1	651 (89.9)
pT2	30 (4.1)
pT3	32 (4.4)
pT4	11 (1.5)
Lymph node metastasis[a]	
Absent (pN0)	315 (43.5)
Central lymph node (pN1a)	346 (47.8)
Lateral lymph node (pN1b)	63 (8.7)
ATA recurrence risk	
Low risk	241 (33.3)
Intermediate risk	358 (49.4)
High risk	125 (17.3)
AJCC cancer staging[a]	
Stage I	623 (86.0)
Stage II	98 (13.5)
Stage III	3 (0.4)
Stage IV	0
BRAF V600E mutation	
Absent	108 (14.9)
Present	616 (85.1)
TERT promoter mutation	
Wild	704 (97.2)
C228T mutation	14 (1.9)
C250T mutation	2 (0.3)
C216T variant	4 (0.6)

ATA, American Thyroid Association; *TERT*, telomerase reverse transcriptase.
[a]All TNM categorization and staging were done according to the 8th American Joint Committee on Cancer (AJCC).

Frequency of *TERT* promoter and *BRAF* V600E mutations

Hotspot-point mutations (C228T and C250T) in the *TERT* promoter were found in 16 (2.2%) patients: 14 with C228T and two with C250T (Table 2, Fig. 1). Four cases had the *TERT* promoter variant of g.1 295 216 C > T (c.–112C > T) (hereafter C216T) (Fig. 1). The *BRAF* V600E mutation was found in 616 (85.1%) patients. Of 20 PTCs with *TERT* promoter aberrations, 19 had coexisting *BRAF* V600E (Table 3, Fig. 2). Fig. 2 summarizes the distribution of histologic variants of PTC and mutational profiles according to the variants. There was no correlation between *TERT* promoter mutations and histologic variants.

Clinicopathologic features of patients with *TERT* promoter mutation

Hotspot mutations in the *TERT* promoter were significantly associated with age ≥ 55 years ($p < .001$), tumor size > 1.0 cm ($p = .001$), extrathyroidal extension ($p = .032$), lateral lymph node metastasis ($p = .041$), and higher ATA recurrence risk ($p < .001$) (Table 2). Compared with patients with hotspot mutations, those with C216T variant were younger ($p = .032$) and had a lower rate of high ATA recurrence risk ($p = .014$). There were no significant differences in the clinicopathologic features between the patients with wild-type *TERT* promoter mutations and those with C216T variant of the *TERT* promoter (Table 2). Table 3 shows the detailed clinicopathologic features of the patients with a *TERT* promoter mutation.

DISCUSSION

The strength of this study stems from the prospectively collected data encompassing all consecutive patients treated for PTC with thyroid surgery. In our study, almost three-quarters of patients with PTC underwent thyroid surgery before the age of 55 years (73.3%) and had microcarcinomas (71.5%). Gross

https://doi.org/10.4132/jptm.2020.05.12

Table 2. Association between *TERT* promoter alterations and clinicopathologic features in 724 consecutive patients with papillary thyroid carcinoma

Variable	*TERT* promoter alteration, n (%)			p-value		
	Wild-type (A)	C228T, C250T (B)	C216T (C)	A vs. B	B vs. C	A vs. C
Age at diagnosis (yr)				<.001	.032	>.99
<55	526 (99.1)	2 (0.4)	3 (0.6)			
≥55	178 (92.2)	14 (7.3)	1 (0.5)			
Sex				.776	.587	.295
Female	515 (97.5)	11 (2.1)	2 (0.4)			
Male	189 (96.4)	5 (2.6)	2 (1.0)			
Tumor size (cm)				.001	.255	>.99
≤1.0	510 (98.5)	5 (1.0)	3 (0.6)			
>1.0	194 (94.2)	11 (5.3)	1 (0.5)			
Histologic variant				.313	.214	.405
Classic[a]	603 (97.4)	12 (1.9)	4 (0.6)			
Classic with TCF	78 (94.0)	5 (6.0)	0			
Tall cell variant	46 (93.9)	3 (6.1)	0			
Follicular variant[b]	16 (100)	0	0			
Other[c]	39 (97.5)	1 (2.5)	0			
Extrathyroidal extension				.032	.162	.645
Absent	274 (98.6)	2 (0.7)	2 (0.7)			
Present[d]	430 (96.4)	14 (3.1)	2 (0.4)			
Pathologic T category				<.001	.267	>.99
pT1-2	667 (97.9)	10 (1.5)	4 (0.6)			
pT3-4	37 (86.0)	6 (14.0)	0			
Pathologic N category				.297	.619	.322
pN0	304 (96.2)	9 (2.8)	3 (0.9)			
pN1	400 (98.0)	7 (1.7)	1 (0.2)			
Lateral lymph node metastasis				.041	>.99	.294
Absent	646 (97.7)	12 (1.8)	3 (0.5)			
Present	58 (92.1)	4 (6.3)	1 (1.6)			
ATA recurrence risk				<.001	.014	.344
Low risk	237 (98.3)	2 (0.8)	2 (0.8)			
Intermediate risk	354 (98.9)	2 (0.6)	2 (0.6)			
High risk	113 (90.4)	12 (9.6)	0			
AJCC cancer staging, 8th edition				.065	>.99	>.99
Stage I/II	702 (97.4)	15 (2.1)	4 (0.6)			
Stage III/IV	2 (66.7)	1 (33.3)	0			
BRAF V600E mutation				.489	>.99	>.99
Absent	107 (99.1)	1 (0.9)	0			
Present	597 (96.9)	15 (2.4)	4 (0.6)			

TERT, telomerase reverse transcriptase; TCF, tall cell features; ATA, American Thyroid Association; AJCC, American Joint Committee on Cancer.
[a]Classic papillary thyroid carcinoma (PTC) included classic PTC (n=490), classic PTC with tall cell features (n=83) and encapsulated classic PTC (n=46); [b]Follicular variant included infiltrative follicular variant (n=10) and invasive encapsulated follicular variant (n=6); [c]Other variants included 15 Warthin-like variant, 8 diffuse sclerosing variant, 8 oncocytic variant, 5 solid variant, 3 hobnail variant, and 1 cribriform-morular variant; [d]Included both microscopic and gross extrathyroidal extension.

extrathyroidal extension was found in only 41 patients (5.7%). No case developed synchronous distant metastasis. Therefore, it stands to reason that the vast majority (86.0%) of patients with PTC were assigned to stage I by the 8th edition of the AJCC staging system. Although *BRAF* V600E mutations were highly prevalent in our study cohort, the frequency of hotspot mutations in the *TERT* promoter was 2.2%, which is far lower than that reported in previous studies for PTC (pooled mean prevalence of 11.3%) [14,23]. These results indicate that most PTC tumors in the current study should have indolent behavior.

In our study, additional benefits were gained by including microcarcinomas in the molecular analysis. Hotspot mutations of the *TERT* promoter were found in five of 518 papillary microcarcinomas (1.0%). Minimal extrathyroidal extension, found in three of the five patients with hotspot mutations, did not affect the pathologic T category. Patient age ranged from 39 to 84

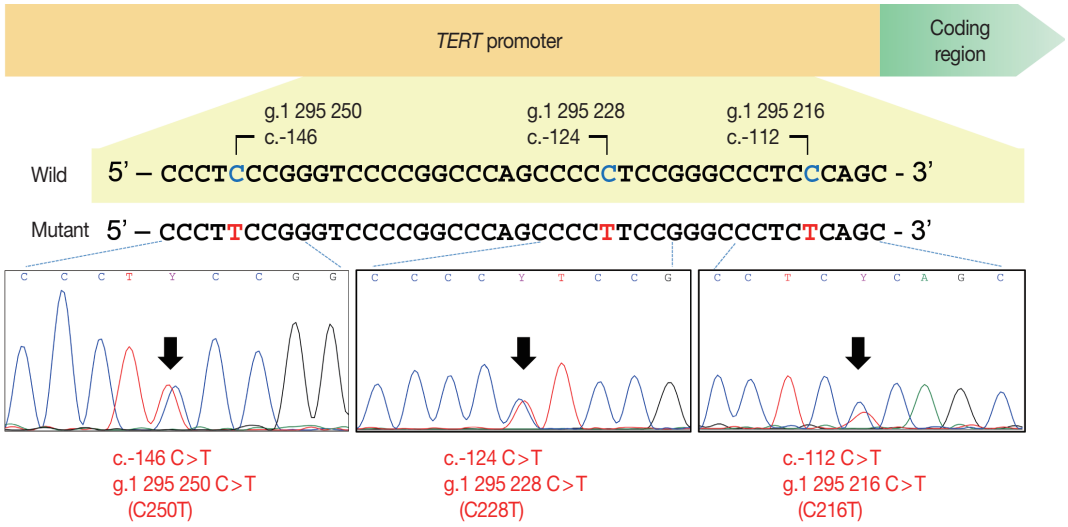

Fig. 1. Schematic figure of the telomerase reverse transcriptase (*TERT*) promoter region and sequencing electropherograms of two hotspot mutations (C228T and C250T) and a C216T variant in the *TERT* promoter. The hotspot mutations resulted from a cytosine-to-thymine transition at genomic loci Chr5:1,295,228 (C228T) and 1,295,250 (C250T), respectively. The C216T variant is a cytosine-to-thymine transition at the 1,295,216 position of Chr5.

Table 3. Clinicopathologic features of papillary thyroid carcinoma patients with *TERT* promoter alterations

Case No.	Age (yr)	Sex	Surgery	Tumor size (cm)	Variant	Multi-focality	ETE	pT	pN	M	Stage	*TERT* promoter	*BRAF*
1	77	F	Isthmusectomy	0.3	Classic	N	Absent	1a	0	0	1	C250T	Wild
2	60	F	Total lobectomy	0.5	Classic, encapsulated	Y	Absent	1a	0	0	1	C250T	V600E
3	55	F	Lobectomy	0.8	Classic	Y	Microscopic	1a	0	0	1	C228T	V600E
4	46	F	Total lobectomy	1.5	Classic	Y	Microscopic	1b	0	0	1	C228T	V600E
5	66	F	Total lobectomy	2.0	Classic	Y	Strap muscle invasion	3b	0	0	2	C228T	V600E
6	57	M	Total lobectomy	2.6	Classic	N	Strap muscle invasion	3b	1b	0	2	C228T	V600E
7	68	M	Lobectomy	2.8	Classic	Y	Microscopic	2	0	0	1	C228T	V600E
8	60	F	Lobectomy	0.7	Classic with TCF	Y	Microscopic	1a	0	0	1	C228T	V600E
9	76	F	Total lobectomy	1.3	Classic with TCF	Y	Microscopic	1b	1a	0	2	C228T	V600E
10	59	F	Total lobectomy	1.6	Classic with TCF	N	Microscopic	1b	0	0	1	C228T	V600E
11	39	F	Total lobectomy	2.1	Classic with TCF	N	Microscopic	2	1b	0	1	C228T	V600E
12	65	M	Total lobectomy	3.2	Classic with TCF	Y	Strap muscle invasion	3b	1a	0	2	C228T	V600E
13	75	F	Total lobectomy	2.0	Tall cell	N	Strap muscle invasion	3b	1a	0	2	C228T	V600E
14	74	M	Lobectomy	2.7	Tall cell	N	Strap muscle invasion	3b	0	0	2	C228T	V600E
15	84	F	Total lobectomy	5.5	Tall cell	N	Esophagus invasion	4a	1b	0	3	C228T	V600E
16	64	M	Total lobectomy	0.7	Oncocytic	Y	Microscopic	1a	1b	0	2	C228T	V600E
17	44	F	Lobectomy	0.4	Classic	N	Absent	1a	0	0	1	C216T	V600E
18	55	F	Total lobectomy	0.5	Classic	N	Absent	1a	0	0	1	C216T	V600E
19	29	M	Total lobectomy	1.0	Classic	Y	Microscopic	1a	1b	0	1	C216T	V600E
20	54	M	Lobectomy	1.2	Classic	N	Microscopic	1b	0	0	1	C216T	V600E

TERT, telomerase reverse transcriptase; ETE, extrathyroidal extension; F, female; M, male; Y, yes; N, no; TCF, tall cell features.

years. Although the frequency of *TERT* promoter mutations is lower than that of previous studies, these findings are in line with a previous Italian study showing no correlation with unfavorable outcomes [24]. The Italian study showed that *TERT* promoter mutations were found in 4.7% of papillary microcarcinomas and were not associated with poor clinical features [24]. As active surveillance is one of the treatment options for low-risk papillary microcarcinomas, the identification of *TERT* promoter mutations may facilitate decision-making on appropriate candidates for active surveillance [21,25]. One Japanese study reported that no *TERT* promoter mutations were found in 25 patients selected from 1,252 patients with low-risk papillary microcarcinoma who were managed with active surveillance [25]. These results, however, need to be validated in further larger studies.

https://doi.org/10.4132/jptm.2020.05.12

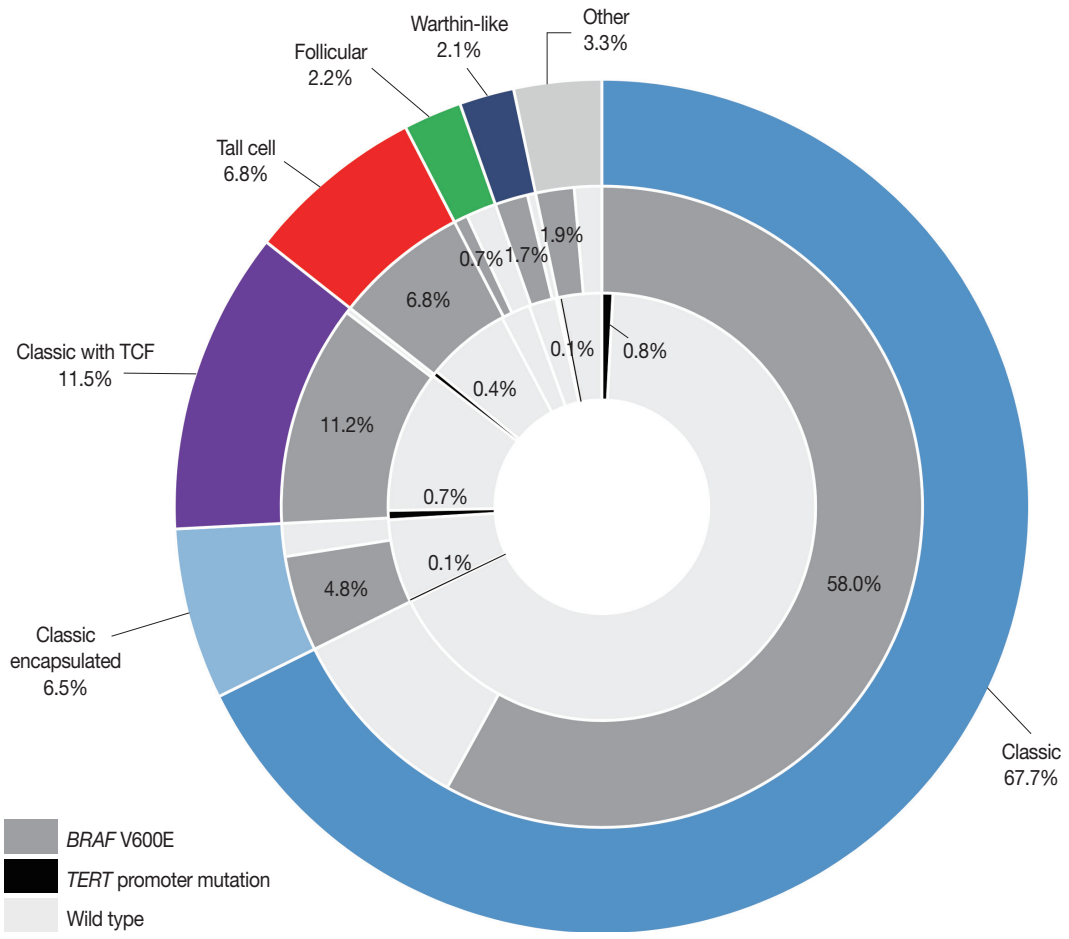

Fig. 2. A pie chart depicting a portion of *BRAF* V600E and telomerase reverse transcriptase (*TERT*) promoter mutations (C228T and C250T) in relation to histologic variants of papillary thyroid carcinoma (n=724). The middle and inner circles show the frequency of *BRAF* V600E and *TERT* promoter mutations, respectively. The other variants included eight diffuse sclerosing, eight oncocytic, five solid, three hobnail, and one cribriform-morular variant. TCF, tall cell features.

Since most studies reported only pathogenic hotspot mutations, little is known about the prevalence and functional role of the *TERT* promoter C216T variant in human cancers. The C216T variant was found in four cases of our study cohort and has been previously reported in two lung adenocarcinomas [26] and one esophageal squamous cell carcinoma [27]. In our study, all four patients with the C216T were younger (range, 29 to 55 years) than those with hotspot mutations and had no unfavorable clinicopathologic features. Therefore, we suggest that the *TERT* promoter C216T variant may be a non-pathogenic DNA polymorphism in PTC.

Many studies have shown synergistic effects of concurrent *BRAF* V600E and *TERT* promoter mutations on the poor prognosis and mortality risk of patients with PTC [8,11,17-19,23]. The C228T and C250T mutations of the *TERT* promoter generate an 11-bp binding motif (5'-CCCCTTCCGGG-3') for E-twenty-six (ETS) transcription factors [13]. Mitogen-activated protein kinase pathway activation by the *BRAF* V600E mutation upregulates ETS transcription factors, which results in increased *TERT* mRNA expression by the binding of the mutated *TERT* promoter to ETS [28]. In our study, all 14 patients with the *TERT* promoter C228T mutation had a concurrent *BRAF* V600E mutation. In Korean patients with PTC and a high prevalence of the *BRAF* V600E, further studies are needed to validate the prognostic utility of risk stratification of patients with PTC by combining *BRAF* V600E and *TERT* promoter mutations.

In summary, this study demonstrated that the *TERT* promoter mutation frequency was 2.2% in prospectively collected patients, and the presently reported frequency is lower than that reported in previous studies. *TERT* promoter mutations were more common in older patients with unfavorable clinicopathologic fea-

tures and a *BRAF* V600E mutation. Although they were observed less frequently than in those with larger tumors, *TERT* promoter mutations also occurred in patients with microcarcinoma and low-risk clinicopathologic features. The C216T variant was found in 0.6% of all PTCs and may be a non-pathogenic DNA polymorphism.

Ethics Statement

This study was approved by the Institutional Review Board of Seoul St. Mary's Hospital, the Catholic University of Korea (KC16SISI0709). Informed consent was obtained from each patient.

ORCID

Sue Youn Kim https://orcid.org/0000-0003-0279-9787
Taeeun Kim https://orcid.org/0000-0001-6945-8616
Kwangsoon Kim https://orcid.org/0000-0001-6403-6035
Ja Seong Bae https://orcid.org/0000-0002-6271-2105
Jeong Soo Kim https://orcid.org/0000-0002-9982-7838
Chan Kwon Jung https://orcid.org/0000-0001-6843-3708

Author Contributions

Conceptualization: CKJ. Data curation: SYK, TK, KK, JSB, JSK, CKJ. Formal analysis: SYK, TK, CKJ. Funding acquisition: CKJ. Investigation: SYK, TK, CKJ. Methodology: SYK, TK, CKJ. Project administration: SYK, CKJ. Resources: SYK, KK, JSB, JSK, CKJ. Software: SYK, CKJ. Supervision: CKJ. Validation: KK, JSB, JSK, CKJ. Visualization: SYK, KK, JSB, JSK, CKJ. Writing—original draft: SYK, CKJ. Writing—review & editing: SYK, TK, KK, JSB, JSK, CKJ. Approval of final manuscript: all authors.

Conflicts of Interest

C.K.J. is the editor-in-chief of the *Journal of Pathology and Translational Medicine* and was not involved in the editorial evaluation or decision to publish this article. All remaining authors declare that they have no potential conflicts of interest.

Funding Statement

This study was supported by a grant (2017R1D1A1B03029597) from the Basic Science Research Program through the National Research Foundation of Korea.

References

1. Vaccarella S, Franceschi S, Bray F, Wild CP, Plummer M, Dal Maso L. Worldwide thyroid-cancer epidemic? The increasing impact of overdiagnosis. N Engl J Med 2016; 375: 614-7.
2. Ahn HS, Kim HJ, Kim KH, et al. Thyroid cancer screening in South Korea increases detection of papillary cancers with no impact on other subtypes or thyroid cancer mortality. Thyroid 2016; 26: 1535-40.
3. Ahn HS, Kim HJ, Welch HG. Korea's thyroid-cancer "epidemic": screening and overdiagnosis. N Engl J Med 2014; 371: 1765-7.
4. Jung KW, Won YJ, Kong HJ, Lee ES. Cancer statistics in Korea: incidence, mortality, survival, and prevalence in 2016. Cancer Res Treat 2019; 51: 417-30.
5. Park S, Oh CM, Cho H, et al. Association between screening and the thyroid cancer "epidemic" in South Korea: evidence from a nationwide study. BMJ 2016; 355: i5745.
6. Jeon MJ, Kim WG, Kim TH, et al. Disease-specific mortality of differentiated thyroid cancer patients in Korea: a multicenter cohort study. Endocrinol Metab (Seoul) 2017; 32: 434-41.
7. Lloyd RV, Osamura RY, Klöppel G, Rosai J. WHO classification of tumours of endocrine organs. 4th ed. Lyon: International Agency for Research on Cancer (IARC), 2017; 65-91.
8. Liu R, Bishop J, Zhu G, Zhang T, Ladenson PW, Xing M. Mortality risk stratification by combining *BRAF* V600E and *TERT* promoter mutations in papillary thyroid cancer: genetic duet of BRAF and TERT promoter mutations in thyroid cancer mortality. JAMA Oncol 2017; 3: 202-8.
9. Kim TH, Kim YE, Ahn S, et al. *TERT* promoter mutations and long-term survival in patients with thyroid cancer. Endocr Relat Cancer 2016; 23: 813-23.
10. Liu X, Qu S, Liu R, et al. *TERT* promoter mutations and their association with *BRAF* V600E mutation and aggressive clinicopathological characteristics of thyroid cancer. J Clin Endocrinol Metab 2014; 99: E1130-6.
11. Melo M, da Rocha AG, Vinagre J, et al. *TERT* promoter mutations are a major indicator of poor outcome in differentiated thyroid carcinomas. J Clin Endocrinol Metab 2014; 99: E754-65.
12. Horn S, Figl A, Rachakonda PS, et al. *TERT* promoter mutations in familial and sporadic melanoma. Science 2013; 339: 959-61.
13. Huang FW, Hodis E, Xu MJ, Kryukov GV, Chin L, Garraway LA. Highly recurrent *TERT* promoter mutations in human melanoma. Science 2013; 339: 957-9.
14. Bae JS, Kim Y, Jeon S, et al. Clinical utility of *TERT* promoter mutations and *ALK* rearrangement in thyroid cancer patients with a high prevalence of the *BRAF* V600E mutation. Diagn Pathol 2016; 11: 21.
15. Xing M, Liu R, Liu X, et al. *BRAF* V600E and *TERT* promoter mutations cooperatively identify the most aggressive papillary thyroid cancer with highest recurrence. J Clin Oncol 2014; 32: 2718-26.
16. Jung CK, Kim Y, Jeon S, Jo K, Lee S, Bae JS. Clinical utility of *EZH1* mutations in the diagnosis of follicular-patterned thyroid tumors. Hum Pathol 2018; 81: 9-17.
17. Landa I, Ganly I, Chan TA, et al. Frequent somatic *TERT* promoter mutations in thyroid cancer: higher prevalence in advanced forms of the disease. J Clin Endocrinol Metab 2013; 98: E1562-6.
18. Liu X, Bishop J, Shan Y, et al. Highly prevalent *TERT* promoter mutations in aggressive thyroid cancers. Endocr Relat Cancer 2013; 20: 603-10.
19. Song YS, Lim JA, Choi H, et al. Prognostic effects of *TERT* promoter mutations are enhanced by coexistence with *BRAF* or *RAS* mutations and strengthen the risk prediction by the ATA or TNM staging system in differentiated thyroid cancer patients. Cancer 2016; 122: 1370-9.
20. Amin MB, Edge S, Greene F, et al. AJCC cancer staging manual. 8th ed. New York: Springer, 2017; 873-90.
21. Haugen BR, Alexander EK, Bible KC, et al. 2015 American Thyroid Association management guidelines for adult patients with thyroid nodules and differentiated thyroid cancer: the American Thyroid Association Guidelines Task Force on Thyroid Nodules and Differentiated Thyroid Cancer. Thyroid 2016; 26: 1-133.
22. Jeong D, Jeong Y, Lee S, et al. Detection of *BRAF*(V600E) mutations in papillary thyroid carcinomas by peptide nucleic acid clamp real-time PCR: a comparison with direct sequencing. Korean J Pathol 2012; 46: 61-7.
23. Yang J, Gong Y, Yan S, Chen H, Qin S, Gong R. Association between *TERT* promoter mutations and clinical behaviors in differ-

entiated thyroid carcinoma: a systematic review and meta-analysis. Endocrine 2020; 67: 44-57.
24. de Biase D, Gandolfi G, Ragazzi M, et al. *TERT* promoter mutations in papillary thyroid microcarcinomas. Thyroid 2015; 25: 1013-9.
25. Yabuta T, Matsuse M, Hirokawa M, Yamashita S, Mitsutake N, Miyauchi A. *TERT* promoter mutations were not found in papillary thyroid microcarcinomas that showed disease progression on active surveillance. Thyroid 2017; 27: 1206-7.
26. Ma X, Gong R, Wang R, et al. Recurrent *TERT* promoter mutations in non-small cell lung cancers. Lung Cancer 2014; 86: 369-73.
27. Zhao Y, Gao Y, Chen Z, Hu X, Zhou F, He J. Low frequency of *TERT* promoter somatic mutation in 313 sporadic esophageal squamous cell carcinomas. Int J Cancer 2014; 134: 493-4.
28. Song YS, Yoo SK, Kim HH, et al. Interaction of *BRAF*-induced ETS factors with mutant *TERT* promoter in papillary thyroid cancer. Endocr Relat Cancer 2019; 26: 629-41.

JPTM
Journal of Pathology and Translational Medicine 2020; 54: 318-331
https://doi.org/10.4132/jptm.2020.02.26

ORIGINAL ARTICLE

Current status of cytopathology practices in Korea: annual report on the Continuous Quality Improvement program of the Korean Society for Cytopathology for 2018

Yosep Chong[1]*, Haeyoen Jung[2]*, Jung-Soo Pyo[3], Soon Won Hong[4], Hoon Kyu Oh[5],
The Committee of Quality Improvement of Korean Society for Cytopathology

[1]Department of Hospital Pathology, College of Medicine, The Catholic University of Korea, Seoul;
[2]Department of Pathology, Eone Laboratories, Incheon;
[3]Department of Pathology, Eulji University Hospital, Eulji University School of Medicine, Seoul;
[4]Department of Pathology, Gangnam Severance Hospital, Yonsei University College of Medicine, Seoul;
[5]Department of Pathology, Daegu Catholic University School of Medicine, Daegu, Korea

Background: The Korean Society for Cytopathology has conducted the Continuous Quality Improvement program for cytopathology laboratories in Korea since 1995. In 2018 as part of the program, an annual survey of cytologic data was administered to determine the current status of cytopathology practices in Korea. **Methods:** A questionnaire was administered to 211 cytopathology laboratories. Individual laboratories submitted their annual statistics regarding cytopathology practices, diagnoses of gynecologic samples, inadequacy rates, and gynecologic cytology-histology correlation review (CHCR) data for 2018. In addition, proficiency tests and sample adequacy assessments were conducted using five consequent gynecologic slides. **Results:** Over 10 million cytologic exams were performed in 2018, and this number has almost tripled since this survey was first conducted in 2004 (compounded annual growth rate of 7.2%). The number of non-gynecologic samples has increased gradually over time and comprised 24% of all exams. The overall unsatisfactory rate was 0.14%. The ratio of the cases with atypical squamous cells to squamous intraepithelial lesions accounted for up to 4.24. The major discrepancy rate of the CHCR in gynecologic samples was 0.52%. In the proficiency test, the major discrepancy rate was approximately 1%. In the sample adequacy assessment, a discrepancy was observed in 0.1% of cases. **Conclusions:** This study represents the current status of cytopathology practices in Korea, illustrating the importance of the Continuous Quality Improvement program for increasing the accuracy and credibility of cytopathologic exams as well as developing national cancer exam guidelines and government projects on the prevention and treatment of cancer.

Key Words: Cytology; Surveys; Statistics; Quality; Accuracy

Received: December 26, 2019 **Revised:** February 19, 2020 **Accepted:** February 26, 2020
Corresponding Author: Hoon Kyu Oh, MD, PhD, Department of Pathology, Daegu Catholic University School of Medicine, 33 Duryugongwon-ro 17-gil, Nam-gu, Daegu 42472, Korea
Tel: +82-53-650-4156, Fax: +82-53-650-3456, E-mail: ap501@cu.ac.kr

*Yosep Chong and Haeyoen Jung contributed equally to this work.

The Korean Society for Cytopathology (KSC) has conducted the Continuous Quality Improvement program for cytopathology laboratories in Korea since 1995 [1]. In 1992, the Committee of Quality Improvement of the KSC (CQIKSC) was first founded. In 1995, the standard operating procedures and documents of quality assurance (QA) were enacted, and the first nationwide survey of annual statistics on cytologic exams of all institutions was conducted. In 1996, the first proficiency tests (PTs) and the certification of participating institutions were performed with 100 institutions. Since 2003, all cytopathology laboratories in Korea have been obliged to submit annual statistics and participate in PTs to be certified by the CQIKSC. The number of participating institutions was 148 in 2004 and increased to 211 in 2018. Currently, the certification awarded through the Continuous Quality Improvement program is regarded as an important standard to qualify individual cytopathology laboratories, especially in conjunction with the National Cancer Screening Program that was started in 1999 [1-3].

pISSN 2383-7837
eISSN 2383-7845

The Continuous Quality Improvement program initially consisted of an annual survey of the statistics on gynecological (GYN) cytologic exams. Recently, the survey has been expanded to cover overall statistics, statistics on the diagnostic category of GYN exams, inadequacy rates, cytology-histology correlation reviews (CHCRs), and the number of discordant cases. PTs were initially performed 2–4 times annually using three slides; however, in 2013, this was adjusted to once annually using five glass slides. Sample adequacy evaluations have been performed with five GYN slides submitted from participating institutions since 2013. Since 2009, six glass slides from each participating institution have been submitted to be used in the PTs for the following years. The statistical analysis of the submitted data has been unofficially performed by CQIKSC to efficiently develop a strategy for quality improvement. Official reports have only been published twice: in 2008 (using data collected before 2007) [1] and 2017 (using data collected before 2016) [4]. A new report using the data collected between 2007 and 2017 is currently being compiled for publication. The Continuous Quality Improvement statistics are very credible and represent the current status of cytopathology practices in Korea [4]. In addition, quality data to support the creation of national policies and strategies in cancer screening are becoming more essential [5]; therefore, CQIKSC has decided to publish the statistics annually.

Thus, we present the results of a nationwide survey on annual statistics from cytologic exams and PTs for 2018.

MATERIALS AND METHODS

The Continuous Quality Improvement program by CQIKSC

As mentioned earlier, the annual Continuous Quality Improvement program consists of four parts: 1, a survey of the statistics on the cytologic exams performed in the last year; 2, a PT using five glass slides; 3, a sample adequacy evaluation of five GYN glass slides submitted by the participating institutions; and 4, submission of six candidate slides by the participating institutions to be used in the PTs of the following years.

Annual survey of cytopathology statistics

A nationwide survey was conducted by CQIKSC from February 11, 2019, to February 22, 2019. The questionnaire and the written informed consent were collected from 211 medical institutions performing cytopathologic examinations in Korea in 2018. The questionnaire included the statistical data on overall cytologic exams, the case number of the GYN exams according to the diagnostic categories, the GYN sample adequacy, the CHCR results, and the number of discordant cases according to the discordant assessment criteria. The diagnostic concordance between the cytologic and corresponding histologic examination of the uterine cervix or endometrium was categorized as either concordant (category O) or one of three discordant categories: category A (minimal clinical impact), category B (minor clinical impact), or category C (major clinical impact). The criteria for CHCR were developed by the individual institutes according to the internal guidelines for laboratory QA. The discordant assessment criteria for PT by CQIKSC were provided to each institute as a reference for the criteria for CHCR (Tables 1–4).

The participating institutions were categorized into three groups: university hospitals, general hospitals, and commercial laboratories. The overall cytologic exam statistics were analyzed by category. The sample categories were as follows: GYN, fine-needle aspiration (FNA), and non-GYN/non-FNA sample exams including urine, body fluids, respiratory tract samples (sputum, bronchial washing, brushing, bronchioloalveolar lavage, etc.), cerebrospinal fluid, etc. Endoscopic bronchial ultrasonography-assisted aspiration cytology samples were classified as FNA samples other than body fluids. The cystic fluids derived from anatomical body cavities, such as the pleural, peritoneal, or pericardial cavities, were classified as body fluids although they were obtained by needle aspiration.

Table 1. Discordance assessment criteria for gynecologic samples, squamous lesions

Original diagnosis	Submitted diagnosis					
	Negative	ASC-US	ASC-H	L-SIL	H-SIL	Carcinoma
Negative	O	A	B	A	B	C
ASC-US	A	O	A	O	A	B
ASC-H	B	A	O	A	O	B
L-SIL	A	A	A	O	A	B
H-SIL	B	B	A	A	O	A
Carcinoma	C	B	B	B	A	O

ASC-US, atypical squamous cells of undetermined significance; ASC-H, atypical squamous cells, cannot exclude H-SIL; L-SIL, low-grade squamous intraepithelial lesion; H-SIL, high-grade squamous intraepithelial lesion.

Table 2. Discordance assessment criteria for gynecologic samples, glandular lesions

Original diagnosis	Submitted diagnosis				
	Negative	AGC	AGC, favor neoplastic	Endocervical AIS	Adenocarcinoma
Negative	O	A	B	B	C
AGC	A	O	A	B	B
AGC, favor neoplastic	B	A	O	A	A
Endocervical AIS	B	B	A	O	A
Adenocarcinoma	C	B	A	A	O

AGC, atypical glandular cells; AIS, adenocarcinoma in situ.

Table 3. Discordance assessment criteria for thyroid fine-needle aspiration

Submitted diagnosis	Original diagnosis								
	Benign, c/w a benign follicular nodule	Benign, c/w chronic lymphocytic (Hashimoto's) thyroiditis	Benign, c/w granulomatous (subacute) thyroiditis	Follicular lesion, conventional type	Follicular lesion, Hurthle cell (oncocytic type)	Papillary carcinoma	Poorly differentiated carcinoma	Medullary carcinoma	Undifferentiated (anaplastic) carcinoma
Benign, c/w a benign follicular nodule	O	A	A	B	B	C	C	C	C
Benign, c/w chronic lymphocytic (Hashimoto's) thyroiditis	A	O	A	B	B	C	C	C	C
Benign, c/w granulomatous (subacute) thyroiditis	A	A	O	B	B	C	C	C	C
Benign, other	A	A	A	B	B	C	C	C	C
AUS or FLUS	A	A	A	A	A	B	B	B	B
Follicular lesion, conventional type	B	B	B	O	A	A	B	B	B
Follicular lesion, Hurthle cell (oncocytic type)	B	B	B	B	O	A	B	B	B
Suspicious for papillary carcinoma	C	C	C	B	B	O	B	B	B
Suspicious for poorly differentiated carcinoma	C	C	C	B	B	B	O	B	B
Suspicious for medullary carcinoma	C	C	C	B	B	B	B	O	B
Suspicious for undifferentiated carcinoma	C	C	C	B	B	B	B	B	O
Suspicious for lymphoma	C	C	C	B	B	B	B	B	B
Suspicious for malignancy, other	C	C	C	B	B	A	B	B	B
Papillary carcinoma	C	C	C	A	A	O	A	A	A
Poorly differentiated carcinoma	C	C	C	B	B	A	O	A	A
Medullary carcinoma	C	C	C	B	B	A	A	O	A
Undifferentiated (anaplastic) carcinoma	C	C	C	B	B	A	A	A	O
Malignant, other	C	C	C	B	B	A	A	A	A

c/w, consistent with; AUS, atypia of undetermined significance; FLUS, follicular lesion of undetermined significance.

Proficiency test

The second part of the Continuous Quality Improvement program, the PT, was performed in 209 medical institutions from May 3, 2019, to May 25, 2019, using a total of 1,045 glass slides. Five glass slides (2 GYN slides, 1 body fluid or urine, 2 respiratory tract sample or FNA slides) were dispatched to the participating institutions by parcel post. The candidate cases for PT, along with their cytologic diagnoses and the corresponding histologic diagnoses, were collected from the participating institutions in 2015 and 2016. The cases were reviewed by members of the CQIKSC and their eligibility for PT was confirmed. The diagnosis submitted by participating institutions was based

https://doi.org/10.4132/jptm.2020.02.26

Table 4. Discordance assessment criteria for body fluid, urine, and other fine-needle aspiration samples

Original diagnosis	Submitted diagnosis				
	Negative or benign	Atypical, favor reactive	Atypical, favor neoplastic	Malignant	Malignant, but different diagnosis
Benign	O	A	B	C	C
Atypical, favor reactive	A	O	A	B	B
Atypical, favor neoplastic	B	A	O	A	A
Malignant	C	B	A	O	A

on the Bethesda system [6] for GYN samples and on the thyroid Bethesda system [7] for thyroid FNA samples. The submitted diagnoses were evaluated using the discordance assessment criteria (Tables 1–4), and the diagnostic concordance was categorized as either concordant (category O) or as one of three discordant categories: category A (minimal clinical impact), category B (minor clinical impact), or category C (major clinical impact). The criteria for PT have been developed and modified by CQIKSC based on the potential clinical impact in relation to the clinical treatment guidelines.

Sample adequacy assessment

The third part of the program was the sample adequacy assessment. Each participating institution was asked to submit five GYN glass slides of any consequent number and the corresponding reported adequacy that were diagnosed in each institution on March 5, 2018. They were submitted to the CQIKSC from September 10, 2018, to September 21, 2018, and the sample adequacy was reevaluated by the members of the CQIKSC.

Submission of samples for the QA program

For the final part of the program, each participating institution was asked to submit six glass slides (2 GYN, 2 non-GYN, and 2 FNA) with confirmed cytologic diagnoses and the corresponding histologic diagnoses from November 26, 2018, to December 7, 2018. The eligibility of the collected samples for the PT was evaluated by the members of the CQIKSC, and eligible samples were archived to be used in the PT in the following years.

Statistical analysis

The correlation between total case numbers, liquid-based preparation (LBP) coverage, atypical squamous cells to squamous intraepithelial lesions ratio (ASC/SIL ratio) of participant institutions in 2018 was done using Pearson correlation analysis with Microsoft Excel 14.0.7237.5000, Microsoft Co. (Redmond, CA, USA).

RESULTS

Participating institutions

Responses were obtained from all 211 medical institutions, including 83 university hospitals (39.3%), 84 general hospitals (39.8%), and 44 commercial laboratories (20.8%) (Fig. 1). The number of participating institutions steadily increased from 148 in 2004 to 211 in 2018. In particular, the number of commercial laboratories significantly increased from 25 (14.6%) in 2009 to 44 (20.8%) in 2018, while the number of general and university hospital laboratories slightly increased.

Overall statistics

The total number of cytopathologic examinations performed in 2018 was 10,057,839; this number was more than triple the number of examinations performed in 2004 (2,891,867, compounded annual growth rate: 7.2%) (Fig. 1). The number of cytologic exams performed was 1,695,625 in university hospitals (16.9%), 732,880 in general hospitals (7.3%), and 7,629,334 in commercial laboratories (75.9%). In 2018, commercial laboratories only comprised approximately 20% of the total institutions but performed over 75% of the total examinations (Supplementary Fig. S1). In 2015, commercial laboratories comprised 17.5% of the participating institutions (36 out of 206) and performed 5,717,336 out of 8,284,952 exams (69.0%), illustrating a significant increase of the segment share (69.0% to 75.9%) and the number of institutions (17.5% to 20.8%). In 2018, the average number of cytologic exams was 20,429 in university hospitals, 8,724 in general hospitals, and 173,393 in commercial laboratories. In 2015, the average number of cytologic exams was 19,320 in university hospitals, 11,080 in general hospitals, and 158,814 in commercial laboratories, illustrating a significant increase in the number of exams in university hospitals and commercial laboratories and a significant decrease in the number of exams in general hospitals.

GYN and non-GYN samples

In 2018, the total number of GYN samples was 7,641,281 (76.0%), and the total number of non-GYN samples was

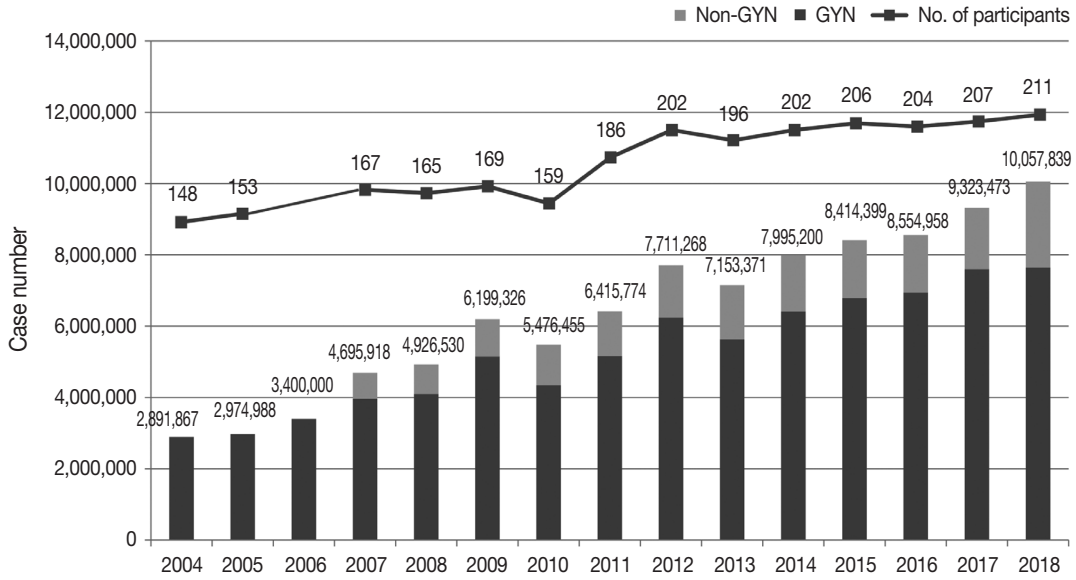

Fig. 1. Overall statistics of cytopathology exams from 2004 to 2018. GYN, gynecologic samples; Non-GYN, non-gynecologic samples.

2,416,558 (24.0%). The percentage of non-GYN samples gradually increased from 14% in 2007 to 24.0% in 2018. The majority (approximately 80.9%) of the GYN samples were analyzed in commercial laboratories (n = 6,181,796), while only 6.7% and 12.5% were processed by general and university hospitals, respectively. The proportion of GYN samples analyzed by commercial laboratories significantly increased from 58.0% in 2004 and 74.2% in 2015 to 80.9% in 2018; however, from 2015 to 2018, this number was similar in university hospitals (13.8% and 12.5%) and significantly decreased in general hospitals (11.1% to 6.7%). The proportion of non-GYN samples was highest in university hospitals (44%), followed by general hospitals (31%) and commercial laboratories (19%).

The primary types of non-GYN samples were body fluids (n = 1,664,313, 68.9%), followed by urine (n = 431,749, 17.9%) and FNA (n = 320,496, 13.3%). The majority of the body fluids were obtained from the respiratory system (e.g., sputum, bronchial washing, or bronchial brushing, n = 1,508,676, 90.6%) (Fig. 2A). Most of the FNA samples were taken from the thyroid (n = 225,511, 70.4%). The FNA and urine samples were more common in the university (17.4% and 30.6%, respectively) and general hospitals (18.9% and 24.2%, respectively), while body fluids from the respiratory tract comprised the majority of the commercial laboratory samples (79.4%) (Fig. 2B).

Conventional and LBP cytology

Of all the samples, 8,030,418 (79.8%) samples were prepared by conventional smear, and 2,027,421 (20.2%) samples were prepared by LBP. The LBP method was used in 19.5% of the GYN (n = 1,493,582) and 22.1% of the non-GYN samples (n = 533,839), including 44.4% of the urine (n = 191,769), 43.6% of the FNA (n = 139,599), and 12.1% of the body fluid (n = 202,471) samples (Fig. 3A). The LBP coverage of the GYN samples slightly decreased from 2017 to 2018 (20.3% to 19.5%). The LBP coverage of the non-GYN samples also decreased from 2017 to 2018 (25.2% to 22.1%), although the coverage was significantly increased in the FNA and urine subsets among the non-GYN samples. This indirectly suggests that from 2017 to 2018 a relatively high increase of GYN and body fluid samples were prepared by conventional methods (Fig. 3A). The LBP coverage of the GYN samples increased from 2017 to 2018 in both university and general hospitals, while it decreased in commercial laboratories (Fig. 3B). This pattern was similar in the non-GYN samples; the LBP coverage decreased only in commercial laboratories in 2018 (Fig. 3C). Among the subsets of the non-GYN samples, the LBP coverage generally increased in the FNA and urine samples of all institutions, while it only decreased in the body fluid samples of the commercial laboratories. (Fig. 3D–F). Chronologically, the LBP coverage in the GYN samples increased from 7.6% in 2004, reached a peak of 29.0% in 2012, and decreased slightly to 19.5% in 2018 (Fig. 3G).

Distribution of the GYN sample cytologic diagnoses

The cytologic diagnoses percentages of the GYN samples are summarized in Table 5. The percentage of the samples with "unsatisfactory adequacy" was 0.14% in 2018. The overall per-

https://doi.org/10.4132/jptm.2020.02.26

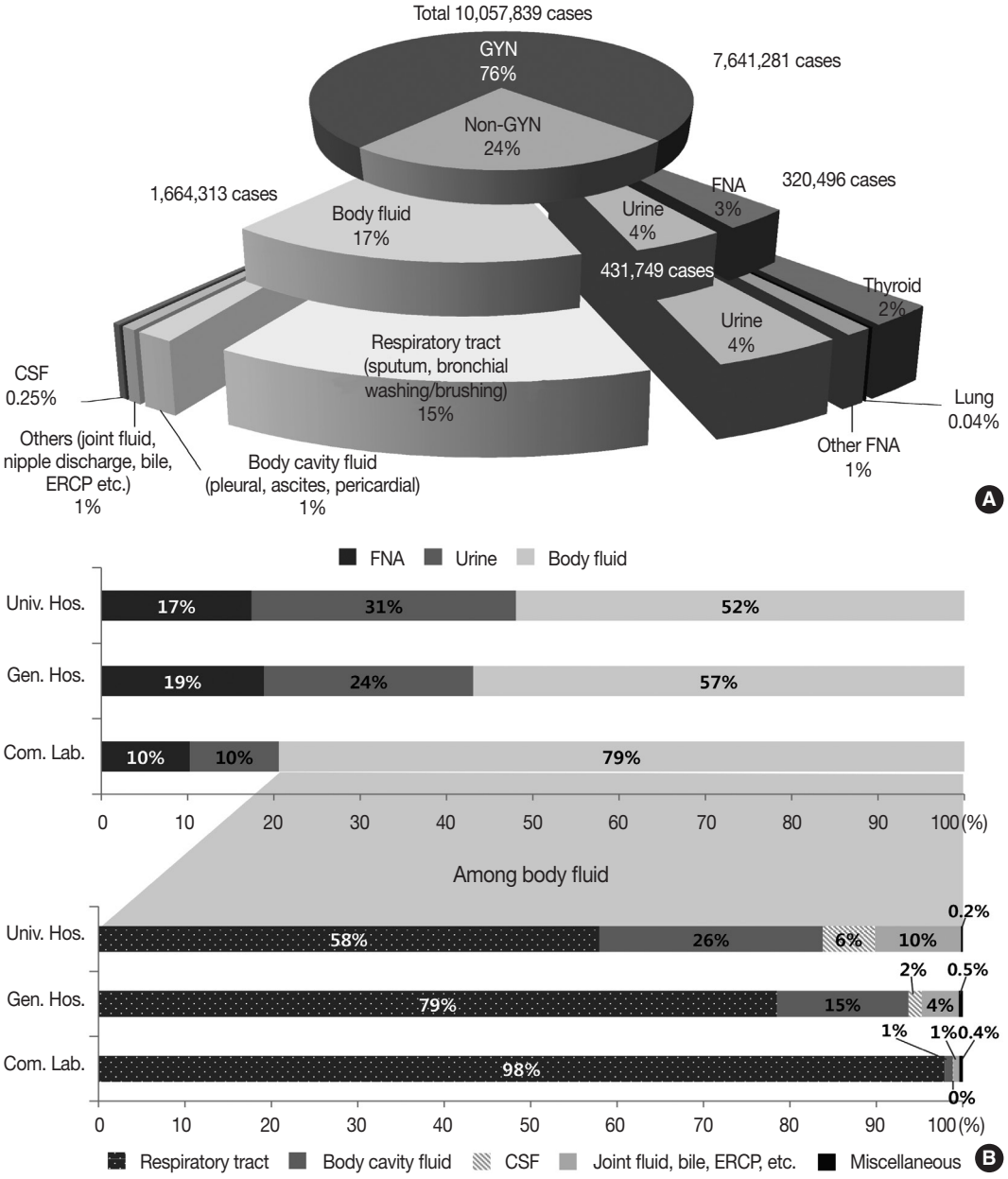

Fig. 2. Number and proportion of cytopathology exams according to types of sample (A) and institution (B). GYN, gynecologic samples; Non-GYN, non-gynecologic samples; FNA, fine-needle aspiration; CSF, cerebrospinal fluid; ERCP, endoscopic retrograde cholangiopancreatography; Univ. Hos., university hospitals; Gen. Hos., general hospitals; Com. Lab., commercial laboratories.

centage of the "negative" samples was 95.29%. The percentage of "atypical squamous cells of undetermined significance" (ASC-US) and "atypical squamous cells-cannot exclude high-grade squamous intraepithelial lesion" were 3.45% and 0.19%, respectively. The percentage of "low-grade squamous intraepithelial lesion" and "high-grade squamous intraepithelial lesion" were 0.65% and 0.19%, respectively. The ratio of ASC-US to squamous intraepithelial lesion (SIL) was 4.25 in 2018. Compared to 2017, the percentage of ASC-US increased from 3.47% to 3.69%, and the percentage of SIL decreased from 0.91% to 0.87%.

Although the total number of GYN samples increased significantly from 5,640,080 in 2012 to 7,706,455 in 2018 as the coverage of the National Cancer Screening Program increased, the total number of SIL and cancer slightly decreased from 71,722 in 2012 to 67,063 in 2018 and 2,847 in 2012 to 2,042 in 2018, respectively (Fig. 4A). In contrast, the atypical squamous cell (ASC) percentage increased slightly from 3.03% in 2012 to 3.69% in

2018. As a result, the ASC/SIL ratio increased from 2.98 in 2012 to 4.24 in 2018. With regard to institutions, the ASC/SIL ratio was steadily maintained at approximately 1.8 in university hospitals and 2.5 in general hospitals; however, it has continuously increased in commercial laboratories from 3.68 in 2012 to 5.65 in 2018 (Fig. 4B). A correlation analysis using the data from all

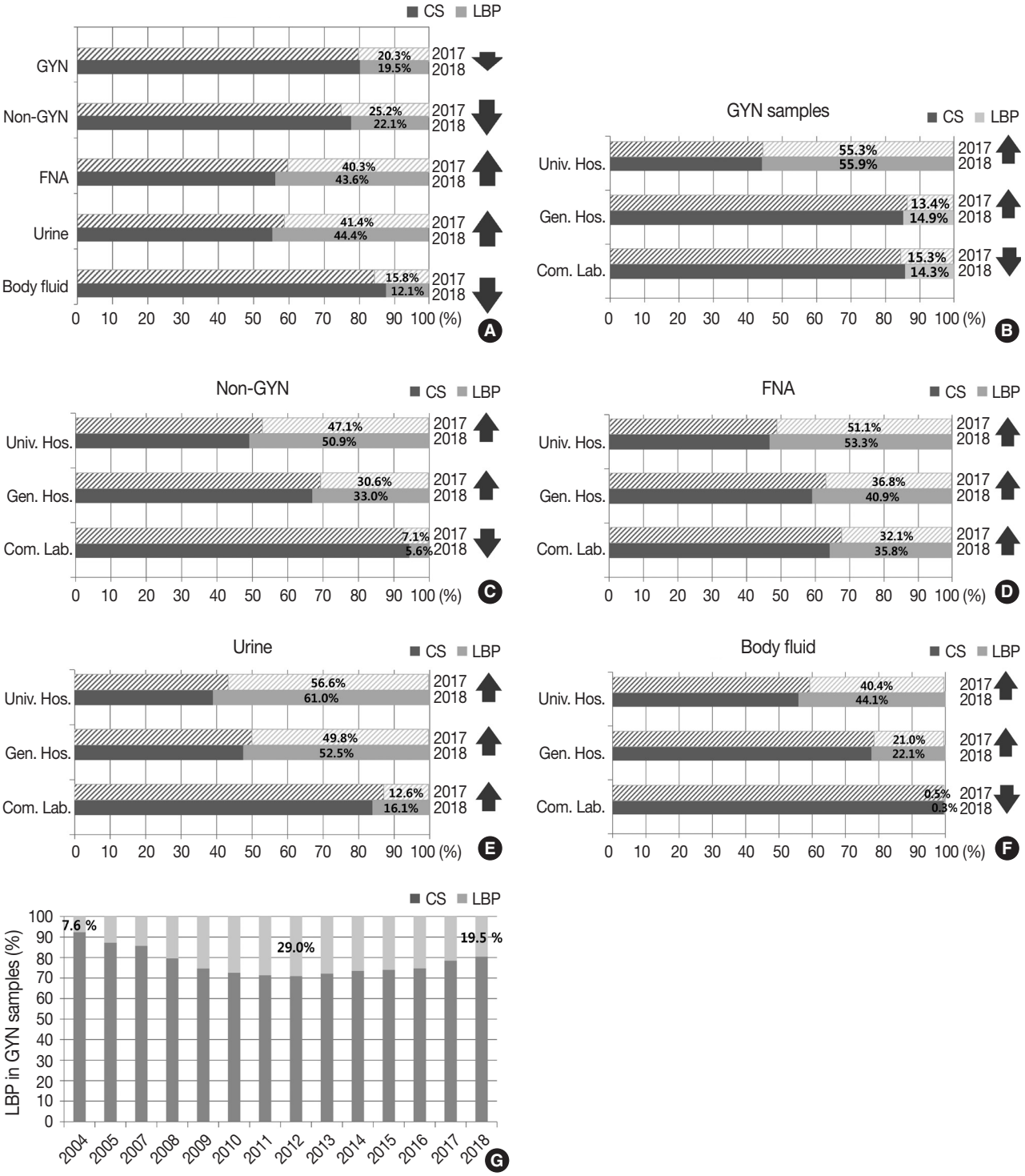

Fig. 3. Proportion of conventional smear (CS) and liquid-based preparation (LBP) cytology. Change in proportion between 2017 and 2018 of all samples (A), gynecologic samples (GYN) (B), non-gynecologic samples (Non-GYN) (C), fine-needle aspiration (FNA) (D), urine (E), and body fluid (F). (G) Proportion of CS and LBP cytology of gynecologic samples from 2004 to 2018. Univ. Hos., university hospitals; Gen. Hos., general hospitals; Com. Lab., commercial laboratories.

https://doi.org/10.4132/jptm.2020.02.26

Table 5. Distribution of the gynecologic sample cytologic diagnoses

Cytologic diagnosis	2017	2018
Unsatisfactory	0.24	0.14
Negative (reactive cellular change, inflammation, atrophy, etc.)	95.10	95.29
ASC	3.51	3.64
ASC-US	3.31	3.45
ASC-H	0.20	0.19
AGC	0.05	0.05
AGC, favor neoplastic	0.01	0.01
L-SIL	0.70	0.65
H-SIL	0.20	0.19
Squamous cell carcinoma	0.02	0.02
Adenocarcinoma	0.00	0.01
ASC/SIL ratio	3.82	4.25

ASC, atypical squamous cells; ASC-US, atypical squamous cells of uncertain significance; ASC-H, atypical squamous cells, cannot exclude H-SIL; AGC, atypical glandular cells; L-SIL, low-grade squamous intraepithelial lesion; H-SIL, high-grade squamous intraepithelial lesion; ASC/SIL ratio, atypical squamous cells/squamous intraepithelial lesion ratio.

211 institutions showed that the laboratories with more cases tended to use less LBP and report a higher ASC/SIL ratio, although these findings were not statistically significant (Fig. 4C, D). Moreover, the laboratories that used more LBP tended to report significantly lower ASC/SIL ratios (Fig. 4E).

CHCR for the GYN cytology

As part of the internal quality control (QC) program, each institution was asked to compare the diagnoses of the cytologic and histologic samples of the same individual whenever possible and to document the degree of discordance between the cytologic and histologic diagnoses according to the institutional criteria. Of 69,808 cases, 60,823 cases showed concordant results between the cytologic and histologic diagnoses (87.1%) (Fig. 5A). Discordance with minimal and minor clinical impact (categories A and B) were found in 6,555 and 2,301 cases, respectively (9.4% and 3.3%) (Fig. 5B). Discordance with major clinical impact (category C) was found in 361 cases (0.52%) (Fig. 5B). Over the past 15 years, while an increasing number of cases have been compared, the discordant rate has been steadily maintained at approximately 15% (Fig. 5A). However, the rates of discordance with minor and major clinical impact (categories B and C) have markedly decreased from 4.40% and 1.5% in 2003 to 3.30% and 0.52% in 2018, respectively (Fig. 5B).

Adequacy of GYN samples

The percentage of the GYN samples with unsatisfactory adequacy in each institution was collected as a part of the annual survey. The overall unsatisfactory rate was 0.14% in 2018 and 0.24% in 2017. It was 0.45% in university hospitals, 0.44% in general hospitals, and 0.07% in commercial laboratories in 2018.

Proficiency test

The PT using 1,045 dispatched glass slides showed 84.6% overall concordance (category O), 12.2% discordance with minimal clinical impact (category A), 2.2% discordance with minor clinical impact (category B), and 0.95% discordance with major clinical impact (category C) (Fig. 6A). The concordance rates reported by the institutions were 86.6% in university hospitals, 85.9% in general hospitals, and 78.1% in commercial laboratories; discordance with major clinical impact (category C) was 1.0% in university hospitals, 1.2% in general hospitals, and 0.5% in commercial laboratories (Fig. 6A). Of the 420 GYN cytology cases, the overall concordance rate was 75.2%, minimal discordance (category A) was 21.0%, minor discordance (category B) was 2.8%, and major discordance (category C) was 0.5% (Fig. 6B). Concordance reported by the institutions was 77.4%, 77.6%, and 67.9% in university hospitals, general hospitals, and commercial laboratories, respectively. Major discordance (category C) was 0.6%, 0.6%, and 0.0% in the university hospitals, general hospitals, and commercial laboratories, respectively (Fig. 6B). Of the 164 thyroid FNA cases, the overall concordance was 95.7%, and the major discordance was 1.2% (Fig. 6C). The concordance rates by institution were similar in the university hospitals (98.5%), general hospitals (95.4%), and commercial laboratories (90.9%). Major discordance was found in only two cases (3.1%) in the general hospitals (Fig. 6C). Of the 300 body fluid cases, the overall concordance was 91.0% and the major discordance rate was 1.0% (Fig. 6D). The concordance rate was 92.4%, 92.6%, and 85.0% in the university hospitals, general hospitals, and commercial laboratories, respectively. Major discordance was found in one case in each institution (0.8%, 0.8%, and 1.7% in university hospitals, general hospitals, and commercial laboratories, respectively) (Fig. 6D). Of the 108 urine cytology cases, the overall concordance rate was 85.2%, and the major discordance rate was 1.9% (Fig. 6E). The concordance rate was 86.0%, 89.1%, and 73.7% in the university hospitals, general hospitals, and commercial laboratories, respectively. Major discordance was found in one case in the general hospitals and in the commercial laboratories (2.2% and 5.3%, respectively) (Fig. 6E). Among 55 other FNA cases, the overall concordance rate was 83.6%, and the major discordance rate was 5.5% (Fig. 6F). The concordance rate was 88.9%, 78.3%, and 85.7% in the university hospitals, general hospitals, and commercial laboratories, respectively. Major

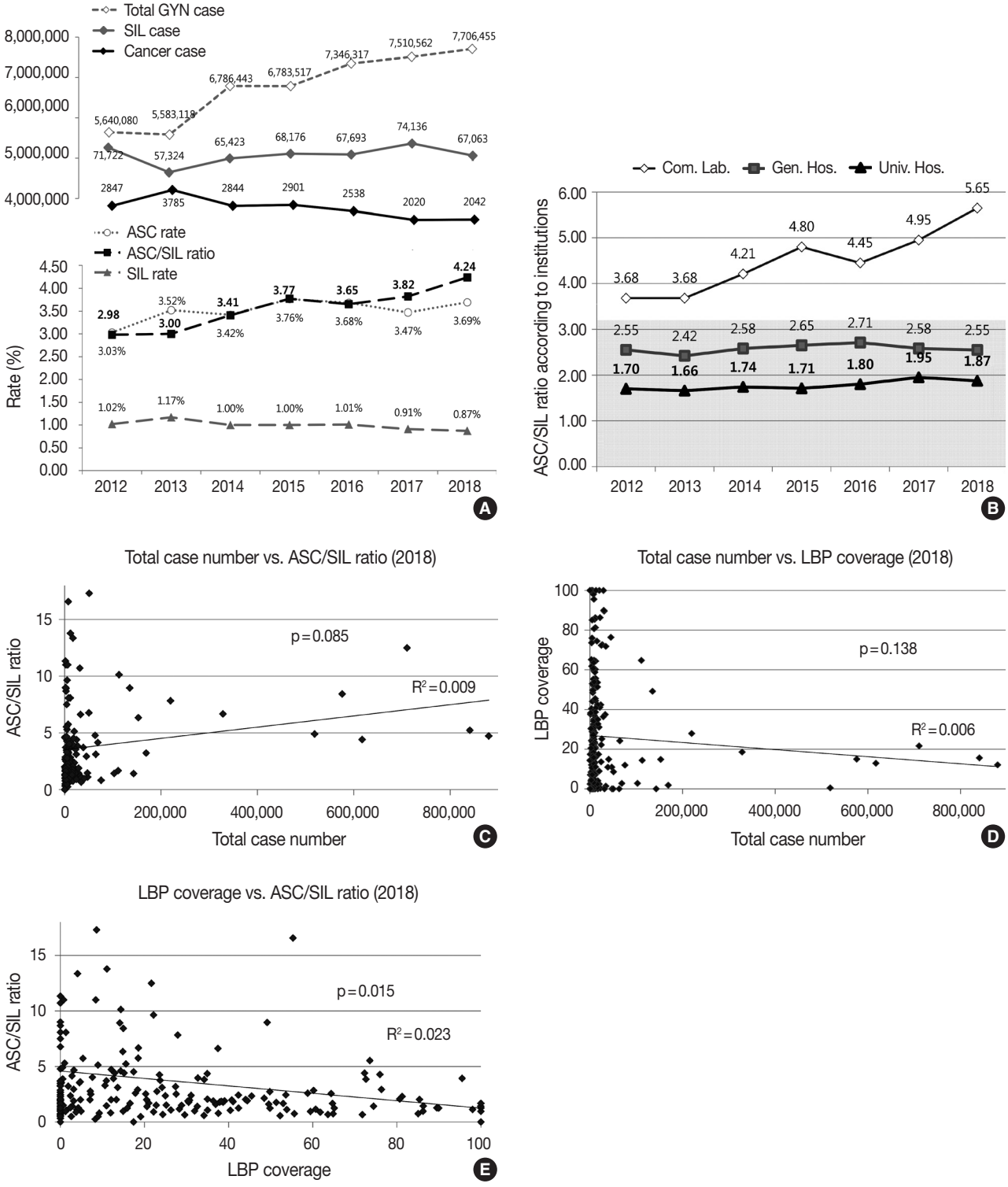

Fig. 4. Trends in gynecologic sample cytologic diagnoses from 2012 to 2018 and correlation analysis according to atypical squamous cells to squamous intraepithelial lesions ratio (ASC/SIL ratio). Trends in the number of total gynecologic (GYN) samples, atypical squamous cells (ASC), squamous intraepithelial lesions (SIL), cervical cancers, and ASC/SIL ratio from 2012 to 2018 (A), ASC/SIL ratio according to institutions (B), correlation of total case number versus liquid-based preparation (LBP) coverage among 211 participating institutions in 2018 (C), correlation of total case number versus ASC/SIL ratio in 2018 (D), correlation of LBP coverage versus ASC/SIL ratio in 2018 (E). Com. Lab., commercial laboratories; Gen. Hos., general hospitals; Univ. Hos., university hospitals.

https://doi.org/10.4132/jptm.2020.02.26

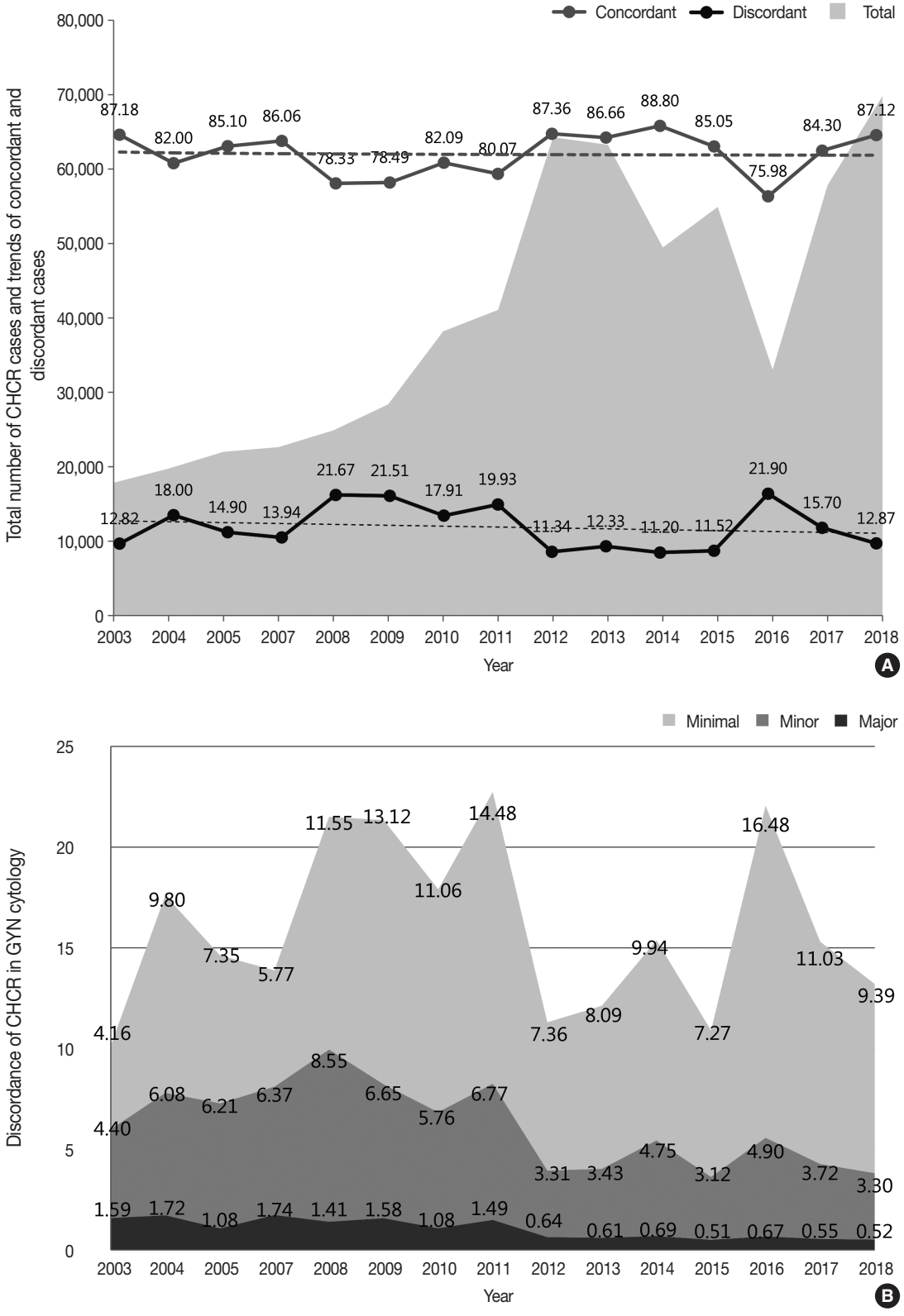

Fig. 5. The results of cytology-histology correlation review (CHCR) from 2003 to 2018. (A) Total number of CHCR cases and trends of the proportions of concordant (category O) and discordant cases. (B) Trends in discordant cases with minimal (category A), minor (category B), and major (category C) clinical impact. GYN, gynecologic samples.

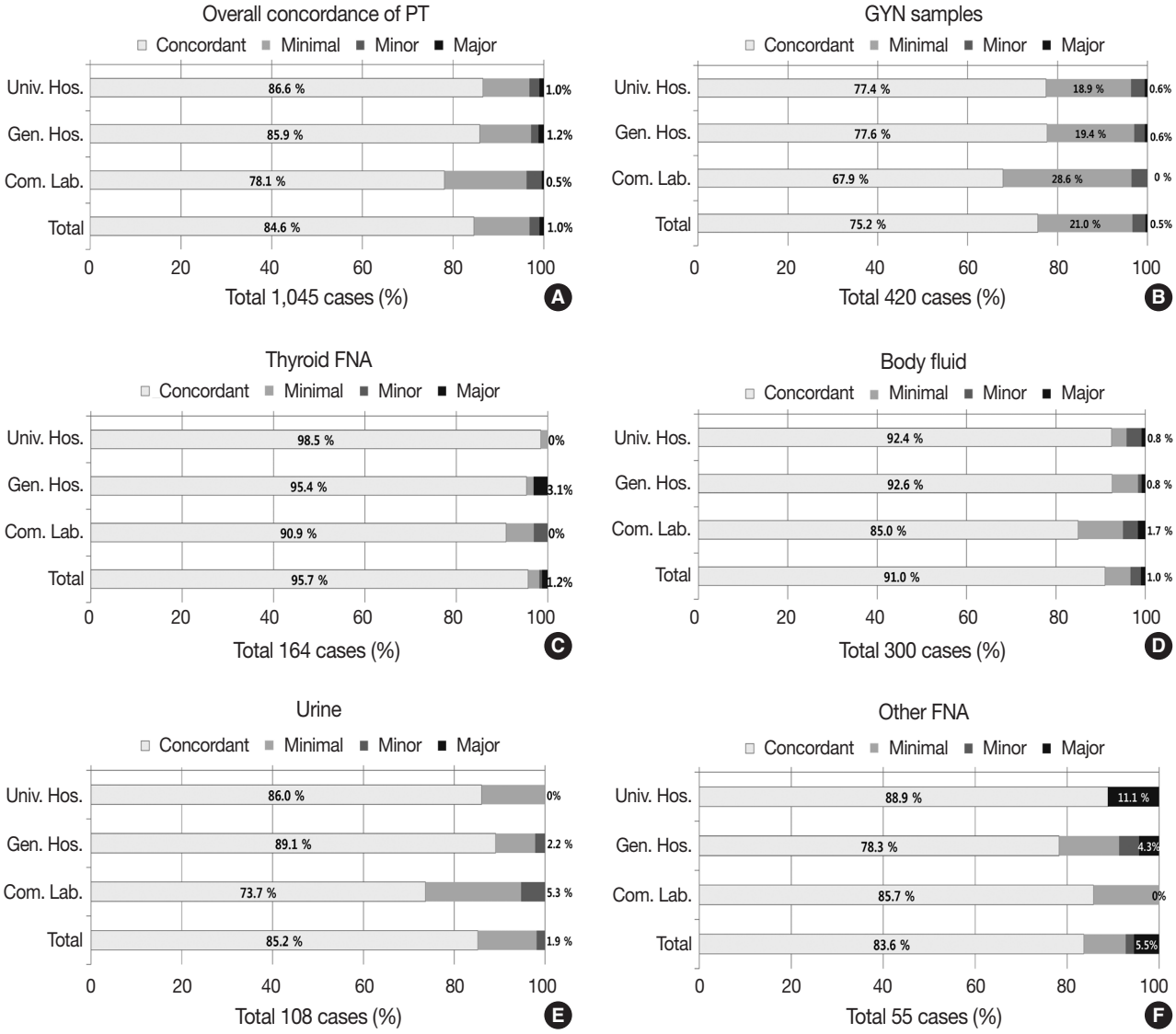

Fig. 6. Proficiency test (PT) results according to institutions in 2018. Overall concordance of PT (A), and concordance of PT in gynecologic samples (B), thyroid fine-needle aspiration (FNA) cytology samples (C), body fluid samples (D), urine (E), and other FNA samples (F). GYN, gynecologic samples; Univ. Hos., university hospitals; Gen. Hos., general hospitals; Com. Lab., commercial laboratories.

discordance was found in two cases and one case in the university and general hospitals, respectively (11.1% and 4.3%, respectively) (Fig. 6F).

Sample adequacy assessment

A total of 193 participating institutions submitted a total of 965 GYN slides of consequent numbers (5 slides from each institution) and their reported adequacy. The sample adequacy assessments reevaluated by the members of the CQIKSC and the reported adequacy of the institutions in all cases were concordant.

Submission of samples for the next QA program

A total of 182 participating institutions submitted 961 glass slides with confirmed cytologic diagnoses and corresponding histologic diagnoses.

DISCUSSION

The key findings of this study are summarized as follows: 1) the total number of cytopathologic exams is continuously increasing, and the proportion of non-GYN samples is gradually increasing over time; 2) the number of cytopathologic exams processed by commercial laboratories is increasing; 3) the LBP coverage is in-

https://doi.org/10.4132/jptm.2020.02.26

creasing in all samples except GYN and body fluid samples processed by commercial laboratories; 4) the total number of GYN exams is increasing, but the number of cancer cases is decreasing; 5) the ASC/SIL ratio is increasing (the ASC percentage is increasing while the SIL percentage is decreasing); 6) the high LBP coverage seems to be lowering the ASC/SIL ratio; 7) the major discordance rate found by the CHCR (internal QC assessment) is decreasing over time; 8) the unsatisfactory rate in GYN samples is well under control; 9) the average diagnosis concordance rate of the PT (external QC assessment) is approximately 85% with a major discordance (category C) rate of less than 1%; and 10) the concordance rate was highest in thyroid FNA, lower in urine and other FNA, and lowest in GYN cytology.

The total number of cytopathologic exams has increased dramatically to over 10 million exams per year. It has more than tripled from the number of total exams in 2004 with a steady compounded annual growth rate of 7.2%. Furthermore, the growth has not slowed but rather reached a peak. In 2018, an annual average of 47,667 cases was processed by individual laboratories that processed only 19,000 cases in 2004. This seems to be primarily due to the introduction of screening cytologic exams in the National Cancer Screening Program [1,2,8]. The proportion of non-GYN samples has also been gradually increasing over time. This is probably because of an overall increase in cytologic exams (the subgroup proportions were not significantly different from the numbers in 2015).

The number of cytopathologic exams processed by commercial laboratories has been increasing. The average number of cytologic exams reported by the institutions showed a bipolar distribution; they significantly increased in university hospitals (19,320 in 2015 to 20,429 in 2018) and commercial laboratories (158,814 in 2015 to 173,393 in 2018) but decreased in general hospitals (11,080 in 2015 to 8,724 in 2018). This finding suggests that university hospitals and commercial laboratories have a need for more manpower.

LBP coverage has generally increased in all samples, especially thyroid FNA and urine samples based on the wide acceptance of the technology in these samples [9]. However, it decreased in the GYN and body fluid samples processed by the commercial laboratories. This seems to be primarily due to the increase in National Cancer Screening Program samples where LBP methods are not covered by insurance. Because the total number of cytologic exams is significantly increasing and cytopathology manpower is limited, expanding LBP coverage in the cancer screening program would be an effective strategy to manage increasing labor demands.

Over the past few years, the total number of GYN exams has been increasing and the number of cancer cases has been decreasing. At the same time, the ASC/SIL ratio, an important QC parameter for GYN cytology exams [10], has been increasing (the ASC rate has been increasing while the SIL rate has been decreasing). This finding seems to be due to the expansion of the recipient age group of the National Cancer Screening Program. Since 2016, the National Cancer Screening Program has covered women over the age of 20 (previously, only women over the age of 30 were covered), and the number of negative or ASC cases has increased while the number of SIL or cancer cases proportionally decreased [8]. The ASC/SIL ratio was more significantly increased in commercial laboratories than in the other institutions (3.68 in 2012 to 5.65 in 2018), which explains the impact of the changes in the National Cancer Screening Program samples. Interestingly, in correlation analyses, the institutions with more samples tended to have less LBP coverage and to report higher ASC/SIL ratios, and high LBP coverage tended to significantly correlate with lower ASC/SIL ratios. As the registered cytotechnologists that perform cytology screening were estimated as 386 in 2017, the average number of GYN samples screened by a cytotechnologist is 19,796.1 cases per year, approximately 79.2 cases per working day, which indicates that cytology laboratories in Korea have a labor-intensive working environment.

The major discordance (category C) rate in the CHCR of the GYN samples has been significantly decreasing over time to a level as low as 0.52%, and the unsatisfactory rate of GYN samples has been well controlled over time (0.14% in 2018). These findings show that the Continuous Quality Improvement program of KSC has gradually contributed to the improvement of cytopathologic exam quality in cytopathology laboratories in Korea over time.

In the PT, the average diagnosis concordance rate was approximately 85%, and the major discordance (category C) rate was less than 1% (0.95%). The concordance rate was the highest in thyroid FNA (95.7%), followed by body fluids (91.0%), urine (85.2%), and other FNA (83.6%); it was the lowest in GYN cytology (75.2%). This finding seems to be due to the sample characteristics and the varying degrees of complexity of the diagnostic categories. In GYN cytology, the major discordance (category C) was less than 0.5%, while the minimal and minor discordance (categories A and B) composed almost one-fourth of the total samples (24.3%). This finding indirectly shows the complexity of the diagnostic category (Bethesda system [6]) of GYN cytology. In contrast, in thyroid FNA, the concordance rate was over 95%. This seems to stem from the monotonous composition of PT samples. The occurrence of the minor categories of

thyroid FNA, such as medullary carcinoma, poorly differentiated, or undifferentiated carcinoma was relatively rare, and these categories were not properly included in the PT sample pools. A more balanced sample composition for the PT should be carefully designed in the future. In comparison with the prior results of PT in 2004 and 2007, the concordant rate slightly but gradually increased from 73.0% in 2004 and 74.5% in 2007 to 75.2% in 2018 [1]. The major discordant rate (category C) also gradually decreased from 2.8% in 2004 and 2.0% in 2007 to 0.5% in 2018 [1]. However, because the discordance assessment criteria for PT have been slightly modified by the CQIKSC during the period as clinical treatment guidelines have changed, it is recommended that this data should be interpreted with care.

For the fourth part of the program, each participating institution has submitted candidate slide samples for the next PT program (182 institutions, 961 slides). However, there are several drawbacks to using these glass slides in the PT program. Not enough samples have been submitted every year. There is a possibility of sample loss or damage during packaging, handling, and storage, which can lead to the leakage of personal information. The level of diagnostic difficulty of each PT sample is variable, and the PT samples may be distributed disproportionately. The PT samples can easily become discolored over time during storage. Because of the aforementioned reasons, the introduction of a digital pathology system in the QC programs is being utilized in other programs such as United Kingdom National External Quality Assessment Site (UKNEQAS) and The Royal College of Pathologists of Australasia Quality Assurance Programs (RCPAQAP) [11,12]. In 2019, CQIKSC will also attempt to adopt the digital pathology system for the Continuous Quality Improvement programs with the collaboration of the Committee of Quality Assurance of the Korean Society of Pathologists. The efficacy of the digital pathology system in the Continuous Quality Improvement program will be assessed during its establishment.

With the results of this study, we confirmed that the Continuous Quality Improvement programs using the annual survey and the internal (CHCR) and external QC tests (PT) in the KSC have contributed to improved cytopathology practice performance quality by enhancing diagnostic accuracy. However, the high ASC/SIL ratio in a few institutions should be further monitored as the National Cancer Screening Programs expand over time. Active intervention and QC surveillance of each institution must be continued.

Supplementary Information

The Data Supplement is available with this article at https://doi.org/10.4132/jptm.2020.02.26.

Ethics Statement

This study was reviewed and approved by the Institutional Review Board of The Catholic University of Korea, Yeouido St. Mary's Hospital (SC19ZCDI0091) with a waiver of consent.

ORCID

Yosep Chong https://orcid.org/0000-0001-8615-3064
Haeyoen Jung https://orcid.org/0000-0001-6950-5144
Jung-Soo Pyo https://orcid.org/0000-0003-0320-8088
Soon Won Hong https://orcid.org/0000-0002-0324-2414
Hoon Kyu Oh https://orcid.org/0000-0001-8793-1948

Author Contributions

Conceptualization: YC, SWH, HKO. Data curation: YC, HKO. Investigation: YC, HKO. Methodology: YC, HKO. Project administration: YC, HJ, JSP, HKO. Resources: YC, HJ, JSP, HKO. Supervision: SWH, HKO. Validation: YC, HKO. Visualization: YC, HJ, JSP. Writing—original draft: YC, HJ, JSP. Writing—review & editing: YC, HJ, JSP, SWH, HKO.

Conflicts of Interest

Y.C., contributing editor and S.W.H., the senior editor of the *Journal of Pathology and Translational Medicine*, were not involved in the editorial evaluation or decision to publish this article. All remaining authors have declared no conflicts of interest

Funding Statement

No funding to declare.

Acknowledgments

We would like to thank Young Dong Seo for reviewing the manuscript and Eun-Mee Jeon for assisting with the data curation.

References

1. Lee HK, Kim SN, Khang SK, Kang CS, Yoon HK. Quality control program and its results of Korean Society for Cytopathologists. Korean J Cytopathol 2008; 19: 65-71.
2. Kim Y, Jun JK, Choi KS, Lee HY, Park EC. Overview of the National Cancer screening programme and the cancer screening status in Korea. Asian Pac J Cancer Prev 2011; 12: 725-30.
3. Suh M, Song S, Cho HN, et al. Trends in participation rates for the national cancer screening program in Korea, 2002-2012. Cancer Res Treat 2017; 49: 798-806.
4. Oh EJ, Jung CK, Kim DH, et al. Current Cytology Practices in Korea: A nationwide survey by the Korean Society for Cytopathology. J Pathol Transl Med 2017; 51: 579-87.
5. Jung M. National Cancer Screening Programs and evidence-based healthcare policy in South Korea. Health Policy 2015; 119: 26-32.
6. Nayar R, Wilbur DC. The Bethesda system for reporting cervical cytology: definitions, criteria, and explanatory notes. 3rd ed. Cham: Springer, 2015.
7. Cibas ES, Ali SZ. The 2017 Bethesda System for Reporting Thyroid Cytopathology. Thyroid 2017; 27: 1341-6.
8. Lim SC, Yoo CW. Current status of and perspectives on cervical cancer screening in Korea. J Pathol Transl Med 2019; 53: 210-6.
9. Chong Y, Ji SJ, Kang CS, Lee EJ. Can liquid-based preparation substitute for conventional smear in thyroid fine-needle aspiration? A

systematic review based on meta-analysis. Endocr Connect 2017; 6: 817-29.
10. Nascimento AF, Cibas ES. The ASC/SIL ratio for cytopathologists as a quality control measure: a follow-up study. Am J Clin Pathol 2007; 128: 653-6.
11. Hodgson C, Cross P. Introduction and development of a digital diagnostic non gynaecological diagnostic cytology interpretative scheme. Cytopathology 2018; 29(Suppl 1): 79.
12. Greaves J, Holzhauser D. Virtual cytopathology in an Austrailian EQA setting. In: 20th International Congress of Cytology; 2019 May 5-10; Sydney, Australia.

JPTM
Journal of Pathology and Translational Medicine 2020; 54: 332-335
https://doi.org/10.4132/jptm.2020.04.20

CASE STUDY

Gastric crystal-storing histiocytosis with concomitant mucosa-associated lymphoid tissue lymphoma

Mee Joo[1], Nam-Hoon Kim[2]

[1]Department of Pathology, Ilsan Paik Hospital, Inje University College of Medicine, Goyang;
[2]Division of Gastroenterology and Hepatology, Department of Internal Medicine, Ilsan Paik Hospital, Inje University College of Medicine, Goyang, Korea

Crystal-storing histiocytosis (CSH) is a rare entity that is characterized by intrahistiocytic accumulation of crystallized immunoglobulins. CSH is not a malignant process per se, but the majority of CSH cases are associated with underlying lymphoproliferative disorder. Although CSH can occur in a variety of organs, gastric CSH is very rare. We present a localized gastric CSH with concomitant mucosa-associated lymphoid tissue (MALT) lymphoma, manifesting as an ulcer bleeding in a 56-year-old man. Histologically, the biopsied gastric mucosa demonstrated expansion of the lamina propria by prominent collections of large eosinophilic mononuclear cells containing fibrillary crystalloid inclusions. Immunohistochemical studies revealed that the crystal-storing cells were histiocytes harboring kappa light chain-restricted immunoglobulin crystals. Within the lesion, atypical centrocyte-like cells forming lymphoepithelial lesions were seen, consistent with MALT lymphoma. Since this entity is rare and unfamiliar, difficulties in diagnosis may arise. Particularly, in this case, the lymphomatous area was obscured by florid CSH, making the diagnosis more challenging.

Key Words: Crystal-storing histiocytosis; Mucosa-associated lymphoid tissue lymphoma; Stomach

Received: March 10, 2020 **Revised:** April 8, 2020 **Accepted:** April 20, 2020
Corresponding Author: Mee Joo, MD, PhD, Department of Pathology, Inje University Ilsan Paik Hospital, 170 Juhwa-ro, Ilsanseo-gu, Goyang 10380, Korea
Tel: +82-31-910-7141, Fax: +82-31-910-7139, E-mail: mjoo@paik.ac.kr

Crystal-storing histiocytosis (CSH) is a rare entity that is characterized by prominent collections of histiocytes with a distinctive intracytoplasmic accumulation of immunoglobulin crystals [1-4]. The name CSH is descriptive and sounds harmless, but up to 90% of cases are associated with an underlying lymphoproliferative or plasma cell disorder, such as multiple myeloma, lymphoplasmacytic lymphoma, or monoclonal gammopathy of undetermined significance [2-4]. That is, CSH is an under-recognized paraneoplastic phenomenon, and the awareness of CSH may help to detect a hidden malignancy. CSH can be overlooked if so subtle, while extensive CSH can obscure a concomitant lymphoma. We herein describe the histologic findings of CSH associated with mucosa-associated lymphoid tissue (MALT) lymphoma in detail, to be aware of this rare entity and facilitate a proper diagnosis.

CASE REPORT

A 79-year-old man was admitted to our hospital with melena and hematemesis lasting for 5 hours. He denied any previous history of gastrointestinal bleeding. His medical history included lacunar infarct, hypertension, and dementia. He was taking Aspirin Protect (100 mg/day). Laboratory test demonstrated anemia (hemoglobin, 9 g/dL; hematocrit, 26.7%), but otherwise normal complete blood counts. Emergency endoscopy and colonoscopy were performed. Colonoscopy showed no bleeding focus. Esophagogastroduodenoscopy revealed a 1 cm-sized active ulcer with an eroded vessel in the high body (Fig. 1A), which was treated with epinephrine injection and argon plasma coagulation. The surrounding mucosa was hyperemic and friable. A flat nodular lesion with irregular margin and discoloration was also seen in the low body (Fig. 1B). Multiple biopsy specimens were obtained from the margin, the surrounding area of the ulcer, and the flat nodular lesion. Microscopically, all biopsy specimens showed marked expansion of the lamina propria by sheets of large mononuclear cells with brightly eosinophilic cytoplasm and eccentric small bland nuclei (Fig. 1C, D). At higher magnification, abundant eosinophilic cytoplasm contained fibrillary,

pISSN 2383-7837
eISSN 2383-7845

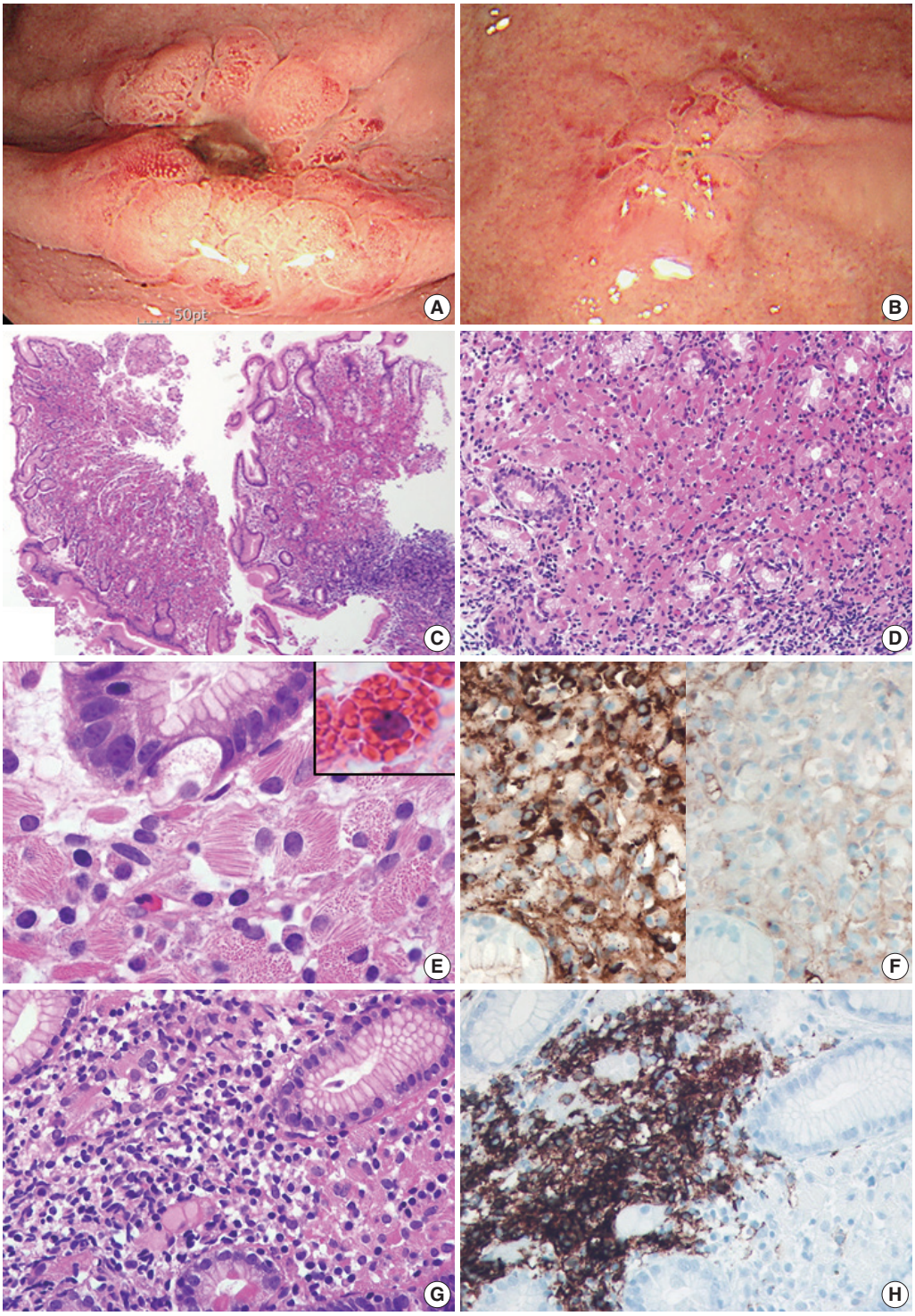

Fig. 1. Esophagogastroduodenoscopy reveals an active ulcer surrounded by elevated hyperemic mucosa in the high body (A) and another flat erosive lesion showing hypertrophic folds and nodularity in the low body (B). (C, D) Microscopically, all the biopsy specimen demonstrates dense infiltration of large eosinophilic mononuclear cells and lymphocytes, along with remarkable decreases in gastric glands. (E) At higher magnification, infiltrating mononuclear cells are packed with eosinophilic, fibrillary, needle-like crystalloid inclusions displacing nuclei, which are different from Mott cells that have grape-like intracytoplasmic spherical inclusions (inset). (F) Immunohistochemically, both crystal-storing cells and lymphoplasma cells show kappa light chain restriction: they are positive for kappa (left) and negative for lambda (right) immunostains. (G) Atypical small- to intermediate-sized lymphoid cells infiltrate adjacent gastric glands to form a lymphoepithelial lesion, which are CD20-positive centrocyte-like cells (H).

Table 1. Clinical and pathological findings of previously published cases of gastric crystal-storing histiocytosis in the English literature

Year	Study	Sex/Age (yr)	Endoscopic finding	*Helicobacter pylori* infection	Associated neoplasm	Ig light chain	Follow-up data
1999	Jones et al. [1]	F/35	NS	NS	Thymic lymphoma	Polyclonal	Persist
2006	Stewart and Spagnolo [7]	M/82	Gastritis	Yes	No	Lambda	Died of unrelated cause
2006	Stewart and Spagnolo [7]	M/81	Gastritis	Yes	No	Insufficient	No symptoms or lesion
2006	Stewart and Spagnolo [7]	F/52	Erosion	Yes	No	Lambda	No symptoms or lesion
2007	Joo et al. [8]	F/56	Polyps	Yes	No	Polyclonal	No residual lesion
2013	Yano et al. [9]	F/55	Discoloration with granularity	Yes	No	Polyclonal	Alive without disease
2014	Vaid et al. [10]	M/NS	Discolored patch	NS	No	Kappa	No
2016	Kanagal-Shamanna et al. [4]	M/43	Nodule	NS	MALT lymphoma	Kappa	Alive without disease
2016	Kanagal-Shamanna et al. [4]	M/51	NS	NS	Multiple myeloma	Lambda	No
2018	Arnold et al. [6]	[a]	Discoloration with granularity	Yes	MALT lymphoma	Kappa	Persist
2018	Arnold et al. [6]	[a]	Discoloration with granularity	Yes	MALT lymphoma	Kappa	Persist
2018	Arnold et al. [6]	[a]	Malignant-appearing mass	No	Mantle cell lymphoma	Lambda	Died of lymphoma
2018	Arnold et al. [6]	[a]	Malignant-appearing mass	No	DLBCL	Kappa	Died of lymphoma
2020	Present case	M/79	Ulcer, flat nodularity	No	MALT lymphoma	Kappa	No

F, female; NS, not stated; M, male; MALT, mucosa-associated lymphoid tissue; DLBCL, diffuse large B cell lymphoma.
[a]Including 2 females and 2 males with age range from 56 to 82.

needle-like, non-refractile crystalloid inclusions (Fig. 1E). Immunohistochemical studies revealed that these crystal-storing cells were histiocytes harboring kappa light chain-restricted immunoglobulin crystals; they were diffusely positive for CD68 and kappa light chain (Fig. 1F, left), but negative for lambda light chain (Fig. 1F, right), desmin, smooth muscle actin, S100 protein, CD117, CD1a, and cytokeratin. Also, there were multifocal aggregates of atypical lymphocytes and plasma cells, which also showed kappa light chain restriction. Atypical lymphocytes forming lymphoepithelial lesions were CD20-positive B cells (Fig. 1G, H), and the diagnosis of CSH associated with MALT lymphoma was rendered accordingly. It was not easy to identify the lymphoepithelial lesions due to overwhelming accumulation of crystal-storing histiocytes. *Helicobacter pylori*–like organisms were not observed histologically, and the result of Campylobacter-like organism test was also negative. The patient refused to undergo bone marrow biopsy. Abdominal and pelvic computed tomography revealed no lymph node enlargement or organomegaly.

DISCUSSION

To date, about 130 cases of CSH have been reported in a wide variety of organs, including bone marrow, lymph nodes, liver, spleen, lungs, gastrointestinal tract, kidney, central nervous system, and skin [1-5]. It may present as either localized (a single deposit involving only one organ or site) or generalized (multiple deposits involving more than one organ or site) forms [2]. Localized CSH is more frequent than generalized CSH (about 70% versus 30%) [2-3,5]. The vast majority of the reported CSH cases had underlying lymphoproliferative or plasma cell disorder with monotypic kappa light chain [2-4]. CSH is extremely rare in the stomach, and until now, 14 cases of gastric CSH (including the present one) have been described in the English literature [1,4,6-10]. The detailed clinical and pathological findings of these patients are summarized in Table 1. The 14 patients reported included 8 men and 6 women with a mean age at diagnosis of 61 years (range, 35 to 82 years). There were one generalized (7.1%) and 13 localized (92.9%) forms. Among them, eight patients (57%) had a concomitant or subsequent lymphoplasmacytic malignancy: four MALT lymphomas with kappa-restriction, one mantle cell lymphoma with lambda-restriction, one diffuse large B cell lymphoma with kappa-restriction, one multiple myeloma with lambda-restriction, and one metachronous thymic lymphoma. Five patients (35.7%) had no associated disease except *H. pylori* infection, and the remaining one patient showed no etiologic condition. Four of the patients who had *H. pylori* infection alone did not develop other gastric lesion or symptoms during the follow up period [7-9]. Compared to other organs, gastric CSH predominantly manifested as a localized form, and about half of the cases were not related to clonal lymphoproliferative disorders: instead, they were frequently associated with *H. pylori*–associated gastritis.

The differential diagnosis of CSH may include a variety of conditions characterized by collections of large eosinophilic tumor cells (adult rhabdomyoma, granular cell tumor, and oncocytic neoplasms) or histiocytic aggregation (Langerhans cell

https://doi.org/10.4132/jptm.2020.04.20

histiocytosis, fibrous histiocytoma, xanthogranuloma, Gaucher's disease, malakoplakia, and mycobacterial or fungal infection) [2-4,6]. However, considering the distinctive intracytoplasmic immunoglobulin crystal and gastric location, Russell body gastritis (RBG) may be the most difficult differential diagnosis. RBG is another rare entity characterized by aberrant immunoglobulin deposits in the stomach [11]. Unlike CSH consisting of predominantly histiocytes with crystallized immunoglobulin in the lysosome, RBG is composed of plasma cells with small condensed spherical immunoglobulin surrounded by endoplasmic reticulum membrane (called Mott cells) [12]. Besides histological picture displaying diffuse proliferation of large eosinophilic mononuclear cells in the lamina propria, RBG cases also share similar features, such as frequent kappa light chain restriction of accumulated immunoglobulin (43%) and strong association with *H. pylori* infection (67%) [11]. There were two cases of RBG related to lymphoplasmacytic neoplasm: one with concomitant MALT lymphoma and another with metachronous multiple myeloma three years after RBG diagnosis [13,14]. However, so far, RBG has been considered a unique inflammatory reaction rather than a paraneoplastic phenomenon. Thus, gastric CSH seems to be more significant than RBG in the aspect of association with lymphoproliferative disorder.

In conclusion, although CSH rarely manifests in the stomach, the recognition of CSH is important to initiate a clinical work-up searching for the underlying neoplasm or associated cause. Therefore, once the diagnosis of CSH is rendered, pathologists have to provide prompt notification to the clinician. Sometimes, CSH can be so extensive as to obscure the concomitant neoplasm. Thus, pathologists should be aware of the detailed histological features of CSH to avoid misdiagnosis and also should have a high level of suspicion for the presence of accompanying lymphoproliferative disorder.

Ethics Statement

This study was approved by the Institutional Review Board of Inje University Ilsan Paik Hospital with a waiver of informed consent (IRB No. ISPAIK 2020-02-004) and performed in accordance with the principles of the Declaration of Helsinki.

ORCID

Mee Joo https://orcid.org/0000-0002-5886-0287
Nam-Hoon Kim https://orcid.org/0000-0002-1063-191X

Author Contributions

Conceptualization: MJ, NHK. Investigation: MJ. Visualization: MJ, NHK. Writing—original draft: MJ. Writing—review & editing: MJ, NHK.

Conflicts of Interest

The authors declare that they have no potential conflicts of interest.

Funding Statement

No funding to declare.

References

1. Jones D, Bhatia VK, Krausz T, Pinkus GS. Crystal-storing histiocytosis: a disorder occurring in plasmacytic tumors expressing immunoglobulin kappa light chain. Hum Pathol 1999; 30: 1441-8.
2. Dogan S, Barnes L, Cruz-Vetrano WP. Crystal-storing histiocytosis: report of a case, review of the literature (80 cases) and a proposed classification. Head Neck Pathol 2012; 6: 111-20.
3. Fang H, Chiu A, Reichard KK. Crystal-storing histiocytosis in bone marrow: a clinicopathologic study of eight cases and review of the literature. Am J Clin Pathol 2018; 149: 148-63.
4. Kanagal-Shamanna R, Xu-Monette ZY, Miranda RN, et al. Crystal-storing histiocytosis: a clinicopathological study of 13 cases. Histopathology 2016; 68: 482-91.
5. Galeano-Valle F, Díaz-Crespo FJ, Melero-Martín R, Apaza-Chávez JE, Del-Toro-Cervera J, Demelo-Rodríguez P. Massive generalized crystal-storing histiocytosis associated with extracellular crystalline nephropathy: clinical, immunohistochemical, and ultrastructural studies of a unique disorder and review of the literature. CEN Case Rep 2019; 8: 166-72.
6. Arnold CA, Frankel WL, Guo L, et al. Crystal-storing histiocytosis in the stomach: a clue to subtle hematolymphoid malignancies. Am J Surg Pathol 2018; 42: 1317-24.
7. Stewart CJ, Spagnolo DV. Crystalline plasma cell inclusions in helicobacter-associated gastritis. J Clin Pathol 2006; 59: 851-4.
8. Joo M, Kwak JE, Chang SH, et al. Localized gastric crystal-storing histiocytosis. Histopathology 2007; 51: 116-9.
9. Yano Y, Nagahama T, Matsui T, et al. Gastric crystal-storing histiocytosis detected with asymptomatic Sjogren's syndrome: report of a case and summary. Clin J Gastroenterol 2013; 6: 237-42.
10. Vaid A, Caradine KD, Lai KK, Rego R. Isolated gastric crystal-storing histiocytosis: a rare marker of occult lymphoproliferative disorders. J Clin Pathol 2014; 67: 740-1.
11. Joo M. Rare Gastric lesions associated with *Helicobacter pylori* infection: a histopathological review. J Pathol Transl Med 2017; 51: 341-51.
12. Hasegawa H. Aggregates, crystals, gels, and amyloids: intracellular and extracellular phenotypes at the crossroads of immunoglobulin physicochemical property and cell physiology. Int J Cell Biol 2013; 2013: 604867.
13. Joo M. Gastric mucosa-associated lymphoid tissue lymphoma masquerading as Russell body gastritis. Pathol Int 2015; 65: 396-8.
14. Altindag SD, Cakir E, Ekinci N, Avci A, Dilek FH. Analysis of clinical and histopathological findings in Russell body gastritis and duodenitis. Ann Diagn Pathol 2019; 40: 66-71.

JPTM
Journal of Pathology and Translational Medicine 2020; 54: 336-339
https://doi.org/10.4132/jptm.2020.02.28

CASE STUDY

Pediatric granular cell tumor in the posterior wall of the larynx extending to the trachea

Jungsuk Ahn[1], Na Rae Kim[1], Yong Han Sun[2]

Departments of [1]Pathology and [2]Pediatrics, Gil Medical Center, Gachon University College of Medicine, Incheon, Korea

Granular cell tumor (GCT) is a slow-growing benign neoplasm that can be found in any organ. Pediatric laryngotracheal GCT is rare. We experienced a 6-year-old boy suffering from a barking cough and symptoms of stridor and croup for one month. Head and neck computed tomography revealed a protruding mass that occluded 60% of the airway lumen. Under the impression of hemangioma or papilloma, excision revealed a submucosal non-encapsulated mass. Histologically, the mass was composed of sheets of large polyhedral-shaped tumor cells containing plump eosinophilic granular cytoplasm and centrally placed, small, bland-appearing nuclei. The tumor cells were positive for S-100 protein, and voluminous eosinophilic cytoplasm was stained by diastase-resistant periodic acid-Schiff. The present report describes a unique case of a huge pediatric laryngeal GCT extending to the subglottic trachea. We also review the clinical course of pediatric laryngotracheal GCT and emphasize the importance of diagnosing GCT in children.

Key Words: Granular cell tumor; Trachea; Larynx; Children

Received: December 10, 2019 **Revised:** February 3, 2020 **Accepted:** February 27, 2020

Corresponding Author: Na Rae Kim, MD, Department of Pathology, Gil Medical Center, Gachon University College of Medicine, 21 Namdong-daero 774beon-gil, Namdong-gu, Incheon 21565, Korea
Tel: +82-32-460-3073, Fax: +82-32-460-2394, E-mail: clara_nrk@gilhospital.com

Granular cell tumor (GCT) has been variably called granular cell myoblastoma, Abrikossoff's tumor, and granular cell schwannoma [1]. As its name indicates, GCT is regarded to be of neural crest Schwann cell origin, like schwannoma, although its pathogenesis is still under debate. Its characteristic granularity is caused by accumulated secondary lysosomes in the cytoplasm of the tumor cells [1]. Recently, we experienced a six-year-old boy with a huge GCT in the larynx that extended to the trachea. Here, we describe a pediatric patient with laryngotracheal GCT who was difficult to diagnose early.

CASE REPORT

A previously healthy 6-year-old boy presented with acute onset noisy breathing, hoarse voice, and symptoms of croup and stridor for three weeks. He had a history of asthma for the previous 1 year, and there was no family history. Physical examination was nonspecific. Laryngoscopy revealed posterior vocal cord swelling and a crust-like lump lesion (Fig. 1A). Laryngitis or tracheitis was suspected. Head and neck computed tomography (CT) showed a 22×9-mm-sized lesion with a lobulated margin and heterogeneous enhancement in the posterior wall of the subglottic trachea, suspicious for papilloma or hemangioma (Fig. 1B). In addition, the mass arose from the cricoid cartilage at the posterior laryngeal wall and extended to the subglottic trachea level. With the patient under laryngeal mask airway general anesthesia, suspension laryngoscope setting bagging was performed using a 4.5-mm endotracheal tube. The posteriorly located glottic mass was incompletely removed using a cup forceps, and the mucosal surfaces of both sides of the mass were left intact to prevent stenosis of the airway.

Histologically, the excised mass from the trachea and glottis was composed of large polyhedral cells arranged in sheets with plump eosinophilic granular cytoplasm (Fig. 2A). Centrally placed small nuclei were bland with or without nucleoli. Mitosis and necrosis were absent. The overlying epithelium was observed as either intact or as occasional erosive squamous epithelium with focal pseudoepitheliomatous hyperplasia. The eosinophilic granular cytoplasm was stained with diastase-resistant periodic acid-Schiff (PAS) (Fig. 2B, left). The polyhedral large cells were

pISSN 2383-7837
eISSN 2383-7845

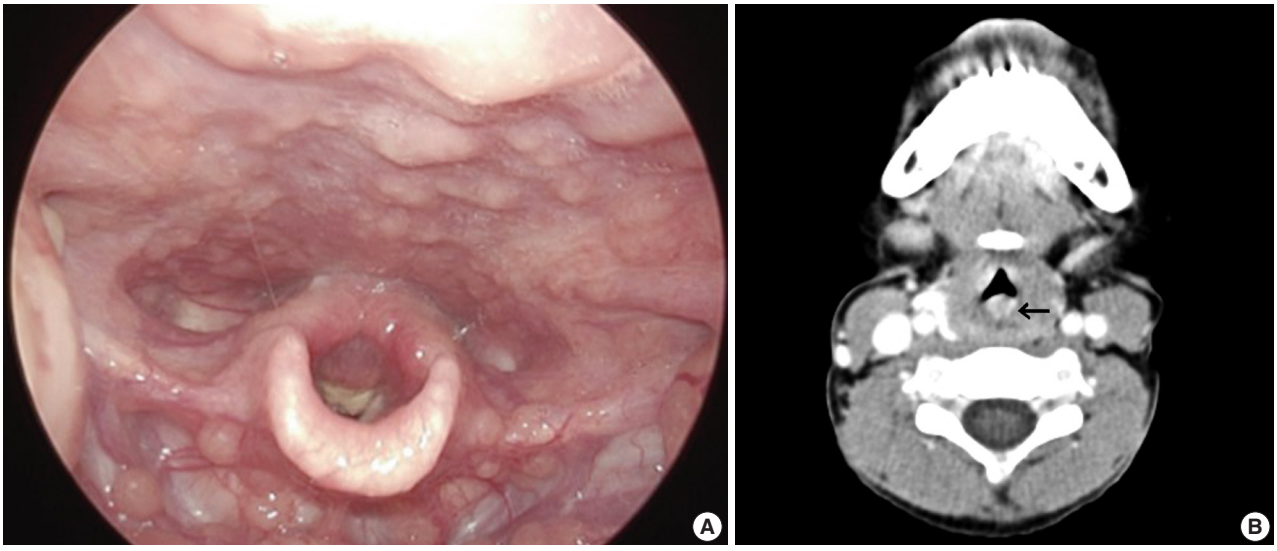

Fig. 1. (A) Laryngoscopy shows scattered swelling and a crust-like lump lesion, causing subglottic stenosis and stricture. (B) Head and neck computed tomography reveals a 2.2-cm-sized lesion (arrow) with heterogeneous enhancement in the posterior wall of the subglottic trachea.

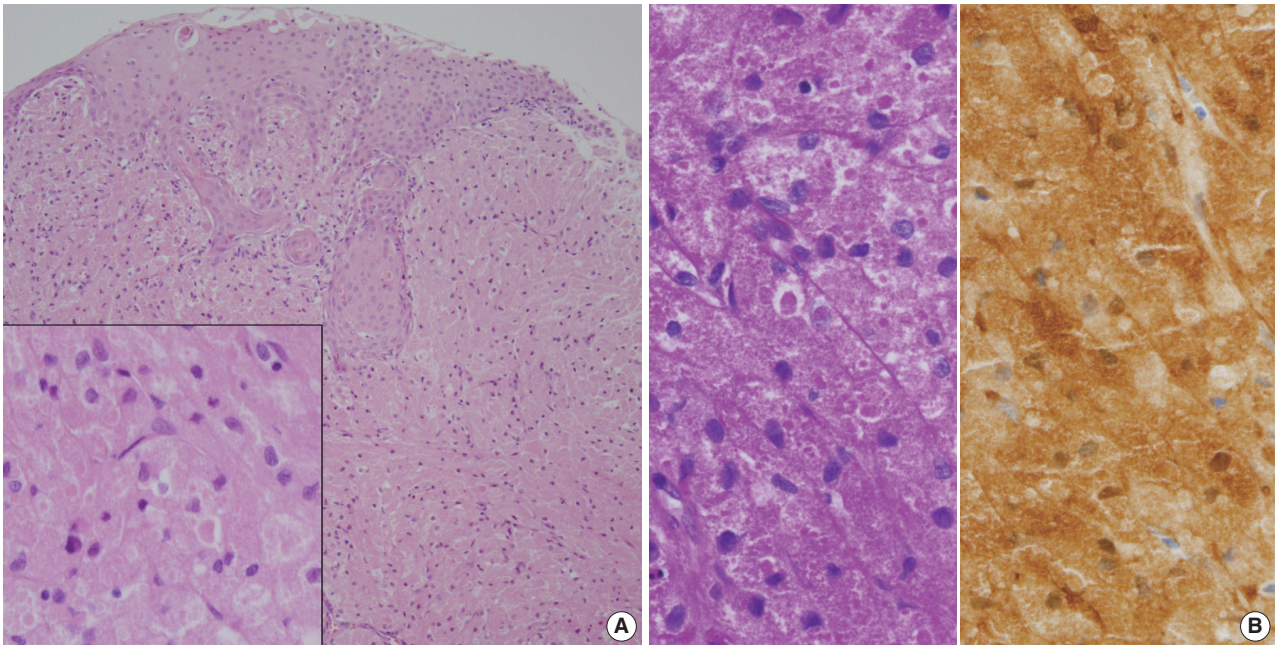

Fig. 2. (A) Large polygonal-shaped tumor cells fill the subepithelial stroma. Note the overlying pseudoepitheliomatous hyperplastic squamous epithelium. The inset indicates tumor cells containing fine granular cytoplasm. (B) Voluminous cells are strongly stained with periodic acid–Schiff with diastase-pretreatment (left) and S-100 protein (right).

positive for S-100 protein (1:600, polyclonal, Dako, Glostrup, Denmark; Fig. 2B, right) and negative for smooth muscle actin (1:100, 1A4, Dako). Because the tissue lacked cellular pleomorphism and mitosis, benign GCT was diagnosed.

Seven months later, the patient is healthy with remaining tumor. A 12-month follow-up visit is planned.

DISCUSSION

Pediatric laryngotracheal tumors are uncommon, accounting for only 2% of laryngeal lesions, and most of them are benign [2]. The most common occurrences are papillomatosis and hemangioma [3]. GCT most commonly affects the posterior portion of the larynx. Pediatric laryngeal GCT is rare [4], with fewer than

20 cases of pediatric laryngotracheal GCTs reported [5]. In addition to its rare incidence, laryngotracheal GCT in children may present with stridor and upper airway obstruction, a very serious clinical presentation, and a long period of time may pass before exact diagnosis. Causes of airway distress vary from infection to rare neoplasm. Furthermore, a preoperative diagnosis of laryngotracheal GCT is not easy because tracheal tumors are infrequent in children. In children, ultrasound is favored over CT. Although preoperative diagnosis of laryngeal GCT may not be easy, its pathologic diagnosis through characteristic histology and immunohistochemical results can be assured, unless the biopsy sample is inadequate. If the diagnostic biopsy is purely superficial, only squamous epithelium will be examined, which may be mistaken as squamous cell carcinoma. Pathologic diagnosis of GCT is based on observation of its classic morphology: overlying pseudoepitheliomatous hyperplasia, submucosal polygonal or elongated cells with small nuclei, and eosinophilic granules stained by S-100 protein and PAS in cellular lysosomes.

Although most GCTs are benign, some show malignant behavior, producing controversial classification between benign, atypical, and malignant GCTs [6]. The pathological criteria of malignancy, i.e., the Fanburg-Smith criteria, have been the most useful. The histopathological diagnosis of malignancy is based on the following six criteria: necrosis, spindling, vesicular nuclei with prominent nucleoli, mitotic activity (> 2 mitoses/10 high-power fields under 200× magnification), high nuclear to cytoplasmic ratio, and pleomorphism. GCTs showing three or more of the criteria are categorized as malignant, those showing one or two criteria are categorized as atypical, and those showing only focal pleomorphism are categorized as benign.

If GCT occurs in multiple locations, it may be the result of multicentric origin rather than metastasis, as in the skin [7]. Multiple GCTs have been reported in the skin of children, and most of those cases were associated with various systemic syndromes, such as neurofibromatosis (NF), Noonan syndrome (NS), Costello syndrome, and mutation of the phosphatase and tensin homologue (*PTEN*) gene. The molecular pathogenesis of multiple GCTs has not yet been clarified. Alterations of the RAS/mitogen-activated protein kinase pathway promoting cellular proliferation and oncogenesis, i.e., gain-of-function mutations, may explain why NF1 and NS patients develop multiple occurrence of GCTs [7]. Therefore, long-term follow-up should be required in patients with pediatric laryngotracheal GCT.

Treatment of laryngotracheal GCT is poorly standardized due to limited data, particularly in children. Most pediatric GCTs take a benign course, unless the patient suffers airway obstructive symptoms, and there is no role for radiotherapy or chemotherapy [8]. Complete excision with a clear resection margin is regarded as the standard of treatment, though therapy may vary from simple observation to laryngotracheal reconstruction [9]. Endoscopic resection may be undertaken as the initial treatment for a small GCT. On the other hand, surgical resection is recommended for laryngotracheal GCTs measuring more than 8 mm or those with full thickness involvement of the airway for maintenance of the airway [10].

Following complete resection, recurrence of GCT is unlikely, and recurrence rates are around 2%–3% if it is completely excised. Recurrence and increased size in benign GCT may be indicators of malignant transformation. Pediatric patients with laryngotracheal GCT and incomplete conservative surgery should be closely and regularly followed to detect late recurrence due to incomplete resection, metachronous multiple occurrence, or systemic manifestation of an underlying syndrome as well as lifetime risk of recurrence.

In conclusion, pediatric GCT involving the trachea and larynx mimics papilloma or hemangioma and poses a challenging diagnosis. The present case was unique for two reasons: first, the laryngotracheal occurrence, an unusual location for GCT; and second, the presentation of acute stridor that necessitated a differential diagnosis that included entities with asthma or bronchitis. Although laryngotracheal GCT is rare, pediatricians and radiologists should bear it in mind when evaluating a patient presenting with respiratory obstructive symptoms.

Ethics Statement

The medical center's institutional review board approved this study with a waiver of informed consent (No. GFIRB2019-243), and the study was performed in accordance with the 1964 Helsinki Declaration and its later amendments.

ORCID

Jungsuk Ahn https://orcid.org/0000-0003-0312-2460
Na Rae Kim https://orcid.org/0000-0003-2793-6856
Yong Han Sun https://orcid.org/0000-0003-1527-6782

Author Contributions

Conceptualization: YHS. Data curation: JA. Investigation: JA, NRK. Resources: YHS. Supervision: NRK. Writing—original draft: NRK, JA. Writing—review and editing: NRK.

Conflicts of Interest

The authors declare that they have no potential conflicts of interest.

Funding Statement

No funding to declare.

References

1. Dunaway CL, Brogdon BG, Robinson AE. Granular cell myoblastoma of the trachea. Pediatr Radiol 1981; 11: 210-1.
2. Burton DM, Heffner DK, Patow CA. Granular cell tumors of the trachea. Laryngoscope 1992; 102: 807-13.
3. Holland RS, Abaza N, Balsara G, Lesser R. Granular cell tumor of the larynx in a six-year-old child: case report and review of the literature. Ear Nose Throat J 1998; 77: 652-60.
4. Amar YG, Nguyen LH, Manoukian JJ, Nguyen VH, O'Gorman A, Shapiro R. Granular cell tumor of the trachea in a child. Int J Pediatr Otorhinolaryngol 2002; 62: 75-80.
5. Spandow O, Lindholm CE. Granular cell tumour in a child's trachea: a diagnostic and therapeutic challenge. Int J Pediatr Otorhinolaryngol 1994; 30: 159-66.
6. Fanburg-Smith JC, Meis-Kindblom JM, Fante R, Kindblom LG. Malignant granular cell tumor of soft tissue: diagnostic criteria and clinicopathologic correlation. Am J Surg Pathol 1998; 22: 779-94.
7. Schrader KA, Nelson TN, De Luca A, Huntsman DG, McGillivray BC. Multiple granular cell tumors are an associated feature of LEOPARD syndrome caused by mutation in PTPN11. Clin Genet 2009; 75: 185-9.
8. White JB, Glade R, Rossi CT, Bielamowicz S. Granular cell tumors of the larynx: diagnosis and management. J Voice 2009; 23: 516-7.
9. Pernas FG, Younis RT, Lehman DA, Robinson PG. Management of pediatric airway granular cell tumor: role of laryngotracheal reconstruction. Int J Pediatr Otorhinolaryngol 2006; 70: 957-63.
10. Daniel TM, Smith RH, Faunce HF, Sylvest VM. Transbronchoscopic versus surgical resection of tracheobronchial granular cell myoblastomas. Suggested approach based on follow-up of all treated cases. J Thorac Cardiovasc Surg 1980; 80: 898-903.

JPTM
Journal of Pathology and Translational Medicine 2019; 53: 340-345
https://doi.org/10.4132/jptm.2020.03.18

CASE STUDY

Primary hepatic extranodal marginal zone lymphoma of mucosa-associated lymphoid tissue

Soyeon Choi[1], Ji Hye Kim[1], Kyungbin Kim[1], Misung Kim[1], Hye Jeong Choi[1,2], Young Min Kim[1,2], Jae Hee Suh[1,2], Min Jung Seo[2,3], Hee Jeong Cha[1,2]

[1]Department of Pathology, Ulsan University Hospital, Ulsan; [2]University of Ulsan College of Medicine, Ulsan; [3]Department of Nuclear Medicine, Ulsan University Hospital, Ulsan, Korea

Extranodal marginal zone lymphoma of mucosa-associated lymphoid tissue (MALT lymphoma), is one of the specific type of low-grade B-cell lymphoma not infrequently found worldwide. It typically involves mucosal sites such as stomach and conjunctiva; however, primary hepatic MALT lymphoma has been extremely rarely reported. We describe a case of hepatic MALT lymphoma in a 70-year-old male patient who underwent left hepatectomy due to the incidentally detected liver masses at a medical checkup. The resected specimen revealed multinodular masses consisting of small-to-intermediate-sized lymphoid cells with serpentine pattern and focal lymphoepithelial lesions. The tumor cells were diffusely positive for CD20 and Bcl-2 but negative for CD3, CD10, CD5, CD23, CD43, and cyclinD1. The Ki-67 labeling index was 10% and immunoglobulin heavy chain gene rearrangement study confirmed monoclonal proliferation. In this paper, we discuss several unique clinicopathologic characteristics which will be helpful to the differential diagnosis of hepatic MALT lymphoma.

Key Words: Lymphoma, B-cell, marginal zone; Mucosa-associated lymphoid tissue; Liver

Received: December 27, 2019 **Revised:** March 10, 2020 **Accepted:** March 17, 2020
Corresponding Author: Hee Jeong Cha, MD, Department of Pathology, Ulsan University Hospital, University of Ulsan College of Medicine, 877 Bangeojinsunhwan-doro, Dong-gu, Ulsan 44033, Korea
Tel: +82-52-250-7261, Fax: +82-52-252-3024, E-mail: heej0124@uuh.ulsan.kr

Extranodal marginal zone lymphoma of mucosa-associated lymphoid tissue (MALT) is one of the specific type of low-grade B-cell lymphoma not infrequently found worldwide. MALT lymphoma represents 7%–8% of all non-Hodgkin's lymphomas in Western countries [1]. In Korea, MALT lymphomas represent 19.0% of non-Hodgkin lymphomas and over half (59.8%) occur in the stomach. Other sites of occurrence include the lung, salivary gland, ocular adnexa, skin, and thyroid [2]. However, lymphoma in the liver as the primary site is very rare. Primary hepatic lymphoma (PHL) comprises 0.016% of non-Hodgkin's lymphoma [3] and MALT lymphoma comprises 2%–4% of PHL [4]. Since it is a rare disease with limited literature, there is no consensus on treatment modalities [5,6]. Here, we report a case of primary hepatic MALT lymphoma.

CASE REPORT

A 70-year-old male patient was referred for liver masses on ultrasonography from a medical checkup at another hospital. He had a history of intracerebral hemorrhage, and coronary stent insertion due to myocardial infarction. A physical examination showed no abnormalities. The laboratory test results were within normal limits. The level of aspartate transaminase was 27 IU/L, alanine transaminase was 24 IU/L, total bilirubin was 0.9 mg/dL, alkaline phosphatase was 96 IU/L, and γ glutamyl transferase was 34 IU/L. The patient was seronegative for hepatitis B and C and tumor markers (α-fetoprotein and protein induced by vitamin K antagonist II) were within normal limits. He was also seronegative for human immunodeficiency virus and was negative for antinuclear antibody. The abdomen ultrasonography showed mild fatty liver. Esophagogastroduodenoscopy showed atrophic gastritis and no other MALT lesion

pISSN 2383-7837
eISSN 2383-7845

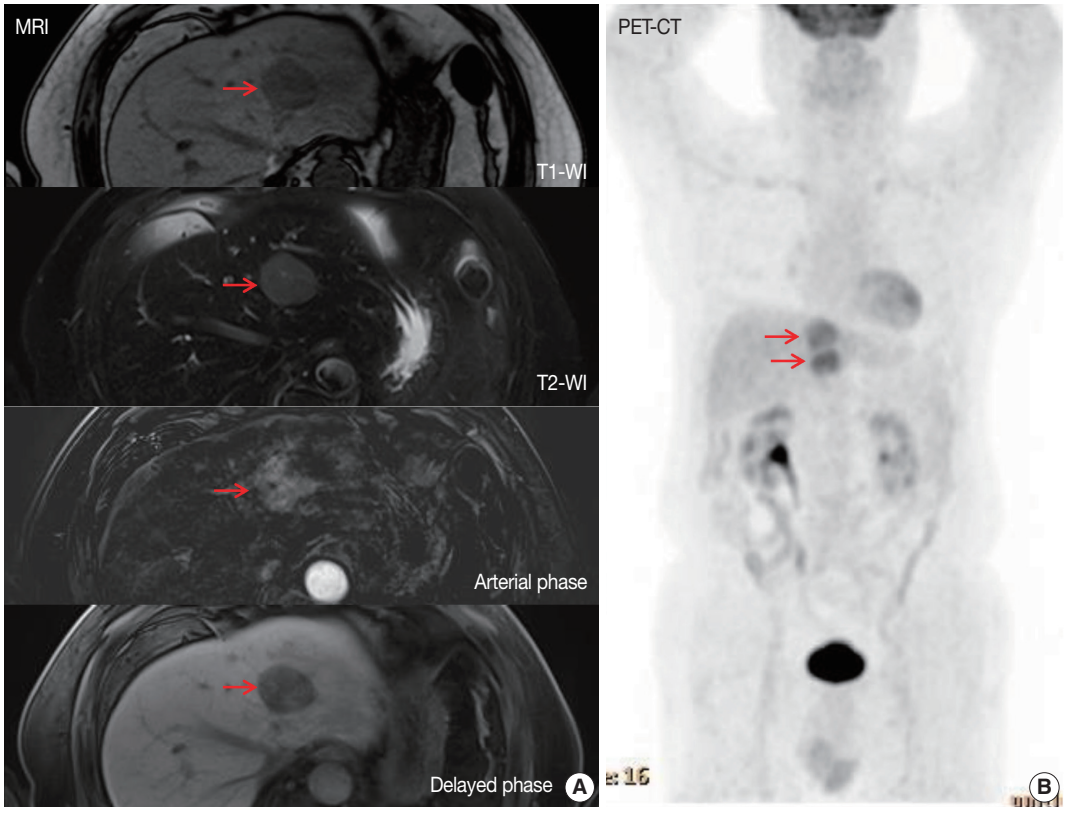

Fig. 1. (A) The magnetic resonance imaging shows a hypointense in T1, and T2, and arterial enhancing lesion in left lateral segment (arrows). (B) The positron emission tomography/computed tomography shows two hypermetabolic masses in left lateral segment (maximal standardized uptake value, 4.4). T1-WI, T1 weighted image; T2-WI, T2 weighted image.

was present. Further imaging studies including computed tomography (CT), magnetic resonance imaging (MRI), and ^{18}F-fluorodeoxyglucose (FDG)-positron emission tomography (PET)/CT were performed. The MRI revealed two arterial enhancing masses measuring 3.6 cm and 3.3 cm in the left lateral segment of the liver, suggesting hepatocellular carcinoma (HCC) (Fig. 1A). The PET/CT revealed the two masses in the left lateral segment of the liver to be hypermetabolic (maximum standardized uptake value of 4.4) (Fig. 1B). No other lymphadenopathy was present. He underwent left hepatectomy.

The liver specimen showed two masses measuring 4.8×4.2×3.3 cm and 4.8×3.8×2.3 cm that were well-demarcated and grayish tan in color in segment 2 (Fig. 2A). On low-power magnification, nodular and serpentine infiltration of lymphocytes was seen (Fig. 2B). On high-power magnification, small-to-intermediate-sized lymphoid cells were present (Fig. 2C). Lymphoepithelial lesions were present in the bile ducts (Fig. 2D), which were highlighted by positive immunoreactivity for cytokeratin 7 by immunohistochemistry (IHC) (Fig. 2E). In other IHC studies, CD20 and Bcl-2 were diffusely and strongly positive, and the tumor cells were negative for CD3, CD10, CD5, CD23, CD43, and cyclinD1 (Fig. 3A–C). The Ki-67 index was about 10%. Immunoglobulin heavy chain (IgH) gene rearrangement study revealed monoclonality of the lymphoid lesion, and all these results were compatible with a diagnosis of MALT lymphoma. The background liver outside the nodules showed portal-to-periportal lymphocytic infiltration (Fig. 3D), however, there was no evidence of autoimmune hepatitis, or primary biliary cirrhosis, or non-alcoholic steatohepatitis. Systemic studies including bone marrow biopsy showed no additional lesions. He was diagnosed with Ann Arbor stage IIE and close follow-up without additional therapy was recommended. After 8 months from the surgery, the patient showed no recurrent disease in the CT scan.

DISCUSSION

Although the incidence of primary hepatic MALT lymphoma is extremely rare, some unique clinical characteristics were reported in the literatures (Table 1) [6-15]. Most of primary hepatic MALT lymphoma cases occurred in elderly people and were presented with incidentally detected liver masses without specific symptoms [6,7]. These features were consistent with

the present case.

Chronic antigenic stimulation such as longstanding inflammation or infection has been suggested as an important etiologic factor of MALT lymphoma. *Helicobacter pylori* has been proved to be the cause of gastric MALT lymphoma and the suggested infectious agents for other sites are *Borrelia burdorferi* for skin, Chlamydophila psittaci for ocular adnexa, *Campylobacter jejuni* for small intestine, and *Achromobacter xylosoxidans* for lung. As

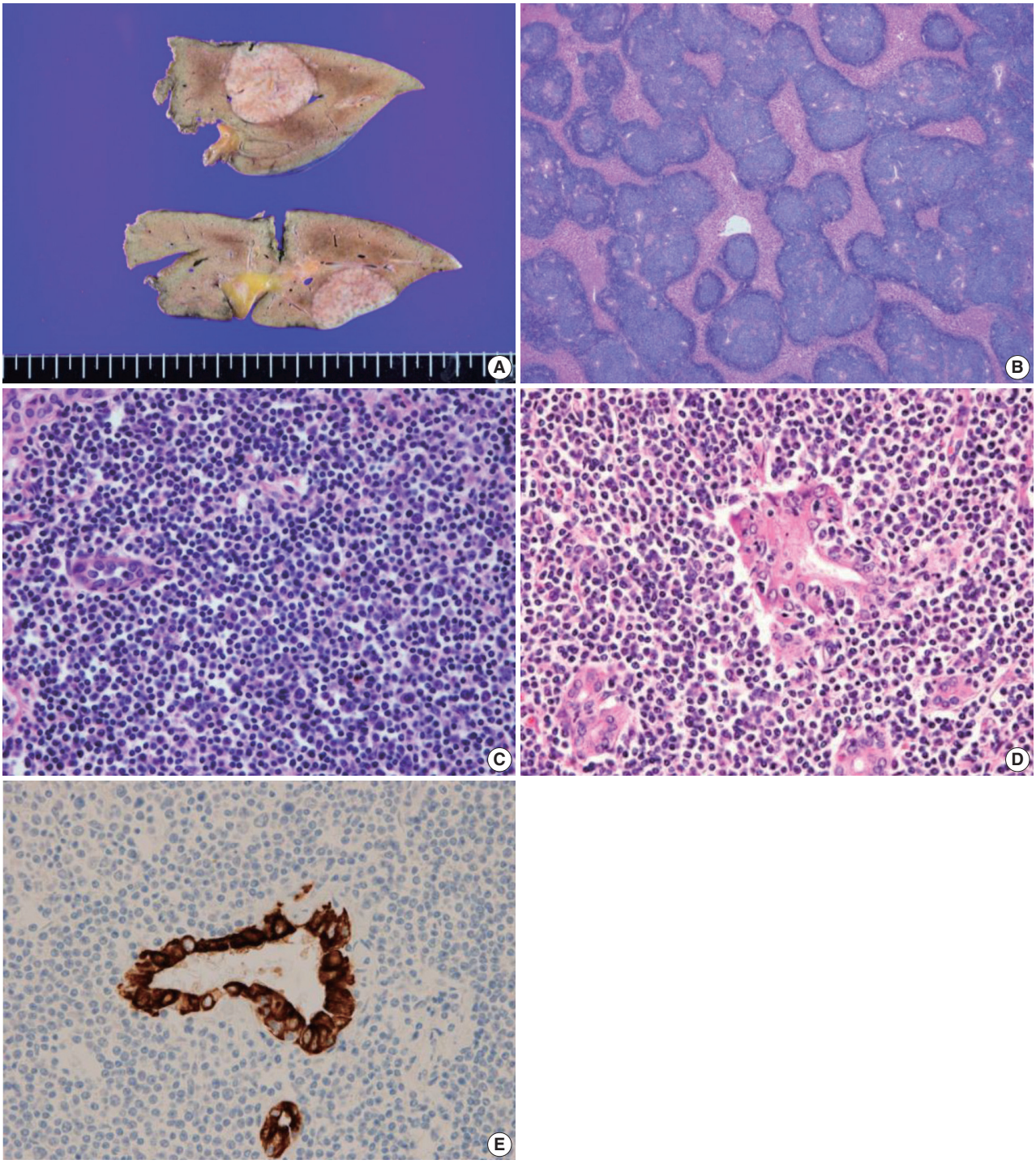

Fig. 2. (A) Gross image of the liver shows well-demarcated and grayish tan masses. (B) Low power view of the lesion demonstrates serpentine infiltrations of lymphoid cells. (C) High power view of the lesion demonstrates small-to-intermediated-size lymphoid cell infiltration. (D, E) Lymphoepithelial lesion is present, which is revealed by cytokeratin 7 immunohistochemical stain.

https://doi.org/10.4132/jptm.2020.03.18

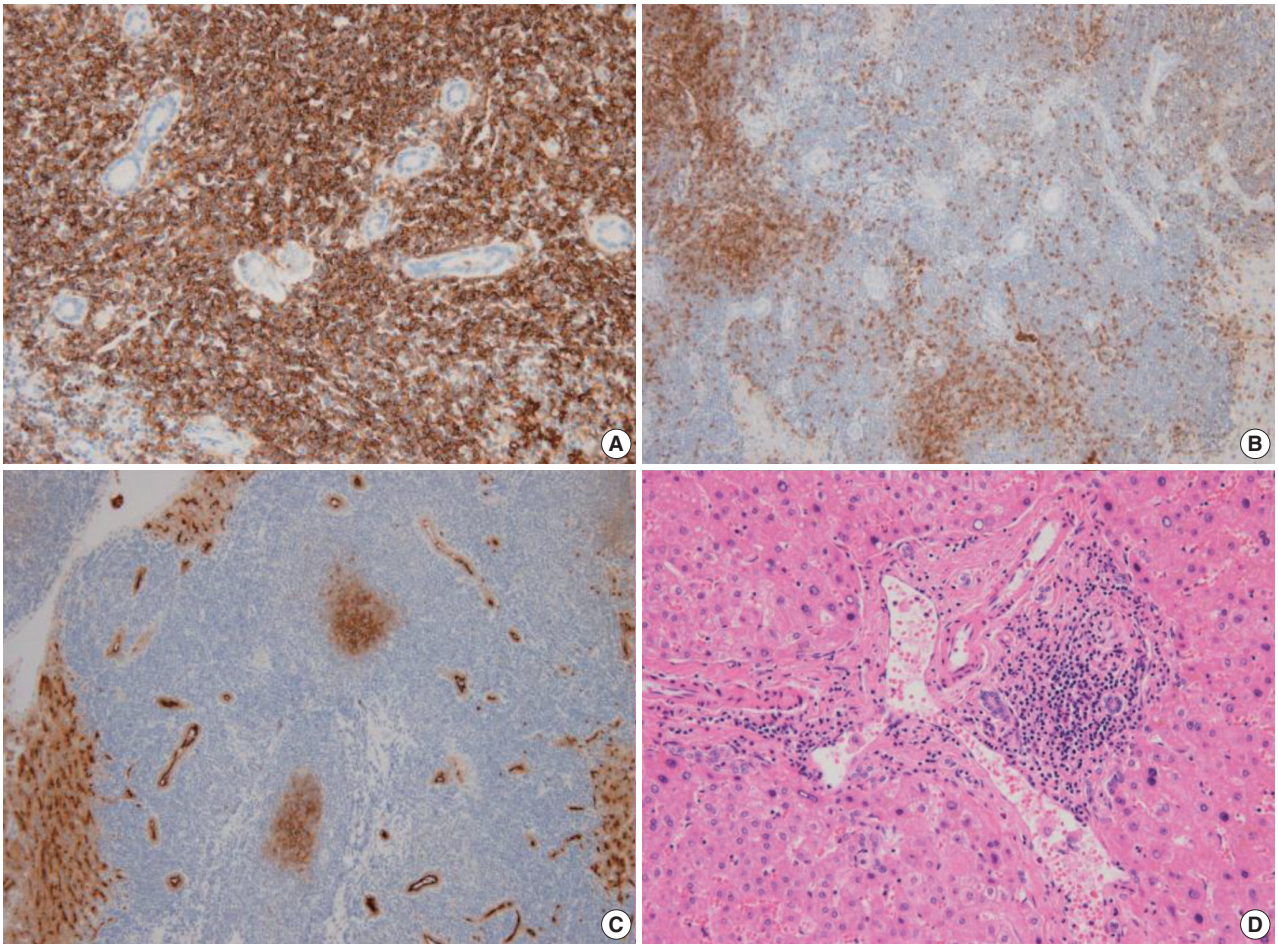

Fig. 3. The lymphoid cells are positive for CD20 (A), and negative for CD3 (B) and CD10 (C). (D) The non-neoplastic liver shows portal to periportal lymphocytic infiltration.

for hepatic MALT lymphoma, hepatitis C viral infection, autoimmune diseases such as Sjogren's disease or Hashimoto's thyroiditis have been reported to have increased the risk of MALT lymphoma [16,17]. Another study proposed that 45% of patients with MALT lymphoma had no concomitant liver diseases [6]. Our patient had no suggested predisposing conditions listed above. The pathogenesis of hepatic MALT lymphoma is still unclear and should be explored in a large-scale study.

In this case, the patient was initially misdiagnosed with HCC by CT and MRI studies. Betianu et al. [8] states that there are no characteristic radiological findings of PHL. After contrast administration, more than 50% of PHLs showed no enhancement, 30% showed patchy enhancement and 15% showed a ring enhancement. On MRI, PHL is hypo- or isointense on T1 and hyperintense on T2 [8]. Thus, when suspected malignant liver masses are seen in imaging studies without elevation of tumor markers, lymphoma should be a differential diagnosis and liver biopsy could be an option. Several articles focus on ^{18}F-FDG PET/CT as a diagnostic modality as for other lymphomas. Bao et al. [9] suggest that ^{18}F-FDG PET/CT is particularly helpful in distinguishing the initial stages of MALT lymphoma, although pathological evidence is needed for definitive diagnosis. It can assist in staging, evaluating treatment responses, and monitoring relapse and recurrence [9]. Our patient had a slightly hypermetabolic mass, considering its indolent nature. The standardized uptake value of primary hepatic MALT lymphoma remains to be validated with more evidence.

Microscopically, in low-power magnification, nodular and serpentine infiltrations of lymphoid cells from the portal area were present. MALT lymphomas are known to predominantly involve the portal fields of the liver, and lymphoepithelial lesions of the bile ducts are known to be typical accompanying findings [18]. The differential diagnoses are HCC, cholangiocellular carcinoma, low-grade B-cell lymphoma including follicu-

Table 1. Reported cases of primary hepatic MALT lymphoma

Case No.	Study	Age (yr)/Sex	HBV	HCV	Comorbidities	Image finding	Treatment	Outcome
1	Xie et al. [6]	73/M	(+)	(–)	None	CT: enhanced in arterial phase MRI: hypointense on T1, hyperintense on T2	Surgery	Alive/6 mo
2	Nagata et al. [7]	74/M	(–)	(–)	Hypertension	CT: no mass MRI: enhanced on T1 in arterial phase, withdrawal in portal venous and delayed phases	Surgery	Alive/2 yr
3	Betianu et al. [8]	47/F	(–)	(–)	None	CT: hypodense mass MRI: hypointense on T1, hyperintense on T2	Surgery and chemotherapy	Alive/9 mo
4	Bao et al. [9]	59/F	(+)	(–)	None	CT: hypodense lesions PET/CT: increased uptake of SUV	Patient refused	ND
5	Obiorah et al. [10]	80/F	(–)	(–)	None	CT: bilobed mass	Surgery, rituximab and idelalisib	Pulmonary recur/1 yr, parotid gland recur/7 yr
6	Obiorah et al. [10]	30/F	(–)	(–)	Autoimmune hepatitis, Hashimoto's thyroiditis	PET/CT: diffuse FDG activity	Rituximab	Alive/3 yr
7	Bohlok et al. [11]	68/M	(–)	(–)	Alcoholic cirrhosis, hemochromatosis	MRI: enhanced in arterial phase and washout in portal phase FDG PET: hypermetabolic tumor	Surgery	ND
8	Khurana et al. [12]	71/F	(–)	(–)	Invasive breast cancer, papillary thyroid carcinoma	PET: FDG hypodense lesion	Surgery	ND
9	Dong et al. [13]	50/M	(–)	(–)	Type 2 diabetes, hypertension	MRI: hypointense on T1 and hyperintense on T2, enhanced in the arterial phase and portal phase	Surgery and Rituximab	Alive/13 mo
10	Li et al. [14]	44/F	(–)	(+)	None	MRI: hyperintense on T1 and T2	Surgery	Alive/27 mo
11	Haefliger et al. [15]	69/M	(–)	(–)	Non-alcoholic steatohepatitis, *Helicobacter pylori*–associated gastritis	MRI: hyperintense on T2, washout on portal venous phase	Rituximab and HP eradication therapy	Alive/6 mo
12	Our case	70/M	(–)	(–)	Intracerebral hemorrhage, myocardial infarction	MRI: enhanced in arterial phase PET/CT: hypermetabolic and isometabolic nodules	Surgery	Alive/8 mo

MALT, mucosa-associated lymphoid tissue; HBV, hepatitis B virus; HCV, hepatitis C virus; M, male; CT, computed tomography; MRI, magnetic resonance imaging; F, female; PET, positron emission tomography; SUV, standardized uptake value; ND, not detected; FDG, fluorodeoxyglucose; HP, *Helicobacter pylori*.

lar lymphoma and small lymphocytic lymphoma, hepatosplenic T-cell lymphoma, pseudolymphoma, and IgG4-related liver disease. IHC with CD5, CD10, CD23, CD43, and cyclinD1 is critically important to further classify low-grade B-cell lymphomas. Hepatic pseudolymphoma is another rare lesion often associated with inflammatory or autoimmune diseases and shows features similar to malignant lesions in imaging. Its histologic findings resemble low-grade lymphoma, particularly extranodal marginal zone lymphoma [19]. It can be distinguished from extranodal marginal zone lymphoma by histology, and IHC studies showing reactive patterns and polyclonality in an IgH gene rearrangement study. The diagnostic features of IgG4-related disease include elevated serum IgG4 concentrations, and histologic features include dense lymphoplasmacytic inflammatory infiltrate with increased numbers of $IgG4^+$ plasma cells, often increased eosinophils, a storiform pattern of fibrosis, and obliterative vasculitis [20]. The histologic findings along with results from IHC study and IgH gene rearrangement study seem to be critical in the differential diagnosis.

H.pylori eradication is a well-established treatment for gastric MALT lymphoma. However, there is no consensus on the treatment for MALT lymphoma in other sites. Expectant observation, surgery, radiotherapy, chemotherapy, and immunotherapy are generally performed, considering site, disease stage, and performance status. For localized diseases, radiation therapy is often a preferred option and surgery can be considered. For advanced stages, observation with monitoring was often proven to be adequate, but when treatment is required, chemotherapy with rituximab and enrollment in controlled clinical trials is suggested [5]. After discussion, our patient was placed under observation. Tumor recurrence has been reported in the literature, with the lung reported as the most common site [10].

https://doi.org/10.4132/jptm.2020.03.18

Primary hepatic MALT lymphoma is a very rare disease. The clinical features are nonspecific and the image findings variable. Histology, IHC studies and an IgH gene rearrangement study are of great importance in accurate diagnosis. The disease characteristics should be disclosed further with more data.

Ethics Statement

This study was approved by the Institutional Review Board of Ulsan University Hospital with a waiver of informed consent (IRB No. 2019-12-002).

ORCID

Soyeon Choi	https://orcid.org/0000-0003-1569-6592
Ji Hye Kim	https://orcid.org/0000-0001-7160-8601
Kyungbin Kim	https://orcid.org/0000-0001-5430-4235
Misung Kim	https://orcid.org/0000-0002-7317-324X
Hye Jeong Choi	https://orcid.org/0000-0002-5124-8589
Young-min Kim	https://orcid.org/0000-0001-8266-4553
Jae Hee Suh	https://orcid.org/0000-0001-7032-0294
Min Jung Seo	https://orcid.org/0000-0001-9037-2155
Hee Jeong Cha	https://orcid.org/0000-0001-8744-5747

Author Contributions

Conceptualization: HJC (Hee Jeong Cha), KK. Investigation: HJC (Hee Jeong Cha), KK, SC. Supervision: HJC (Hee Jeong Cha). Visualization: HJC (Hee Jeong Cha), KK, MJS. Writing—original draft: HJC (Hee Jeong Cha), KK, SC. Writing—review & editing: JHS, YMK, HJC (Hye Jeong Choi), HJC (Hee Jeong Cha), KK, MK, MJS, JHK, SC.

Conflicts of Interest

The authors declare that they have no potential conflicts of interest.

Funding Statement

No funding to declare.

References

1. A clinical evaluation of the International Lymphoma Study Group classification of non-Hodgkin's lymphoma. The Non-Hodgkin's Lymphoma Classification Project. Blood 1997; 89: 3909-18.
2. Schreuder MI, van den Brand M, Hebeda KM, Groenen PJ, van Krieken JH, Scheijen B. Novel developments in the pathogenesis and diagnosis of extranodal marginal zone lymphoma. J Hematop 2017; 10: 91-107.
3. Freeman C, Berg JW, Cutler SJ. Occurrence and prognosis of extranodal lymphomas. Cancer 1972; 29: 252-60.
4. El-Fattah MA. Non-Hodgkin lymphoma of the liver: a US population-based analysis. J Clin Transl Hepatol 2017; 5: 83-91.
5. Rosand CB, Valla K, Flowers CR, Koff JL. Effective management strategies for patients with marginal zone lymphoma. Future Oncol 2018; 14: 1213-22.
6. Xie H, Lv J, Ji Y, Du X, Yang X. Primary hepatic mucosa-associated lymphoid tissue lymphoma: a case report and literature review. Medicine (Baltimore) 2019; 98: e15034.
7. Nagata S, Harimoto N, Kajiyama K. Primary hepatic mucosa-associated lymphoid tissue lymphoma: a case report and literature review. Surg Case Rep 2015; 1: 87.
8. Betianu CI, Dima A, Pavaloiu G. Primary hepatic mucosa-associated lymphoid tissue lymphoma in a patient with no chronic liver disease: Case report. Radiol Case Rep 2017; 12: 715-9.
9. Bao C, Wei J, Zhao X, et al. Prognostic value of fluorine-18-fluorodeoxyglucose positron emission tomography/computed tomography in primary hepatic mucosa-associated lymphoid tissue lymphoma: a case report and review of the literature. Medicine (Baltimore) 2018; 97: e9877.
10. Obiorah IE, Johnson L, Ozdemirli M. Primary mucosa-associated lymphoid tissue lymphoma of the liver: A report of two cases and review of the literature. World J Hepatol 2017; 9: 155-60.
11. Bohlok A, De Grez T, Bouazza F, et al. Primary hepatic lymphoma mimicking a hepatocellular carcinoma in a cirrhotic patient: case report and systematic review of the literature. Case Rep Surg 2018; 2018: 9183717.
12. Khurana A, Mukherjee U, Patil N. An unusual case of hepatic lymphoma with multiple epithelial malignancies. Indian J Pathol Microbiol 2018; 61: 585-6.
13. Dong S, Chen L, Chen Y, Chen X. Primary hepatic extranodal marginal zone B-cell lymphoma of mucosa-associated lymphoid tissue type: a case report and literature review. Medicine (Baltimore) 2017; 96: e6305.
14. Li LX, Zhou ST, Ji X, et al. Misdiagnosis of primary hepatic marginal zone B cell lymphoma of mucosa-associated lymphoid tissue type, a case report. World J Surg Oncol 2016; 14: 69.
15. Haefliger S, Milowich D, Sciarra A, et al. Primary hepatic marginal B cell lymphoma of mucosa-associated lymphoid tissue (MALT) and non-alcoholic steatohepatitis (NASH): more than a coincidence? Ann Hematol 2019; 98: 1513-6.
16. Zucca E, Bertoni F, Vannata B, Cavalli F. Emerging role of infectious etiologies in the pathogenesis of marginal zone B-cell lymphomas. Clin Cancer Res 2014; 20: 5207-16.
17. Kleinstern G, Maurer MJ, Liebow M, et al. History of autoimmune conditions and lymphoma prognosis. Blood Cancer J 2018; 8: 73.
18. Baumhoer D, Tzankov A, Dirnhofer S, Tornillo L, Terracciano LM. Patterns of liver infiltration in lymphoproliferative disease. Histopathology 2008; 53: 81-90.
19. Kwon YK, Jha RC, Etesami K, Fishbein TM, Ozdemirli M, Desai CS. Pseudolymphoma (reactive lymphoid hyperplasia) of the liver: a clinical challenge. World J Hepatol 2015; 7: 2696-702.
20. Weindorf SC, Frederiksen JK. IgG4-related disease: a reminder for practicing pathologists. Arch Pathol Lab Med 2017; 141: 1476-83.

JPTM
Journal of Pathology and Translational Medicine 2020; 54: 346-350
https://doi.org/10.4132/jptm.2020.05.14

CASE STUDY

Atypical femoral neck fracture after prolonged bisphosphonate therapy

Kwang-kyoun Kim[1], Young-wook Park[2], Tae-hyeong Kim[1], Kyung-deok Seo[1]

Departments of [1]Orthopaedic Surgery and [2]Pathology, Konyang Unversity Hospital, Daejeon, Korea

Of the drugs developed to prevent and treat osteoporosis, bisphosphonate has played a very important role in preventing osteoporotic fractures. However, case reports describing atypical femoral fractures in patients using long-term bisphosphonates have emerged. The majority of atypical femur fractures occurs in the lateral aspect of the subtrochanteric or femur diaphysis, which is explained by accumulation of tensile stress in these areas. Although the superior cortex of the femur neck withstands maximum tensile stress, to our knowledge, there have been only two reports (three cases) of atypical femoral neck fracture. In addition, none of those case reports revealed detailed pathology related to suppressed bone turnover rate. We encountered an incomplete femoral neck fracture and diagnosed it as "atypical" on the basis of the patient's lack of trauma and medication history and pathological findings. For patients with groin pain, minimal or no trauma, and a history of long-term bisphosphonate use, an atypical femoral neck fracture should be considered.

Key Words: Atypical femur fracture; Femur neck fracture; Tensile strength; Bisphosphonate

Received: April 7, 2020 **Revised:** May 4, 2020 **Accepted:** May 14, 2020
Corresponding Author: Kwang-kyoun Kim, MD, Department of Orthopaedic Surgery, 158 Gwanjeodong-ro, Seo-gu, Daejeon 35365, Korea
Tel: +82-42-600-6902, Fax: +82-42-600-9964, E-mail: kimajouos@gmail.com

Bisphosphonates reduce the overall risk of osteoporotic fractures and have a long-term beneficial effect. However, they reduce bone turnover and allow micro-cracks to accumulate over time, leading to atypical femoral fracture (AFF) [1]. There have been many reports of AFF in the subtrochanter or the diaphysis that were attributed to accumulation of tensile stress in these regions [2]. According to Koch [3], the greatest tensile strength occurs at the superior cortex of the femoral neck. However, to our knowledge, there have been only three cases of atypical femoral neck fracture (AFNF) [4,5]. In addition, none of those case reports revealed evidence related to suppressed bone turnover rate. Here, we report a case of AFNF with detailed pathological findings and a literature review.

CASE REPORT

A 71-year-old female was referred to our clinic with a 3-month history of pain in the right groin. Her pain was not preceded by a fall or any injury. Three weeks before presenting to our clinic, the pain worsened so that she could not bear weight on the right hip, and she underwent hip radiography and magnetic resonance imaging (MRI) at the referring hospital, where she was conservatively treated for a bone contusion. The patient had been taking 3 mg of intravenous ibandronate sodium every 3 months over the previous 4 years for osteoporosis. At admission, the bone mineral densities (T-score) of the lumbar spine, total hip, and femoral neck were –3.6, –1.4, and –1.2, respectively. On physical examination, there was pain limitation to range of motion and a positive log roll test for the right hip.

Laboratory tests showed normal adjusted serum calcium (8.9 mg/dL; normal range, 8.0 to 10.5), inorganic phosphorus (3.2 mg/dL; normal range, 2.5 to 4.5), serum creatinine (0.7 mg/dL; normal range, 0.6 to 1.1), and alkaline phosphatase (85 IU/L; normal range, 40 to 120). However, 25-hydroxycholecalciferol (17.8 ng/mL; normal range, 30 to 80) and urinary excretion of the N-telopeptide of type I collagen (8 nM bone collagen equivalents/nM creatinine; normal range, 11 to 91) were decreased.

Hip radiograph performed at our hospital upon admission showed a more definite and extended incomplete right femoral neck fracture (Fig. 1A, B), whereas a 1.5T MRI conducted at the referral hospital had shown a decreased signal intensity without fracture on the right femur neck (Fig. 1C).

A specimen that included the fracture line was obtained and stained with hematoxylin and eosin (H&E) (Fig. 2A). The frac-

pISSN 2383-7837
eISSN 2383-7845

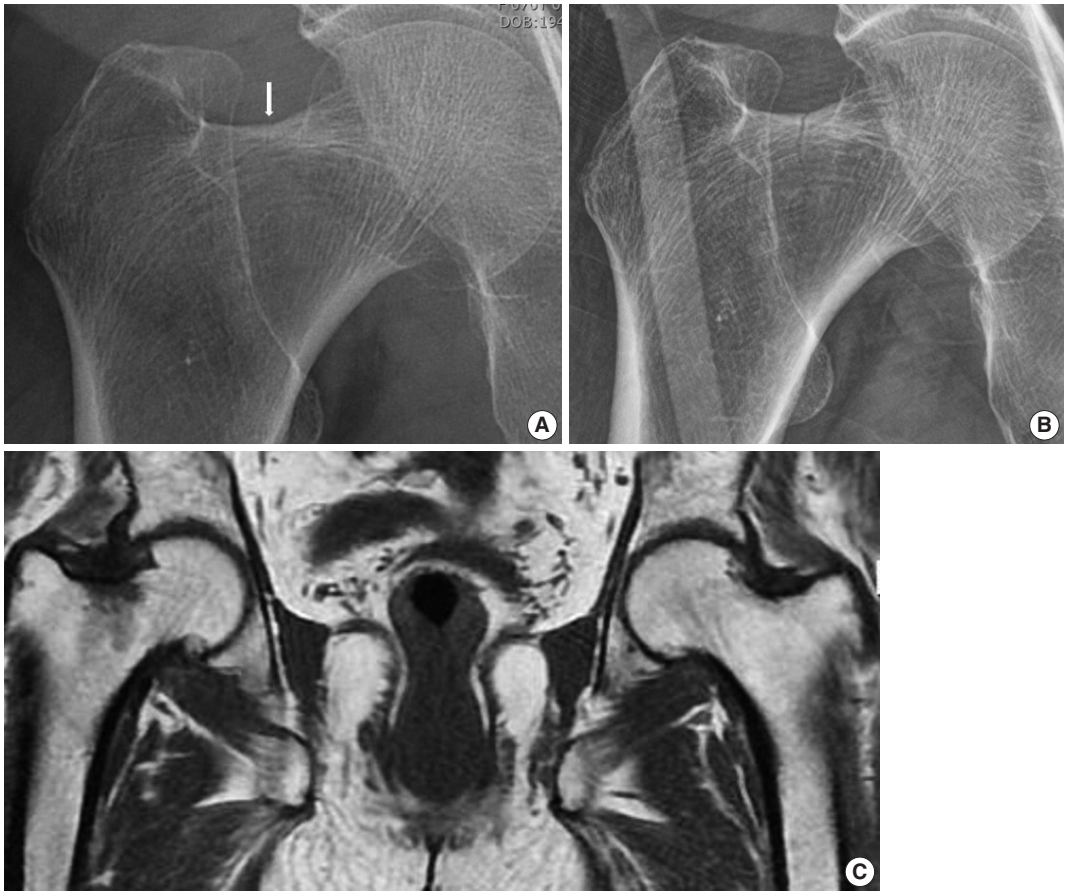

Fig. 1. (A) A radiograph performed 3 weeks before referral to our hospital shows a minimal fracture line (white arrow) on the superior cortex of the right femoral neck. (B) A radiograph performed at our hospital at admission shows a more definite and nearly vertical radiolucent line (fracture) in the right femoral neck. (C) T1 magnetic resonance imaging shows a decreased signal intensity in the superior and central aspect of the right femoral neck, which represents bone marrow edema.

ture gap appeared as a vertical, nearly empty crack, ≤0.1 mm wide, and containing mainly amorphous acellular material. No hematoma, vessels, chondrocytes, or inflammatory cells were seen within the fracture gap (Fig. 2B). The deep portion of the fracture was mostly replaced by fibrovascular tissue with a focal area of osteoid formation, indicating fracture healing (Fig. 2C). Increased remodeling activity (active osteoblastic rimming and osteoclast proliferation) was seen around the fracture gap (Fig. 2D). Osteoclasts were widely distributed, except within the fracture gap (Fig. 2). There were giant multinucleated osteoclasts, with more than 8 detached from the shallow resorption cavity (Fig. 3). The patient was diagnosed with AFNF based on history of long-term bisphosphonate therapy, suppressed bone turnover marker (urinary excretion of the N-telopeptide of type I collagen), and radiologic and pathological findings.

Because the patient required early weight bearing, bipolar arthroplasty was performed rather than internal fixation. Bisphosphonate treatment was discontinued, oral supplemental vitamin D was prescribed, and teriparatide was administered subcutaneously to prevent osteoporotic fracture. The patient was able to bear full weight immediately after the operation, and no pain was felt in either hip at 3 months postoperatively.

DISCUSSION

To our knowledge, only three cases of atypical femoral neck fractures have been previously reported with little evidence. Khan et al. [5] reported the pathological findings of disconnected, mainly thin trabecular bone with necrosis, hemorrhaging, and acute inflammatory cells. However, these pathological findings are not specific to AFF and are considered evidence of acute fracture in osteoporotic patients [6,7]. However, the pathology from the present case showed that the fracture gap contained amorphous acellular material and no living cells. Con-

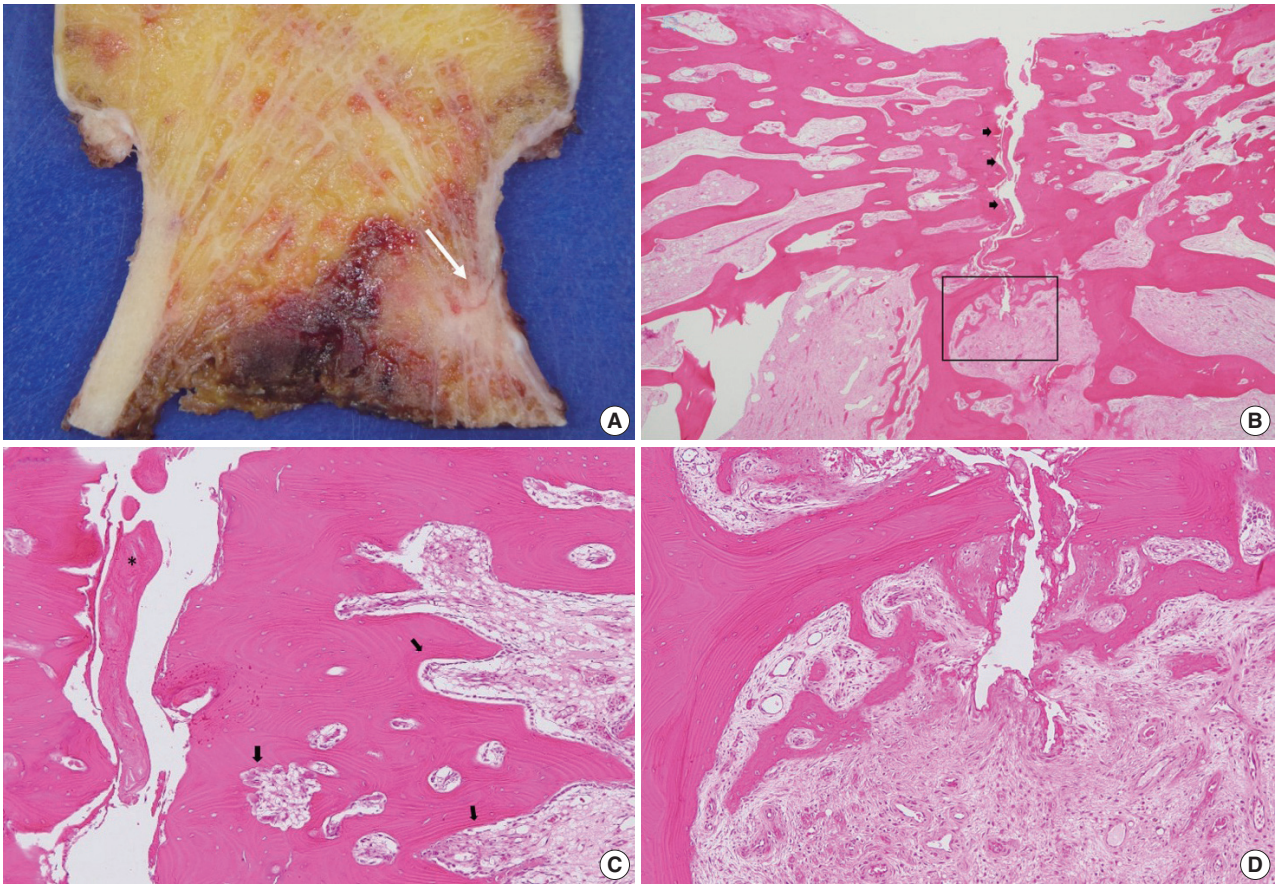

Fig. 2. (A) Specimen shows a definite incomplete fracture of the superior femoral neck (arrow). (B) A thin fracture line (arrows) extends through the entire thickness of the cortex. (C) A thin fracture gap contained amorphous acellular material (asterisk) but no hematoma, vessels, chondrocytes, or inflammatory cells. However, remodeling cavities with increased cellular activity are seen in the bone adjacent to the fracture gap (arrows). (D) A deep portion of the fracture site is mostly replaced by fibrovascular tissue with a focal area of osteoid formation representing the fracture-healing process (magnification of square area of B).

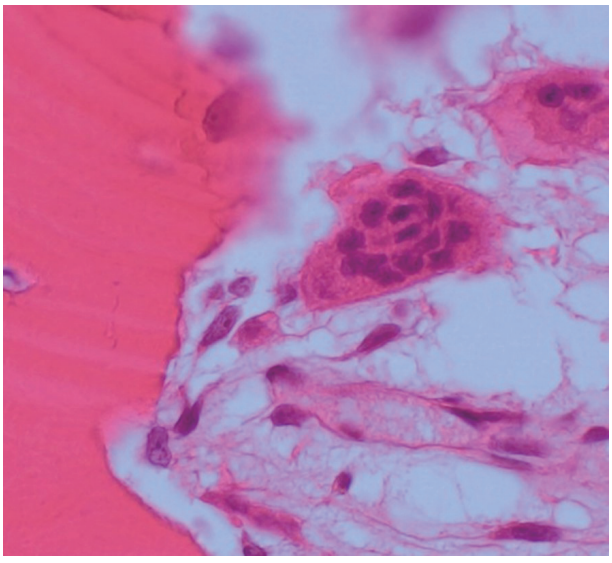

Fig. 3. A giant multinucleated osteoclast with more than 8 nuclei detached from the shallow resorption cavity.

versely, the adjacent bone revealed living cells, including active osteoclasts. These findings show that the present case was not an acute fracture, but a stress fracture.

Osteoclasts normally contain up to eight nuclei before apoptosis, but in the present case, there were giant multinucleated osteoclasts with more than 8 nuclei detached from the shallow or absent resorption cavity. This is as a characteristic finding of bisphosphonate-related atypical fractures [8-10]. Osteoclast apoptosis is likely due to exposure to a high extracellular concentration of calcium released during bone absorption [11,12]. Bisphosphonate inhibits formation of the guanosine triphosphate-binding protein necessary for osteoclasts to form the ruffled border necessary for adhesion and resorption on bone surface; therefore, calcium concentration in the resorption cavity does not increase due to loss of absorption from long-term bisphosphonate use [13]. As a result, by reducing the signal (high extracellular calcium concentration), which is important

https://doi.org/10.4132/jptm.2020.05.14

for osteoclast apoptosis, the lifespan of the osteoclast increases; therefore, the number of osteoclasts does not decrease, and fusion continues to form giant multinuclear cells [8,14]. Giant multinuclear cells are also found in Paget's disease, secondary hyperparathyroidism, giant cell tumor, and fibrodysplasia. However, these conditions can be pathologically differentiated by number, size, and apoptosis of osteoclasts; amount of osteoids; and condition of the hematopoietic bone marrow.

Fractures originating in the femoral neck and in the intertrochanteric femur are excluded from the case definition of AFF because they are more likely to be associated with other causes such as trauma or osteoporosis. However, given that atypical fractures are clustered at the region of maximal tensile loading, the superior cortex of the femoral neck withstands maximum tensile stress, putting it at risk of atypical fractures [2,3]. We assumed that the paucity of reports on AFNFs was related to the fractures being mistaken for the transverse type of osteoporotic insufficiency fractures [15]. In osteoporosis, the pathology shows thin trabeculae disconnected from each other, enlarged areolar tissue, and increased resorption cavity, and the increased bone turnover marker is shown in laboratory testing. In the present case, urinary excretion of the N-telopeptide of type I collagen was reduced, reflecting a decrease in bone remodeling due to bisphosphonate [16,17]. Recently, atypical fractures were also reported in the ulna, tibia, ilium, and pubis [18-20]. Therefore, I propose that the case definition of AFF be limited to femoral subtrochanter and shaft that require supplementation.

There is a limitation in this study. Histomorphometry of giant multinuclear osteoclasts (i.e., scale, shape, and position) and number of giant multinuclear osteoclasts were not detailed, as only H&E staining was performed.

In conclusion, the patient in the present case had no trauma history, long-term bisphosphonate use, reduced urinary excretion of the N-telopeptide of type I collagen, and a pathological finding of bisphosphonate-related atypical fracture comprised of amorphous acellular material and no living cells in the fracture gap and giant multinucleated osteoclast detached from the bone perimeter. For patients with groin pain with minimal or no trauma and a history of prolonged bisphosphonate use, the possibility of AFNF should be considered.

Ethics Statement

The Institutional Review Board of Konyang University Hospital (KYUH 2019-10-014) approved this study, and we received informed consent from the patient.

ORCID

Kwang-kyoun Kim https://orcid.org/0000-0002-6844-5431
Young-wook Park https://orcid.org/0000-0002-7976-6644
Tae-hyeong Kim https://orcid.org/0000-0001-7410-8813
Kyung-deok Seo https://orcid.org/0000-0001-7227-0710

Author Contributions

Conceptualization: KKK. Data curation: KKK, KDS. Investigation: KKK, YWP. Methodology: YWP, KKK. Project administration: KKK. Resources: KKK. Software: KKK. Supervision: KKK. Validation: KKK, THK. Visualization: YWP, KKK, THK. Writing—original draft: KKK. Writing—review & editing: KKK. Approval of final manuscript: all authors.

Conflicts of Interest

The authors declare that they have no potential conflicts of interest.

Funding Statement

No funding to declare.

Acknowledgments

Thanks to Change-jin Kim and Pan-jo Kim, who assisted me in finding giant multi-nucleated cells in a cold pathology room.

References

1. Shane E, Burr D, Ebeling PR, et al. Atypical subtrochanteric and diaphyseal femoral fractures: report of a task force of the American Society for Bone and Mineral Research. J Bone Miner Res 2010; 25: 2267-94.
2. Koh JS, Goh SK, Png MA, Ng AC, Howe TS. Distribution of atypical fractures and cortical stress lesions in the femur: implications on pathophysiology. Singapore Med J 2011; 52: 77-80.
3. Koch JC. The laws of bone architecture. Am J Anat 1917; 21: 177-298.
4. Kim DH, Lee EC, Kang SK. Insufficiency fracture of ipsilateral femur neck in patient treated with long term bisphosphonate treatment: a case report. J Bone Metab 2012; 19: 159-62.
5. Khan SK, Savaridas T, Hemers JS, Maarouf Z, Orgee JM, Orr MM. Atraumatic intracapsular neck of femur fractures after prolonged bisphosphonate treatment: a new atypical variant? Clin Cases Miner Bone Metab 2016; 13: 38-41.
6. Schilcher J, Sandberg O, Isaksson H, Aspenberg P. Histology of 8 atypical femoral fractures: remodeling but no healing. Acta Orthop 2014; 85: 280-6.
7. Kajino Y, Kabata T, Watanabe K, Tsuchiya H. Histological finding of atypical subtrochanteric fracture after long-term alendronate therapy. J Orthop Sci 2012; 17: 313-8.
8. Weinstein RS, Roberson PK, Manolagas SC. Giant osteoclast formation and long-term oral bisphosphonate therapy. N Engl J Med 2009; 360: 53-62.
9. Whyte MP, Wenkert D, Clements KL, McAlister WH, Mumm S. Bisphosphonate-induced osteopetrosis. N Engl J Med 2003; 349: 457-63.
10. Jain N, Weinstein RS. Giant osteoclasts after long-term bisphosphonate therapy: diagnostic challenges. Nat Rev Rheumatol 2009; 5: 341-6.
11. Lorget F, Kamel S, Mentaverri R, et al. High extracellular calcium concentrations directly stimulate osteoclast apoptosis. Biochem Biophys Res Commun 2000; 268: 899-903.

12. Nielsen RH, Karsdal MA, Sorensen MG, Dziegiel MH, Henriksen K. Dissolution of the inorganic phase of bone leading to release of calcium regulates osteoclast survival. Biochem Biophys Res Commun 2007; 360: 834-9.
13. Rogers MJ, Crockett JC, Coxon FP, Mönkkönen J. Biochemical and molecular mechanisms of action of bisphosphonates. Bone 2011; 49: 34-41.
14. Cremers S, Papapoulos S. Pharmacology of bisphosphonates. Bone 2011; 49: 42-9.
15. Parks TG, Baird DS, Wilson RI. Stress fractures of the neck of the femur. Ulster Med J 1970; 39: 111-8.
16. Bone HG, Hosking D, Devogelaer JP, et al. Ten years' experience with alendronate for osteoporosis in postmenopausal women. N Engl J Med 2004; 350: 1189-99.
17. Greenblatt MB, Tsai JN, Wein MN. Bone turnover markers in the diagnosis and monitoring of metabolic bone disease. Clin Chem 2017; 63: 464-74.
18. Osada R, Zukawa M, Kimura T. Atypical ulnar fracture associated with long-term bisphosphonate use. J Orthop Sci 2015; 20: 1132-5.
19. Breglia MD, Carter JD. Atypical insufficiency fracture of the tibia associated with long-term bisphosphonate therapy. J Clin Rheumatol 2010; 16: 76-8.
20. Patel V, Graves L, Lukert B. Pelvic fractures associated with long-term bisphosphonate therapy-case report. J Musculoskelet Neuronal Interact 2013; 13: 251-4.

 https://doi.org/10.4132/jptm.2020.05.14


JPTM
Journal of Pathology and
Translational Medicine